Evaluation of the Cruden Motorcycle Simulator

B.E. Westerhof

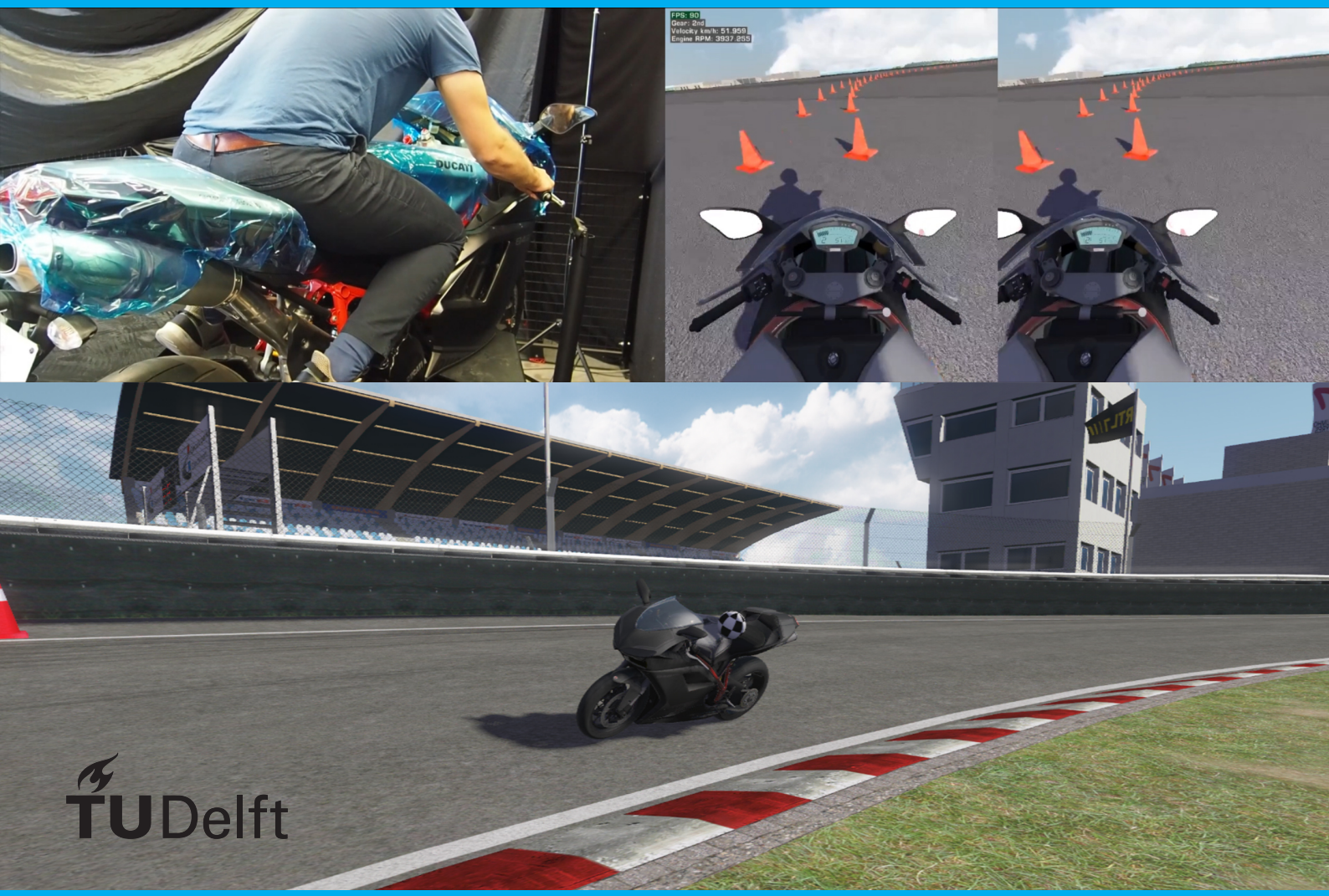

TU Delft

Evaluation of the Cruden Motorcycle Simulator

by

Bernhard E. Westerhof

to obtain the degree of Master of Science
at the Delft University of Technology,
to be defended publicly on Friday, August 31, 2018 at 08:30 AM.

Student number:	4230809	
Project duration:	November 13, 2017 – August 21, 2018	
Thesis committee:	Dr. ir. R. Happee,	TU Delft, Chairman
	Dr. ir. Arend L. Schwab,	TU Delft, Supervisor
	Dr. ir. B. Shyrokau,	TU Delft, Independent
	Dr. ir. Edwin J.H. de Vries,	Supervisor Cruden B.V.

An electronic version of this thesis is available at http://repository.tudelft.nl/.

TU Delft

Abstract

Research in the motorcycle industry is lagging behind research in the automotive industry. Especially with respect to safety, more research is needed, since motorcycles are overrepresented in the number of road casualties and injuries. Important tools in vehicle research are vehicle simulators. The use of motorcycle simulators enables manufacturers to develop new motorcycle technologies and could make motorcycles safer. Unfortunately, few motorcycle simulators are available, and even fewer are used in the development of new motorcycles and motorcycle safety systems. Furthermore, validation of the available motorcycle simulators is lacking and little design knowledge is available.

This thesis evaluates the Cruden motorcycle simulator and shows that it can be used in motorcycle research. This evaluation consists of three parts. First, a new motorcycle dynamics model based on existing literature is developed and validated using parameter estimation methods on virtual simulation data. It is shown that the capsize and weave eigenmodes are present and that these eigenmodes show qualitatively similar behavior as is observed in real motorcycles.

The motorcycle simulator uses a Stewart platform and handlebar control loader to provide motion cues to the user. In the second part, these two systems are evaluated. For both systems, specific input sequences are used to gather output data. Using a system identification approach, the dynamics properties of the motion platform and handlebar control loader are evaluated. The dynamics properties are compared to what is required from the motorcycle dynamics model and it is shown that the Stewart platform and handlebar control loader have enough bandwidth and sufficiently small phase delays to accurately simulate the motorcycle dynamics.

In the third and final part, a human research approach is used to further evaluate the motorcycle simulator. In a speed perception experiment, where participants were asked to ride three different speeds on an infinite highway, it is shown that speed perception on the motorcycle simulator shows correspondence to what is observed in real life: participants underestimated their riding speed as a group. It was also observed that speed perception at higher speeds is relatively more accurate than at lower speeds, which corresponds to findings in literature too.

Two other questions which were asked in this part of the research were whether the motorcycle simulator actually needs platform motion and upper body tracking. To answer these questions, participants were asked to ride the motorcycle on a trajectory with four semicircular corners separated by short straights. Objective metrics like steering torque and lane deviation and subjective metrics like workload and simulator sickness were compared. Finally, it is shown that platform motion significantly improves the rider's performance and perception of the motorcycle simulator, but that no significant findings on upper body tracking could be established.

Preface and Acknowledgments

When I was around 14 years old, a friend of mine got a Zündapp ZD40 50cc two stroke moped from his uncle. After some tinkering, we got the moped to run again, but we didn't stop there. Honing the inlet manifolds, using larger size carburettors and changing the air filters were just a few of the tricks we used to get the moped to run faster. All we wanted to do was learn everything there is about mopeds with the goal to make them faster and faster. In retrospective, I think my wish to become a mechanical engineer started here. Or maybe it already started with al the Lego's played with as a child. Anyhow, it seems only fitting that in my final research project I learned a great deal more about mopeds.

First of all I would like to thank Dr. de Vries for his daily supervision and I greatly appreciated that he shared his invaluable knowledge on vehicle dynamics. I very much enjoyed the moments in which he gave me more insight into vehicle dynamics and modeling techniques.

It has been an honor to be supervised by Dr. Schwab, an authority on bicycle dynamics and multi-body dynamics, for whom I have great respect.

I would like to express my gratitude to Dr. Happee for helping me give my research a clear direction and his helpful feedback in the final stages of my thesis.

Advice given by Dr. de Winter with respect to my experimental design and statistical analysis was greatly appreciated.

I am particularly grateful for the opportunity given by Cruden to do my thesis on their motorcycle simulator. I would like to explicitly mention Martijn de Mooij and Jelle van Doornik and Kay Hagenaars for their help, but everyone at Cruden has been most friendly to me and helped me whenever possible. It has been a fantastic experience to work with the talented people at Cruden and the high-tech simulators they make.

I would also like to thank my friends from Delft and my colleagues at Cruden who participated in my experiments. It gives me great joy that they were willing to give up their free time to help me with my thesis.

Finally, I would like to thank my girlfriend Lianne and my parents for their support and motivation throughout my time working on this thesis.

Bernhard E. Westerhof
Amsterdam, August 21, 2018

Contents

1 Introduction **1**
- 1.1 A brief literature review . . . 2
- 1.2 Problem description . . . 2
- 1.3 Research questions . . . 3
- 1.4 Outline . . . 4

2 The Cruden Motorcycle Simulator **5**
- 2.1 Motorcycle simulator hardware . . . 5
- 2.2 Motorcycle dynamics model . . . 6
  - 2.2.1 Geometry . . . 7
  - 2.2.2 Suspension . . . 7
  - 2.2.3 Tire-road forces . . . 9
  - 2.2.4 Driveline . . . 10
  - 2.2.5 Brakes . . . 10
  - 2.2.6 Aerodynamics . . . 12
  - 2.2.7 Data logger . . . 12
- 2.3 Motion cueing . . . 12
  - 2.3.1 Motion platform . . . 12
  - 2.3.2 Control loader . . . 13
- 2.4 Upper Body Tracking . . . 14
- 2.5 The Visual System . . . 14
- 2.6 Cruden Panthera software . . . 16

3 Motorcycle Dynamics Evaluation **17**
- 3.1 Method . . . 17
  - 3.1.1 Eigenvalue identification . . . 17
  - 3.1.2 Identification maneuvers . . . 18
- 3.2 Results . . . 18
- 3.3 Discussion . . . 20

4 Motion Platform **23**
- 4.1 Method . . . 23
  - 4.1.1 Steering assembly frequency response analysis . . . 23
  - 4.1.2 Stewart platform analysis . . . 24
- 4.2 Results . . . 24
  - 4.2.1 Steering assembly . . . 24
  - 4.2.2 Stewart platform . . . 25
- 4.3 Discussion . . . 27

5 Human Research **31**
- 5.1 Method . . . 31
  - 5.1.1 Participant recruitment . . . 31
  - 5.1.2 Test track development . . . 31
  - 5.1.3 Experimental design . . . 32
  - 5.1.4 Data acquisition and performance metrics . . . 34
  - 5.1.5 Statistical analysis . . . 37
- 5.2 Results . . . 37
  - 5.2.1 Velocity estimation . . . 37
  - 5.2.2 Trajectory tracking . . . 38

5.3 Discussion 41
5.3.1 Speed perception experiments 46
5.3.2 Trajectory tracking experiments 46

6 Conclusion **49**

7 Future Work **51**

Bibliography **53**

A Participant Demographics **57**

B Questionnaires **59**

C Steps for Conducting the Experiments **69**
C.1 List of Steps. 69
C.2 Order of Administration. 70

D Informed Consent Form **71**

1 Introduction

Motorcycles are used worldwide for a wide variety of purposes such as commuting, racing and leisure. One of the biggest advantages of motorcycles with small displacement combustion engines is that they are very fuel efficient, making them extremely popular in developing countries. But also a motorcycle's performance for a reasonable cost and the thrill of riding a motorcycle are appealing to their owners. Unfortunately, motorcyclists were 35 times more likely to die in a crash compared to car drivers, per mile traveled, in the U.S. in 2007 [22]. Therefore, research in the field of motorcycle safety is necessary for the development of safer motorcycles to decrease the number of deaths.

Motorcycles have not received the same attention in the development of safety mechanisms as passenger cars and trucks. This could partially be explained by a lack of motive for motorcycle manufacturers, as fast motorcycles sell better than safe motorcycles. But next to that, the means for the development of safety mechanism for motorcycles have also been less available. One of the reasons for this unavailability is that motorcycle simulators are rare and even more rarely used in the development of motorcycle safety systems and design. This is interesting to see, as simulators are widely used throughout the aviation and car industry for development of new technologies and training pilots and drivers. After all, simulators offer great flexibility and control over the independent variables, which is not possible in the real world, let alone for safety reasons.

Nevertheless, a motorcycle simulator has been developed by Cruden, a company that designs, manufactures and integrates simulators for the automotive, motorsport and marine industries. Figure 1.1 shows the Cruden motorcycle simulator. This simulator has been made available by Cruden for research and this thesis sets out to evaluate the Cruden motorcycle simulator and to obtain new knowledge with respect to motorcycle simulators in general.

Figure 1.1: Picture of the Cruden motorcycle simulator. The simulator consists of a Ducati 848 Evo motorcycle mock up mounted on a Stewart platform.

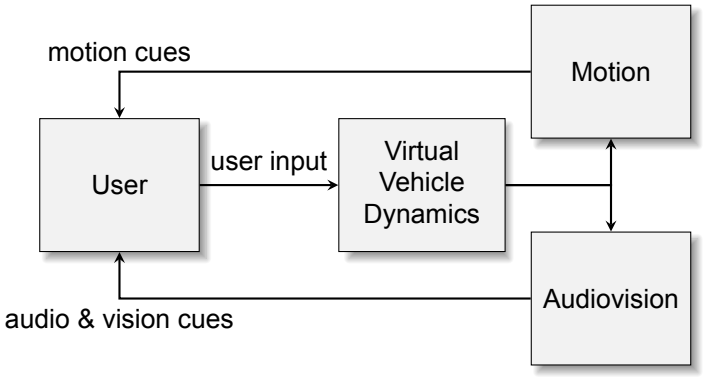

Figure 1.2: Basic vehicle simulator loop. The user provides a certain input to a measurement device which sends the input to a computer with a vehicle dynamics model. The virtual vehicle dynamics model calculates the new states of the model. These states are used for simulation of motion by a motion platform and simulation of other sensory inputs like vision and sound.

1.1. A brief literature review

A wide variety of simulators exist, all with their specific purposes and strengths. One of the areas in which simulators differ from each other is the use of motion simulation [41]. The simplest simulators are fixed based and do not provide the user with motion cues. The most complex simulators provide the user with motion cues in all six degrees of freedom (6DoF), like the Daimler-Benz and the NADS-1 driving simulators [8, 28, 33]. Providing motion in all six degrees of freedom is often done by means of a Stewart platform [35].

Vehicle dynamics play a crucial role in the simulation of motion and therefore in motorcycle simulators, as can be seen in Figure 1.2, where a simplified architecture of a motion simulator is shown. Fortunately, research in motorcycle and bicycle dynamics already has a long history, with one of the first papers written by Whipple in 1899 on the stability of bicycles [42]. Contributors in the field of motorcycle dynamics include among others Sharp, Koenen and Cossalter [3, 18, 32]. See [20] for a comprehensive overview on motorcycle dynamics and modeling. Interestingly, Sharp already mentioned in 1971 that theoretical studies on car steering behavior helped the car industry develop better vehicles and that he wanted to do the same for motorcycles [30]. In later years, his contributions helped identify motorcycle instabilities like wobble and weave and paved the way for more complex motorcycle dynamics research.

The first motorcycle simulator was developed by Honda as the Japanese government required simulator training as a part of obtaining the motorcycle license [46]. Other noteworthy motorcycle simulators have been developed over the years by YNL Tokyo, MORIS, Stedmon et al., SIMACOM and SafeBike [1, 5, 9, 21, 34]. Other interesting research with motorcycle simulators has been performed at the WIVW in Germany [44].

1.2. Problem description

Even though some motorcycle simulators exist, the use of motorcycle simulators in industry is very limited. The lack of simulators limits the extent to which manufacturers and suppliers can test new motorcycle designs, safety systems and perform validation in an early stage of development. Unfortunately, little information is available on the design of motorcycle simulators and their performance.

With respect to the vehicle dynamics of the simulator, Limebeer gives a good overview of what is needed to model the most important dynamics properties of a motorcycle by for example using a multibody dynamics modeling approach [20]. These dynamics properties include the motorcycle's eigenmodes and input-output behavior. Furthermore, results published by Cossalter showed resemblance between an instrumented motorcycle and the SafeBike motorcycle simulator [4]. Looking at the motion platform however, it is suggested that roll and pitch motion are the most important, but a comparative research has not been successfully done yet for motorcycle simulators. Since riding a motorcycle is such a dynamic endeavor, it may very well be that the only way of accurate simulation is by providing motion in all degrees of freedom. If, however, motion cues in only certain directions provide satisfactory results, it could be concluded that cheaper simulator constructions can do the job just as well. Numerous studies on the influence of motion have been done in the aviation industry

[13, 25] and the car industry [16, 26, 43]. A general conclusion is that motion cueing is preferred by the users and that motion sickness is reduced, thus improving the subjective quality of the simulator. Yet, it remains a challenge to prove an increase in simulator validity and objective performance metrics by using motion.

It is suggested that the most important steering input is the handlebar torque [20]. Hence, all motorcycle simulators measure the torque the rider inputs on the the simulator's handlebar. However, another interesting topic is rider motion. As every motorcyclist knows, moving your body on a motorcycle steers the motorcycle [2]. In a study where a 12-DoF rider model has been developed, rider motion did show to influence the motorcycle's behavior [14]. Two examples where rider motion is accounted for are the Safebike motorcycle simulator, where load cells in the foot-pegs are used to account for rider motion and the DESMORI simulator, where an induced roll torque in the simulator is measured resulting from the rider shifting weight [4, 44]. Assessing how riders actually steer their bike would be a valuable contribution to motorcycle research. Using the upper body tracking sensors available on the Cruden Motorcycle Simulator, this study will explore the benefits of implementing body steer in a motorcycle simulator.

Since the dynamics of a motorcycle strongly depend on the motorcycle's velocity, it is important to know whether users of a motorcycle simulator are able to estimate their speed correctly. Surely, if the perception of velocity on a motorcycle simulator is completely different from that of a real motorcycle, then the motorcycle's dynamics will also be perceived differently. One problem often encountered is that humans are relatively poor in estimating their velocity. For a car, Recarte and Nunes showed that participants underestimated all speeds, with worst underestimation at 60 km/h with a 39 percent error and best underestimation at 120 km/h with an 11 percent error [24]. For example, participants estimated on average that they were driving 48.3 km/h while in reality they were driving 60 km/h.

The Cruden Motorcycle Simulator uses a Head-Mounted Display (HMD) to present the visual information to the rider. Another example of a motorcycle simulator using an HMD is the YNL Tokyo simulator [1]. Unfortunately, HMD's and projection methods have not been systematically compared for motorcycle simulators. Nevertheless, Kemeny and Panerai describe some favorable properties present in HMD's like motion parallax and stereopsis, which could help in the correct perception of speed [16]. Sound also plays an important role in speed perception giving cues about for example engine RPM and wind noise. Like HMD's, sound has not been explicitly validated with respect to speed perception. If the same behavior of speed perception is observed in the motorcycle simulator, it can at least be concluded that the cues provided by the simulator are correct.

For motorcycle simulators, Will has performed extensive studies in speed perception in motorcycle simulators for different sensory inputs [44]. He used mainly presence as a measure of simulator quality. In his research, he used a real motorcycle for his speed perception experiments, and showed that participants underestimated speed with 13 percent error at 50 km/h. However, participants were able to estimate their speed correctly at 100 km/h. As Kemeny and Panerai describe, visual cues are essential for speed perception [16]. Little is known however on the performance of head-mounted displays in simulator speed perception.

1.3. Research questions

With this research, new knowledge about motorcycle simulators is obtained by using a 6-DoF motorcycle simulator developed at Cruden with a 15-DoF motorcycle model. The motorcycle model has been developed in the scope of this work, based on a Honda CB750 described in [31]. This motorcycle simulator can be used to address the questions on motion cueing, rider movement on the motorcycle and speed perception and is described in detail in Chapter 2. This research is subdivided in three categories, where category two and three follow a human research approach. The first category focuses on the performance of the motion platform itself and whether it can simulate some important properties of a motorcycle. The second category investigates speed perception on the motorcycle simulator with the Oculus Rift. The third category evaluates the motorcycle simulator by investigating the importance of platform motion and upper body tracking.

For the first category, the hypotheses are formulated as follows:

- The motion platform can simulate the motorcycle's dynamics under normal operation.
- The motion platform can capture the capsize, weave and wobble eigenmodes of the motorcycle dynamics.

In the speed perception category, the hypotheses are based on the work of Recarte and Nunes and are [24]:

- On average, riders have the best speed perception at 120 km/h, underestimating within 5 percent error.
- On average, riders have the worst speed perception at 50 km/h, underestimating within 30 percent error.
- On average, riders have medium speed perception at 80 km/h, underestimating at 20 percent error.
- Speed estimation error conforms to experiments in previous work.

And in the final category, the hypotheses are:

- With motion cueing and body tracking, the rider performs best, reports the lowest effort and sickness and highest presence.
- With either motion or body tracking turned of, performance worsens, higher values for effort and sickness are reported and presence is lower.
  - Motion plays a more important role than body tracking.

1.4. Outline

This report is structured as follows. First, Chapter 2 gives a detailed description of the motorcycle simulator used in this research. This chapter also describes what changes have been made in preparation of this research. Chapters 3, 4 and 5 each have a method, results and discussion section for their respective subjects: Chapter 3 contains the evaluation of motorcycle dynamics, 4 the evaluation of the motion platform and the human research experiments are explained in Chapter 5. Finally, Chapter 6 concludes this research, and Chapter 7 outlines some possibilities for future work.

2

The Cruden Motorcycle Simulator

This chapter describes Cruden's motorcycle simulator in some detail. Also, several changes that were made to the simulator before the start of the experiment are mentioned. Section 2.1 discusses the hardware of the motorcycle simulator. For other sections is this chapter, Figure 2.1 shows a representation of the used Simulink subsystems and indicate in which sections relevant information can be found. Section 2.3 explains what motion cueing strategy is used in the simulator and Section 2.5 explains how the visuals are created. Section 2.6 shows insight in the Panthera software, which is used to run the simulator.

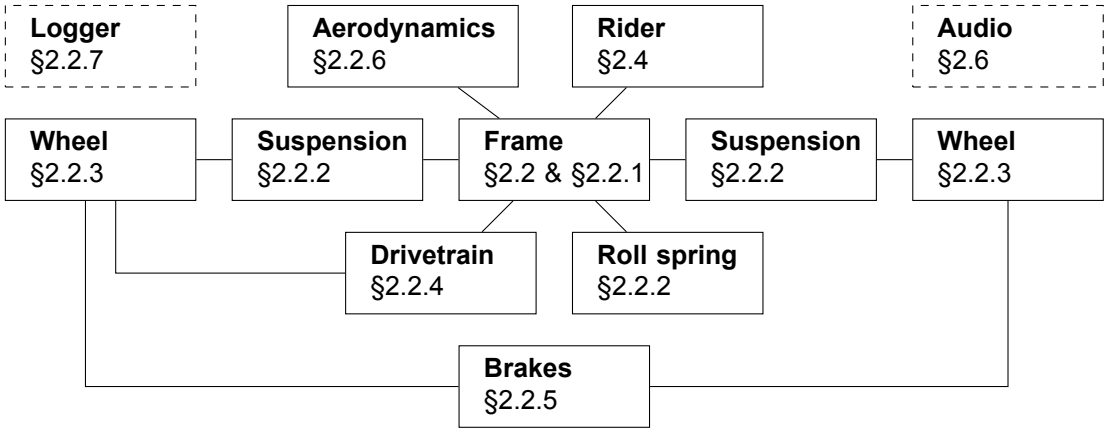

Figure 2.1: Representation of the used Simulink model and description of where each subsystem is described in this chapter. The dashed boxes show subsystems that are only used to output data and do not otherwise influence the dynamics of the motorcycle.

2.1. Motorcycle simulator hardware

The hardware of the motorcycle simulator can be subdivided in the motion platform, motorcycle mock-up, vision hardware, audio hardware and computer hardware. Table 2.1 shows the specifications of the motorcycle simulator.

Table 2.1: Cruden motorcycle simulator specifications. Note that the hardware for the computers differs per computer, but that the specific hardware for the HMD PC (Master) are given explicitly.

Motion Platform	
Manufacturer	E2M
Stewart platform	E2M eM6-300-1500 [37]
Control loader	E2M eF-DD-50 [36]
Real-time PC	Linux RT/Xenomai + eMoveRT controller
Communication protocol	UDP + EtherCAT

Motorcycle Mock-Up	
Manufacturer	Cruden/Ducati
Model	Ducati 848 Evo
Steering torque sensor	Loadcell Transducer Techniques
Body position sensor	Intel RealSense SR300 Dev kit (2x) [38]
Throttle position sensor	Potentiometer 75mm PM2S-75-5K
Gear selection sensor	Interlock Switch shifter unit
Clutch sensor	Brake sensor, 250 bar
Front brake sensor	Brake sensor, 250 bar
Rear brake sensor	Brake sensor, 250 bar
Kill cord for interlock	Demon Tweeks: Bike-It Universal Kill Switch With Tether
Computer hardware	
Manufacturer	Cruden/Generic
Computers	- Operator/Database PC - Telemetry PC - GPS tracker PC - Spectator PC - HMD PC
Graphics cards	NVIDIA GeForce GTX 1080
Processors	Intel i7-6700K (Master) Intel Xeon X3350 (Others)
Memory	16 GB at 1666MHz
Sound Card(s)	Creative Soundblaster Z PCIe
Communication	Ethernet
Video	
Manufacturer	Oculus Rift
Type	Head mounted display
Display	2,160 x 1,200 pixels, OLED
Refresh rate	90 Hz
Audio	
Mixer	Allen & Heat GR4 4ch mixer with ducking
Amplifiers	Yamaha P2500S Amp (3x)
Speakers	Yamaha SW115W Subwoofer
Speakers	Yamaha SM10V Floor monitor (4x)
Speakers	Yamaha MS101 III Active speaker for intercom talk-back

The interfaces between the hardware are defined as follows and can be seen in Figure 2.2. The five computers are used as operator, master, spectator, GPS and logger. The operator controls the four other computers and has control over the simulation. With this approach, one operator computer is needed to control several simulation aspects simultaneously. The master runs the vehicle dynamics model, communicates with the motion platform and sends the visuals and audio to their respective devices. The spectator shows 'TV-like' live footage of the simulation. Data logging and telemetry analysis is handled by the fourth computer. The five computers all communicate over Ethernet. Communication with the real-time PC is also established over Ethernet. The Oculus Rift uses a standard HDMI interface.

2.2. Motorcycle dynamics model

For this research, a new motorcycle model based on the Honda CB-750 described by Sharp and Alstead has been developed [31]. This motorcycle model contains the parametric description of the Honda CB-750 combined with several components already developed within Cruden, like the tires, driveline and brake systems. This section gives a detailed overview of the design of the motorcycle model used in this research.

The motorcycle dynamics model is developed in MATLAB®R2013b 32-bit and Simulink® using the

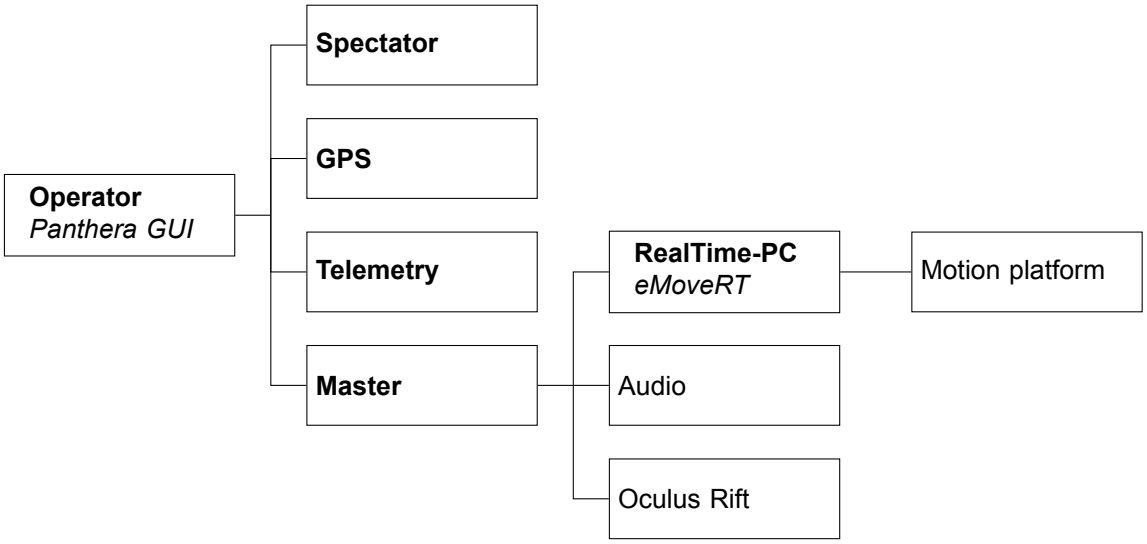

Figure 2.2: Block diagram of the PC communication architecture. The PC names are boldfaced. Specific software on these computers is shown in italic.

Simscape Multibody™first generation toolbox. It consists of the following six bodies, shown in figure 2.3, resulting in a total of 15 degrees of freedom:

Rear frame six degrees of freedom.

Front frame two degrees of freedom with respect to rear frame, steer angle and frame twist.

Front wheel two degrees of freedom with respect to front frame, one rotational, one prismatic along the front fork rake angle.

Rear wheel two degrees of freedom with respect to rear frame, one rotational, one vertical prismatic.

Rider upper body two planar degrees of freedom with respect to rear frame, longitudinal and lateral.

Crankshaft one rotational degree of freedom with respect to rear frame.

Figure 2.4 shows how the bodies are connected to each other in the multibody dynamics modeling approach. The universal joint between the rear frame and the front frame allows for two rotational degrees of freedom around a rotated x'-z' coordinate system. The z' axis corresponds to the steer axis and the x' axis to the frame flexibility axis. Around the steering axis, only a damping of 5 Nms/rad is applied. Around the frame flexibility axis, a stiffness of 102 kN/rad and a damping of 2 kNms/rad is applied, where the stiffness is derived from Sharp and Alstead and the damping is added to keep the simulation numerically stable [31]. The frame flexibility spring damper system is modeled using a native Simscape First Generation Joint Spring & Damper block. The Rear Hub and Front hub are massless bodies without inertia.

2.2.1. Geometry

As mentioned before, the geometry of a motorcycle plays an essential role in its performance. Figure 2.5 gives a schematic representation of the motorcycle's key parameters. Table 2.2 shows the values for the parameters in Figure 2.5, combined with mass and inertial properties. Subscript $_f$ and $_r$ correspond to front and rear respectively. Subscript $_b$ corresponds to the rider's body and subscript $_e$ to the engine's crankshaft. Subscript $_w$ indicates a wheel property and subscripts $_{x,y}$ and $_z$ correspond to their respective axes.

2.2.2. Suspension

Both the front and rear suspension exert forces in the direction of the prismatic joint between their respective bodies. The rear suspension is modeled using a Joint Spring & Damper block native to

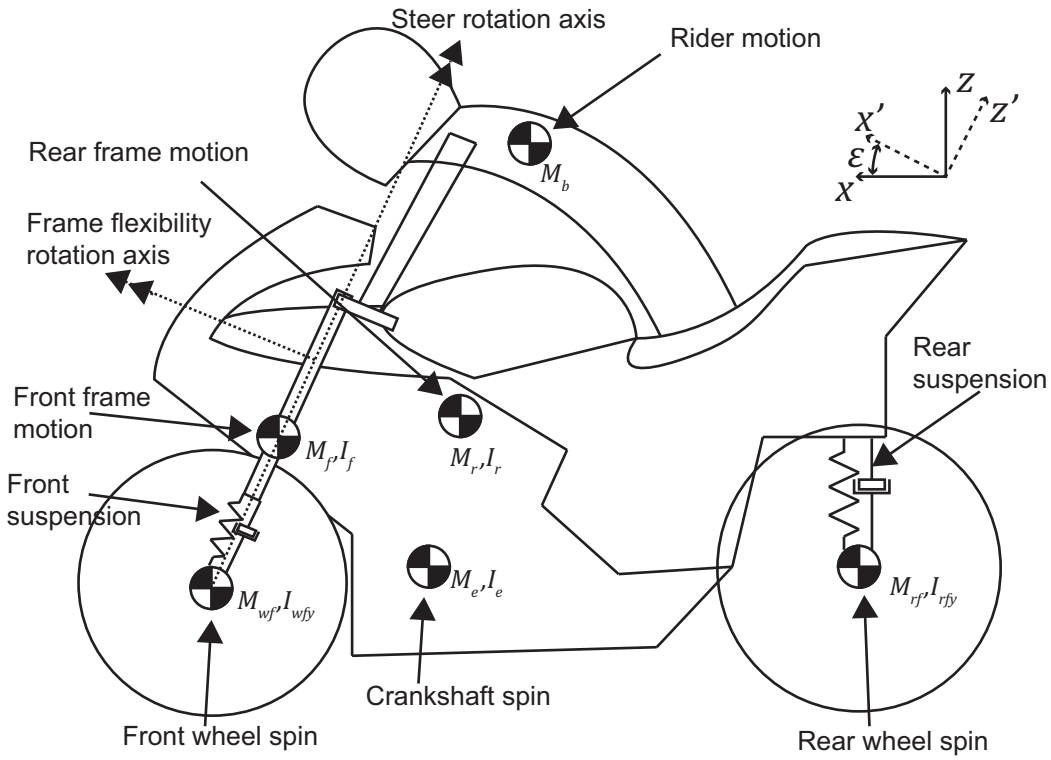

Figure 2.3: Representation of the Honda CB-750 motorcycle indicating the centers of gravity for all bodies accounted for in the motorcycle dynamics model. Based on the work of Sharp and Alstead [31].

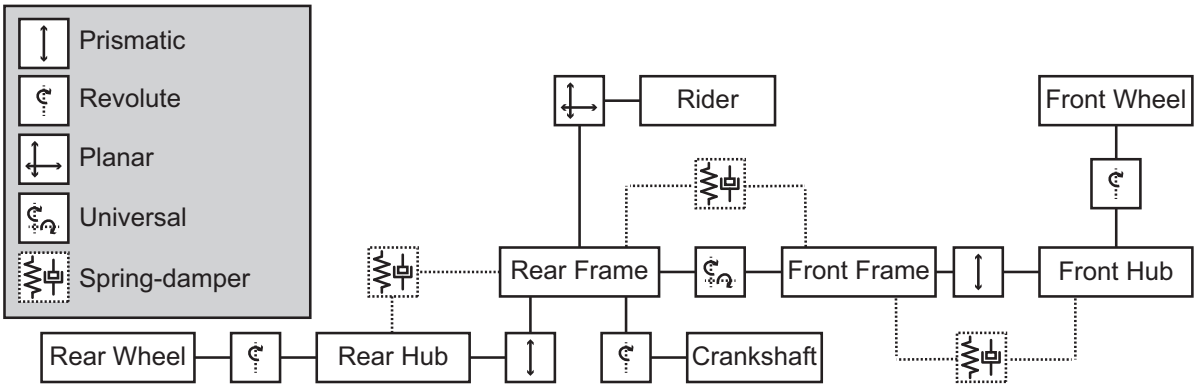

Figure 2.4: Kinematics of the Honda motorcycle model.

Table 2.2: Parameter set for the Honda model based on the work of Sharp and Alstead [31]. Values with a [1] are estimated and not taken from Sharp and Alstead to accommodate the pitch dynamics and upper body dynamics.

Parameter	Value	Unit	Parameter	Value	Unit	Parameter	Value	Unit
b	0.50	m	M_f	25	kg	I_{rx}	32	kgm^2
e	0.05	m	M_r [1]	200	kg	I_{ry} [1]	60	kgm^2
h	0.60	m	M_b [1]	30	kg	I_{rz}	22	kgm^2
j	0.55	m	M_{wf}	10	kg	I_{fx}	3.8	kgm^2
l	0.92	m	M_{wr}	10	kg	I_{fy} [1]	0.0	kgm^2
R_f	0.32	m	M_e [1]	20	kg	I_{fz}	0.3	kgm^2
R_r	0.31	m				I_{wfy}	0.8	kgm^2
t	0.10	m				I_{wry}	1.1	kgm^2
ε	0.47	rad				I_{ex} [1]	0.1	kgm^2
s	0.87	m				I_{ey} [1]	0.1	kgm^2
h_b [1]	0.40	m				I_{ez} [1]	0.1	kgm^2

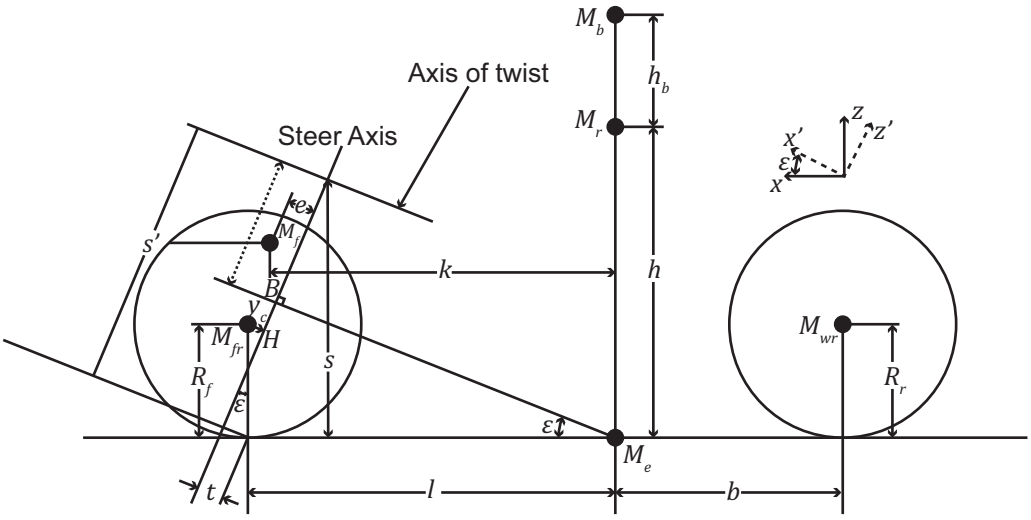

Figure 2.5: Parametrization of the Honda model, based on the work by Sharp and Alstead [31].

Table 2.3: Spring-damper characteristics for the front and rear spring-damper systems.

	Spring Constant	Damper Constant	Spring Offset
Rear	50 kN/m	2 kNs/m	-0.02 m
Front	20 kN/m	*lookup-table*	0.00 m

Simscape First Generation with properties shown in Table 2.3. For the front suspension, Cruden's spring damper Simulink subsystem is used, featuring end-stops, bump-stops and non-linear damping characteristics implemented both in normal Simulink blocks and S-Functions. These spring damper subsystems are used in most vehicle models developed by Cruden.

Besides the conventional suspension, a virtual roll spring is used to facilitate take off from a standing start with the motorcycle simulator. At 0 velocity, this roll spring exerts a torque

$$M_x = -k\phi - c\dot{\phi}, \tag{2.1}$$

where ϕ is the roll angle in radians and k and c are spring and damper constants respectively. For higher velocity, M_x is multiplied with $f(v)$, where

$$f(v) = -0.5(\tanh(v - v_{ref}) - 1). \tag{2.2}$$

In 2.2, v is the motorcycle's velocity and v_{ref} is the reference fade out velocity. For the human research experiments and the majority of the other experiments, k, c and v_{ref} were 100 kNm/rad, 10 kNms/rad and 2 m/s respectively.

2.2.3. Tire-road forces

Tire road contact forces are calculated using an extended version of the Magic Formula. Tire deflection is calculated via road height input and tire position. The crown radius is accounted for and the tire model also incorporates camber thrust forces, which play an important role in motorcycle tire dynamics [3, 7]. The lateral camber thrust force component $F_{y,\gamma}$ for both the rear and front tire is calculated by

$$F_{y,\gamma} = -0.65F_z \arcsin(\gamma), \tag{2.3}$$

where γ is the camber angle, F_z is the tire force in vertical (z) direction and 0.65 is an experimentally determined value. Several tire properties are shown in Table 2.4.

Table 2.4: Some tire properties used in simulation of the motorcycle tire dynamics.

	Front ($F_z = 1184\,\mathrm{N}$)		**Rear** ($F_z = 1710\,\mathrm{N}$)	
	longitudinal	*lateral*	*longitudinal*	*lateral*
Stiffness	331.2 kN/m	150.47 kN/m	341.1 kN/m	150.47 kN/m
Slip stiffness	40.84 kN	69.28 kN/rad	64.29 kN	99.41 kN/rad
Relaxation length	61.57 mm	115.1 mm	94.28 mm	165.2 mm

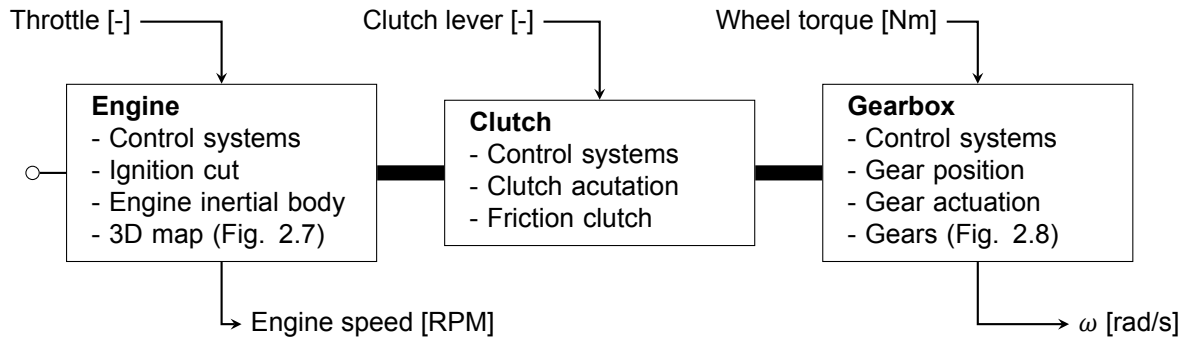

Figure 2.6: Drivetrain system. The thick black lines represent a Simscape SimDriveline connection between the three subsystems. The line to the left of the engine subsystem represents the mechanical connection to the revolute joint with the rear frame. Signals coming from the top are inputs, signals coming from the bottom of the subsystems are outputs.

2.2.4. Driveline

The motorcycle model uses a complex driveline modeled in Simmechanics SimDriveline, which is shown in Figure 2.6. Using throttle position and engine RPM as inputs, a 3D map is used to calculate the engine torque. Figure 2.7 shows the 3D engine map used in the model. Initially, an engine map for a car was used in the motorcycle dynamics. However, it was found that specifically engine braking was absent. Unfortunately, typical torque curves are often only measured with full throttle on a dynamometer making the development of a 3D engine map a difficult process. The full throttle curve is based on that of a real motorcycle. Half-throttle and no-throttle curves are guessed and entered by hand in the curve. With subjective evaluation the engine braking proved to be satisfactory. A normalized torque output of 1 corresponds to 96 Nm.

The crankshaft torque is controlled via several mechanisms such as ignition cut and engine cut and is then imposed on a Simscape driveline. The Simscape driveline uses a main clutch which is actuated by the rider and uses a control mechanism to determine among others ignition cut out. The next part in the driveline system is the gearbox. Via the gear position lever, the rider provides an input which goes through a gear control system. The gear control system actuates the synchromeshes (much stiffer versions of a normal clutch) which make the connection between different gear ratio blocks. Figure 2.8 shows how the gears with synchromeshes are modeled. The gearbox consists of six of these systems; one for each gear. When a gearshift takes place, the input signal changes from zero to one, engaging the synchromesh (clutch) of the new gear while simultaneously the previously engaged gear is disconnected. Finally, the driveline imposes motion on the wheel, and the tire road contact moments are imposed on the driveline in turn. Simply put, the driveline consists of the following elements:

- Engine with 3D torque map and control systems
- Clutch with control systems
- Gearbox with control systems

Most control mechanisms are implemented as S-functions. Table 2.5 shows the gear ratios used in motorcycle model, much like the Cruden spring damper subsystems.

2.2.5. Brakes

Both the front and rear brake are controlled independently. The brake signal is converted to a pressure signal, which is send to a Simulink S-Function which uses brake pressure, tire velocity, brake temperature, ambient temperature and brake force as inputs and outputs the brake force, brake moment, brake

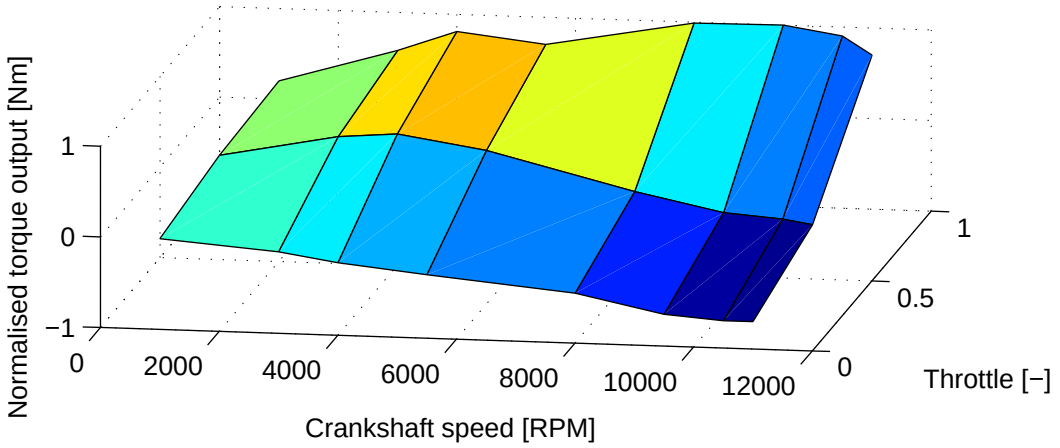

Figure 2.7: 3D engine torque map. Inputs to the torque map are crankshaft speed and throttle position. The output is normalized crankshaft torque.

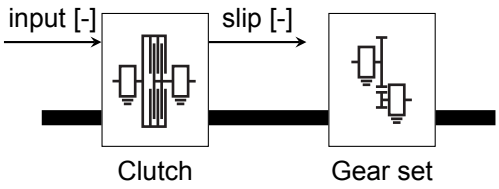

Figure 2.8: Model of single gear set with synchronizer in the Simmechanics SimDriveline Gearbox. The thick black line represents the SimDriveline connection.

Table 2.5: Gear ratios used in the Honda motorcycle model.

Primary	1st	2nd	3rd	4th	5th	6th
4.9524	2.4666	1.7647	1.4000	1.1818	1.0435	0.9683

friction and brake temperature. The brake system S-Function has been developed at Cruden and is used in several vehicle dynamics models where it has shown satisfactory results.

2.2.6. Aerodynamics

The aerodynamics are modeled according to

$$F = \frac{1}{2}\rho C_d A v^2, \tag{2.4}$$

where F is the aerodynamic friction force, C_d the coefficient of drag linearized at 0.4, A the frontal area at 0.7 m^2 and v the motorcycle's speed in m/s. ρ is calculated according to the general gas law

$$\rho = \frac{p}{RT}M, \tag{2.5}$$

where R is the gas constant, M is the mass of 1 mol of gas, p the atmospheric pressure and T the air temperature. In the simulation, the ratio $\frac{M}{R}$ is approximated as 3.46e-3 KJ^{-1}. Hence, the aerodynamic drag can be influenced by the external control of pressure and ambient temperature.

It is possible to decrease the frontal area and coefficient of drag using the pitch angle from the body tracking system, but for this research that feature has been disabled and constant coefficient of drag and frontal area are assumed.

2.2.7. Data logger

The data logger has no influence on the behavior of the motorcycle simulator. However, it does play an important role in saving data from the virtual motorcycle model during operation. All signals in the simulation can be logged at 100 Hz in single-precision floating-point accuracy.

2.3. Motion cueing

The rider experiences the motorcycle's mechanical motion in two ways: (1) the acceleration from the Stewart platform and (2) the movement of the handlebar. This section discusses how both systems are controlled. The visual motion perception is discusses in Section 2.5

2.3.1. Motion platform

Since a motion platform is limited by its workspace and dynamics, it is impossible to cue all accelerations exactly as experienced in a vehicle. Therefore, to have a user of a motion platform experience accelerations as good as possible, motion cueing algorithms are used [6]. To do this, acceleration, velocity and position signals coming from the vehicle dynamics model can either be scaled, filtered, or otherwise modified to keep the motion platform within its bounds. The motion cueing algorithm on the motorcycle simulator is based on a classical washout filter design, but with several modifications. Figure 2.9 shows a schematic of the motion cueing strategy. Here, DWM is short for Direct Workspace Management, an E2M propriety optimal washout method. This washout method uses a real-time optimization approach with a tunable penalization function. Note that, instead of sending reference acceleration signals for the roll and pitch angles, the angular positions are sent. As the pitch and roll angle of the motorcycle are bounded by its natural physical properties, the motion platform can cue these angles directly by making use of scaling factors. Motion cueing is handled by eMoveRT on the RealTime PC (Fig. 2.2)

Specific attention has been given on cueing of the roll angle. When riding a steady state corner on a bicycle, the vector combination of lateral acceleration a_y and gravity g pushes the rider right into the saddle. Unfortunately, a constant lateral acceleration a_y cannot be cued by a Stewart platform. This is why only the gravity vector g is discussed now.

When considering a motorcycle, two factors should to be taken into account: crown radius (Figure 2.10a) and upper body displacement (Figure 2.10b). Taking a closer look at Figure 2.10a reveals that, due to the crown radius, the contact point with the road is not exactly in the middle of the tire. To have g go through the contact point, the combined center of mass actually has to roll into the turn. On the other hand, when looking at Figure 2.10, the upper body displacement of the rider could also be accounted for. Suppose that a turn is negotiated, than g should go through the contact point. If the rider is hanging off of the motorcycle into the turn, than actually the difference $\phi - \phi'$ needs to be cued to have the real

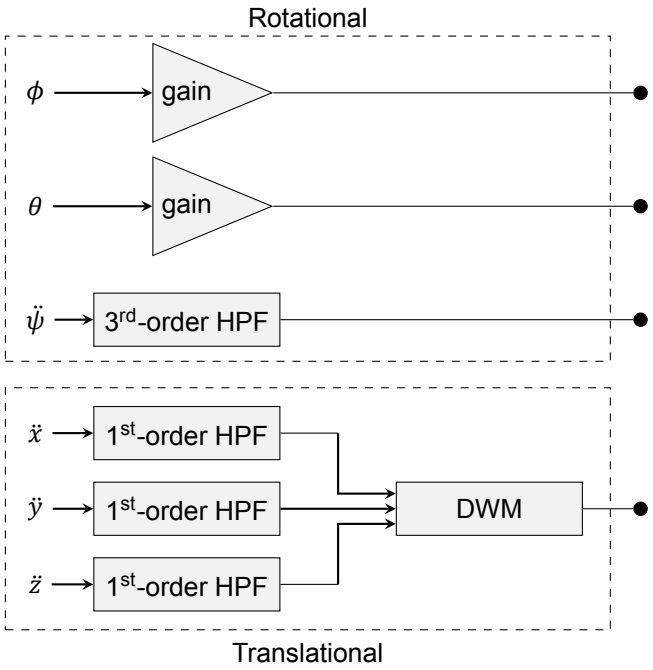

Figure 2.9: Schematic of the motion cueing strategy on the Cruden motorcycle simulator. Note that the roll (ϕ) and pitch (θ) are position reference signals and not acceleration reference signals like the other signals. HPF is short for high-pass filter and DWM is short for Direct Workspace Management.

gravity align with the virtual gravity vector (originated in M_{r+b}), resulting in the motorcycle simulator actually leaning out of the turn.

Practically, the roll cueing has been implemented as cueing a percentage of the motorcycle roll as defined by ϕ in Figure 2.10b. As a result, the initial roll moment corresponds to that of what would be experienced on a real motorcycle. In their research on motorcycle roll cueing, Shahar et al. showed that their participants also favored roll in turn cueing [29].

2.3.2. Control loader

The handlebar is the most important control mechanism for controlling a motorcycle. Therefore, correctness of it's dynamics are of great importance. With automotive and airplane simulators, steer angle or position is used as input for the control loader, and the output is a torque or force respectively. For the motorcycle simulator however, this causality is reversed and the rider's input is steering torque, where the control loader controls towards a handlebar angle. The E2M eMoveRT controller offers this possibility by making use of the jam-override control scheme in Figure 2.11. The virtual vehicle dynamics dictate the reference angle θ_{ref} for the handlebar. The jam-override control loop outputs a reference angle for the servo dynamics θ_{servo}. The limiter is programmed in any control loader system to ensure that no excessive forces can be generated which could eventually hurt or injure the user.

The jam-override systems is based on simple spring damper dynamics. The angle error $\theta_{ref} - \theta_{servo}$ is multiplied with spring stiffness k to obtain a virtual torque on an inertia of 1 kgm^2. The difference between this torque and a damping torque due to c is consequently limited for the servo dynamics. The extremes of this limiter can be manually changed. Following the two integrators, the limited torque is converted to a speed and reference angle again.

Ignoring the limiter and substituting $c = 2\zeta\omega_0$ and $k = \omega_0^2$, the transfer function

$$\frac{\theta_{serv}(s)}{\theta_{ref}(s)} = H(s) = \frac{\omega_0^2}{s^2 + 2\zeta\omega_0 s + \omega_0^2} \tag{2.6}$$

is obtained. Here, s is the Laplace complex variable. This transfer function is in fact a second order filter where the corner frequency is given by ω_0 and the damping by ζ. These two variables can be modified externally, like the limiter extremes.

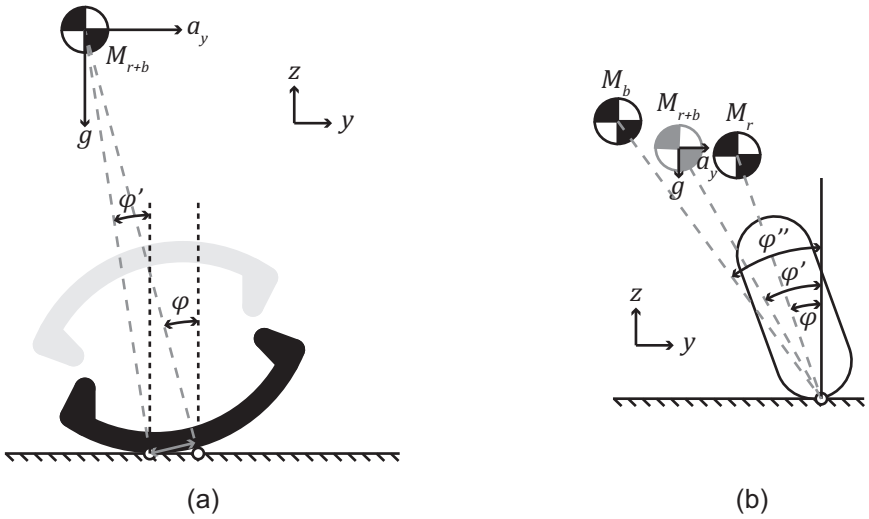

Figure 2.10: (a) shows a representation of a motorcycle tire with large crown radius and the physical contact point of the tire under lean angle. (b) shows a motorcycle under lean with the centers of mass for the rider M_b and rear frame M_r. The combined center of mass is given by M_{r+b}. Different interpretations of lean are given by ϕ, ϕ' and ϕ''.

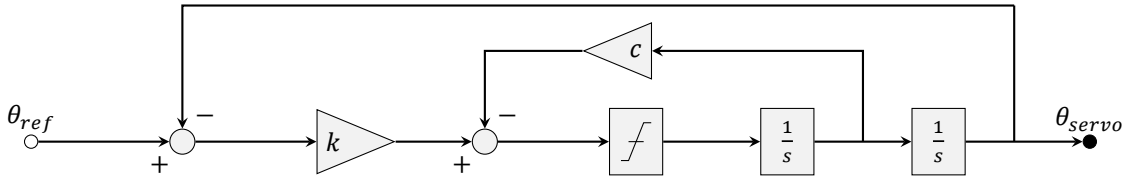

Figure 2.11: Block diagram representing the jam-override control scheme containing gains, sums, integrators and a limiter block.

2.4. Upper Body Tracking

For the upper body tracking, two Intel RealSense SR300's are used [38]. These cameras use coded light, also known as structured light to estimate 3d features at a distance from 0.2 m – 1.5 m. Each camera features a full 1080p color camera at 30 frames per second to reconstruct hand gestures, shapes or facial features. Using data from both camera's, the upper body position from the rider is estimated with software developed by Cruden. Finally, Simulink receives signals with the longitudinal and lateral position and the pitch of the rider's body. For the experiments described in this thesis, only the lateral displacement of the upper body has been used, practically reducing the model order to 14-DoF.

To further illustrate the implementation of the planar joint as described in Section 2.2, one can image the rider's center of gravity m_b to move frictionless along a prismatic line in the y-direction of the motorcycle (Figure 2.12) as no longitudinal displacement is present. Since m_b is free to move along the y-axis, no reaction moments $\vec{M}_z$ and $\vec{M}_y$ are created due to moving the upper body. Only the gravity vector $\vec{F}_z$ creates a torque as a result of upper body displacement.

$$\vec{M}_x = \vec{\delta} \times \vec{F}_z \tag{2.7}$$

around the x-axis.

2.5. The Visual System

An Oculus Rift is used to provide the rider with visual cues. Some important aspects of how the Rift is set up are discussed in this section. The Oculus Rift uses two different systems to track the user's head position. The first system is called the constellation sensor, which is in fact an infrared sensor. Embedded inside the Rift are a number of infrared LEDs, which can be tracked by the constellation sensor. The second system is located inside the Rift self, featuring a magnetometer, a gyroscope and an accelerometer. At 1000 Hz, information from these sensors is combined to estimate the acceleration

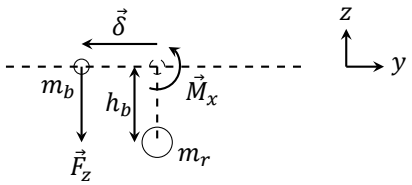

Figure 2.12: Example of how only gravity, due to the rider upper body mass m_b, creates a torque on the motorcycle frame m_r. To keep a distinction between torque and mass, the masses in this figure are lower case.

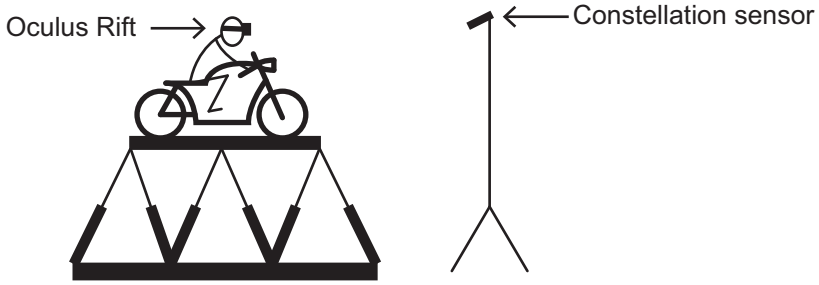

Figure 2.13: The constellation sensor is fixed in the real world. The Oculus Rift is worn by the rider on the motorcycle simulator.

of the Rift. Combining the information from the constellation sensor and the systems inside the Rift, the Oculus software is able to give an accurate estimation of the 6-DoF motion of the Oculus Rift in the real world. Figure 2.13 shows how the constellation sensor is positioned in the real world.

The Panthera Software, which will be discussed in more detail in Section 2.6, accounts for the motion of the Stewart platform. By calibrating the Oculus Rift if the motion platform is engaged but in resting state, the head position of the user can be accurately estimated. All translations and rotations from the motion platform are consequently compensated for as such that the visuals send to the Oculus Rift correspond to where the user's head is in the virtual world.

To take a constant roll angle of 32° as an example, the motion platform cues 7° of roll and the Oculus Rift's horizon cues the complete 32° (Figure 2.14). Note that the Rift cues 32° because it is level with respect to the motion platform. If the user would keep his head level with respect to the earth, the horizon displayed in the Rift would be $32^\circ + 7^\circ = 39^\circ$. To further illustrate this example, if the rider would actually align his vision with the Rift's horizon, he would in fact lean out of the turn on the simulator with a roll angle of $7^\circ - 32^\circ = -25^\circ$ in the real world.

In case the roll angle would be cued 1:1 at 32°, or on the other hand not at all, and the rider would sit upright along the motion platform's local z-axis, the same visuals would still be presented at 32°. In short: the visual roll cueing is independent of the physical roll cueing.

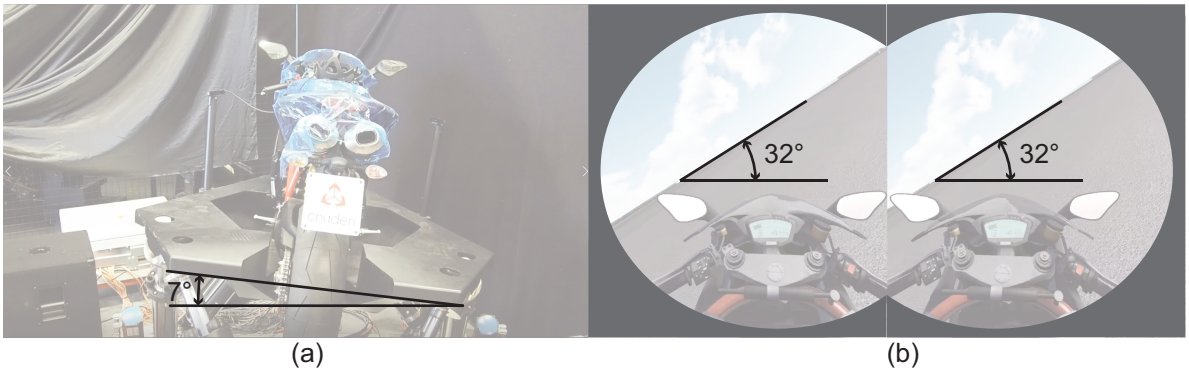

Figure 2.14: Roll cueing with the Stewart platform and the Oculus Rift. The Oculus Rift cues the complete roll angle (b), whereas the motion platform only cues a percentage (a).

2.6. Cruden Panthera software

The software developed by Cruden that integrates the vehicle dynamics, vision, audio and motion platform control is called Panthera. The Panthera software runs on all PC's in Figure 2.2 except for the E2M RealTime PC. For the motorcycle simulator specifically, a Dynamic Link Library (DLL) file is build from the Simulink vehicle dynamics model. Panthera consequently uses this DLL file to run simulations on the Master PC. Several tasks Panthera takes care of are:

- Generating visuals
- Generating audio
- Simulation control
- Session managing: a GUI for operating the simulator
- Communication with the slave PC's from the operator PC
  - Master PC (runs simulation)
  - Spectator PC (shows cinema-like real-time footage)
  - Logger PC (logs real-time data)
  - E2M real-time PC (controls the motion platform)
- Sensor reading/fusion

An important feature of Panthera is that all signals first have to pass through it. One of the problems that often arises with motion simulation and vehicle simulation in general is that 0 velocity simulation is problematic because of division by 0. Panthera avoids this problem by dividing by a small number $\neq 0$ instead, to ensure that no numerical singularities terminate simulation. Also, road roughness and road height calculation is done by Panthera, among several other tasks to ensure smooth simulation.

Finally, sound generation is another important aspect taken care of by Panthera. Simulink sends several signals among which vehicle velocity, engine RPM, gearbox signals and brake signals to Panthera. The engine RPM signal is for example used to modulate the engine noise. Gearbox and brake signals, which are often booleans, are used to trigger short audio fragments like, for example, the sound of a gear shift. Velocity is used as input for the magnitude of wind noise.

3

Motorcycle Dynamics Evaluation

Correct motorcycle dynamics play an essential role in simulating a motorcycle. In this chapter, the methods used for evaluating the dynamics of the motorcycle are explained. The results of the motorcycle dynamics analysis are shown and afterwards discussed.

3.1. Method

In this section, it is explained how an eigenvalue identification method was used to identify the motorcycle model's eigenvalues using specific identification maneuvers. Besides the eigenvalue identification method, steer torque step inputs have also been used to show the motorcycle's response in the time domain.

3.1.1. Eigenvalue identification

According to Limebeer and Sharp, capsize, weave and wobble are the most important eigenmodes of a motorcycle [20]. If it can be shown that these eigenmodes are present, it can be concluded that the motorcycle dynamics are correct. Since a multibody dynamics modeling approach is used in this research, the eigenvalues cannot be easily extracted from linearized state equations. A general way of obtaining linearized state equations form a Simulink model is using `linmod`. This method is unfortunately not robust enough to be used on the motorcycle dynamics model. For that reason, a similar approach as by Kooijman, Schwab and Meijaard was used to find the eigenvalues of the motorcycle [19]. This method utilizes the fact that the set of linear state equations

$$\dot{\mathbf{x}}(t) = \mathbf{A}\mathbf{x}(t), \tag{3.1}$$

where $\mathbf{x} \in \mathbb{R}^{n\times 1}$ and $\mathbf{A} \in \mathbb{R}^{n\times n}$ and has solutions in the form

$$\mathbf{x}(t) = c_1 e^{\lambda_1 t}\mathbf{u_1} + c_2 e^{\lambda_2 t}\mathbf{u_2} + \ldots + c_n e^{\lambda_1 n}\mathbf{u_n}, \tag{3.2}$$

has eigenvalues $\lambda_1, \lambda_2, \ldots, \lambda_n$, eigenvectors $\mathbf{u_1}, \mathbf{u_2}, \ldots, \mathbf{u_n}$ and arbitrary constants $c_1, c_2, \ldots, c_n$. Suppose that a complex conjugate eigenvalue pair

$$\lambda_{1,2} = a \pm bi \tag{3.3}$$

is of interest. Then a solution in the form

$$y(t) = e^{at}[c_1 \cos(bt) + c_2 \sin(bt)] \tag{3.4}$$

exists. Next, suppose that it is possible to measure $y(t)$ in the direction (or close to that) of its eigenvector, than the eigenvalues can be determined using a parameter fit method. For this approach, a parameter fit function in the form of

$$\dot{\phi} = c_1 + e^{dt}[c_2 \cos(\omega t) + c_3 \sin(\omega t)] \tag{3.5}$$

for the capsize mode and a fit function in the form of

$$\dot{\phi}/\dot{\delta} = c_1 + e^{d_1 t}[c_2 \cos(\omega_1 t) + c_3 \sin(\omega_1 t)] + e^{d_2 t}[c_4 \cos(\omega_2 t) + c_5 \sin(\omega_2 t)] \tag{3.6}$$

for the weave ($\dot{\phi}$) and wobble ($\dot{\delta}$) mode were used. Here, $\dot{\phi}$ corresponds to the roll rate and $\dot{\delta}$ to the steer rate. The steer and roll rate were used as it is supposed that these are close to the eigenvectors corresponding to capsize, weave and wobble [18, 19].

For the parameter fit function itself, MATLAB's nonlinear multidimensional optimization function `fminsearch` has been used. The implementation of this function in this research aims to minimize the 2-norm between a measured time signal and either Equation 3.5 or 3.6 by varying the constants c_x, damping values d_x and frequency values ω_x.

The starting vector and time window play an important role for the optimization function. Here, the method was to find a starting vector which gave good results for the lowest speed experiment. The final solution obtained here would be the starting vector for a higher velocity maneuver. For the capsize motion, the time frame was the total length of the experiment. For the weave and wobble motion, the time frame was at least 0.6 s.

3.1.2. Identification maneuvers

To gather data to be used in the identification procedure, several simulations have been conducted. The general procedure was to generate a model with specific properties like initial speed and a predefined maneuver, and to run this model in Cruden's virtual environment. Data during the simulation was logged and could afterwards be analyzed in MATLAB. A P-control speed controller with deadzone of ± 0.2 m/s was used to keep the motorcycle at the prescribed speed.

For the capsize eigenmode identification, the motorcycle was just initialized in the virtual world with an initial speed. After a short period of time, the motorcycle would start to lean over to one side. Speeds of 0-40 m/s in increments of 5 m/s were used to generate data.

For the weave and wobble eigenmodes, a steer torque (in [Nm])

$$T_\delta(t) = \begin{cases} 0 & \text{if} \quad t < 5.1 \\ 10 & \text{if} \quad t = 5.1 \quad \text{and} \quad t < 5.2 \\ 0 & \text{if} \quad t \geq 5.2 \end{cases} \tag{3.7}$$

was used to excite the motorcycle and induce the vibrational modes of interest. For the weave and wobble, speeds of 5-50 m/s with 5 m/s increments were used to generate the data.

3.2. Results

To demonstrate the non-minimum phase behavior, Figure 3.1 shows the time history response behavior of two step steering torques. In both cases, the transient from a negative to positive steering angle can be observed for a negative steering torque. The same behavior holds for the lateral displacement, showing a transient from positive lateral displacement to negative lateral displacement.

As described in Section 3.1.1, the second step of evaluating the motorcycle simulator was by validating its dynamics model and retrieving its eigenvalues. Figure 3.2 shows an example of how the function fit has performed for a weave maneuver and a capsize maneuver. In both cases, it can be observed that the function fit curve almost exactly overlaps the data. If the capsize figure is observed closely, it can be seen that the blue line appears thicker than for the weave figure. This is the result of a noisier data signal, which has been blurred slightly by the thickness of the blue line. Nevertheless, the unstable and slow capsize behavior can easily be derived from this data. Interestingly, one can see in the weave figure that the roll rate does not return to zero. This is in fact correct, as the slow unstable capsize starts to manifest itself at this point and the roll rate will only keep decreasing over a longer period of time. However, choosing a longer time window makes it harder for the optimization function to find a good fit.

Unfortunately, not all function fits have shown good results. For example, it proved not to be possible to identify the wobble mode using the steer rate nor the roll rate. Figure 3.3 shows a curious difference between the identification maneuver at 25 m/s and 30 m/s, as the latter shows a high frequency oscillation. This same behavior is observed for 10, 15, and 35 m/s, but not for 20, 25, 40, 45 and 50 m/s. In any case, the function fit was able to find a parameter match for the data, but as the

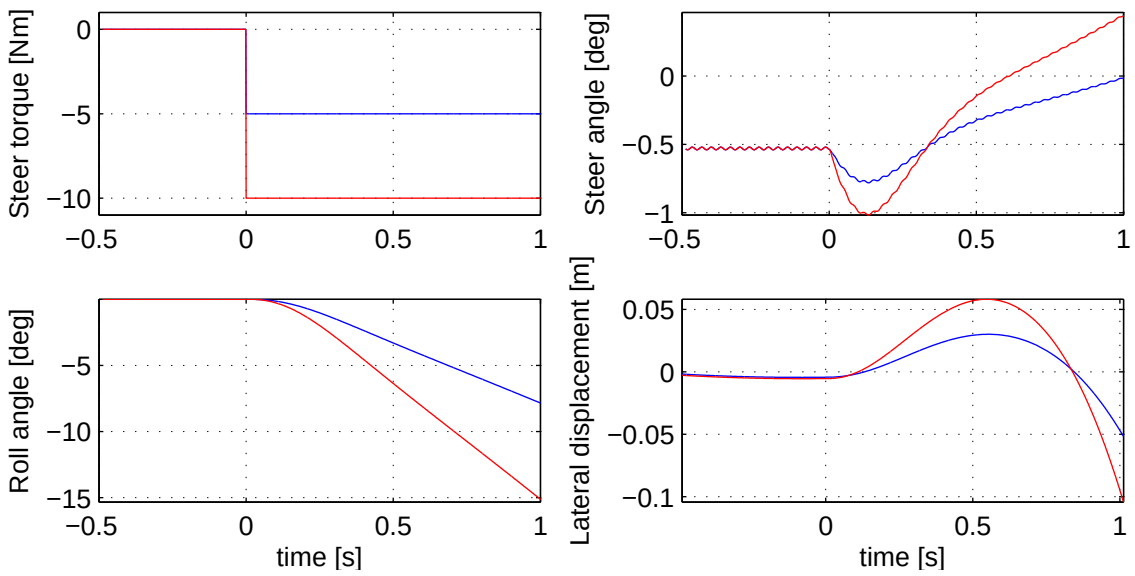

Figure 3.1: Steering torque step input effects on the motorcycle's behavior (blue -5 Nm, red -10 Nm). The top left plot shows the steering torque step, the top right input the handlebar angle, the bottom left shows the roll angle and the bottom right shows the lateral displacement as a consequence of the step torque input.

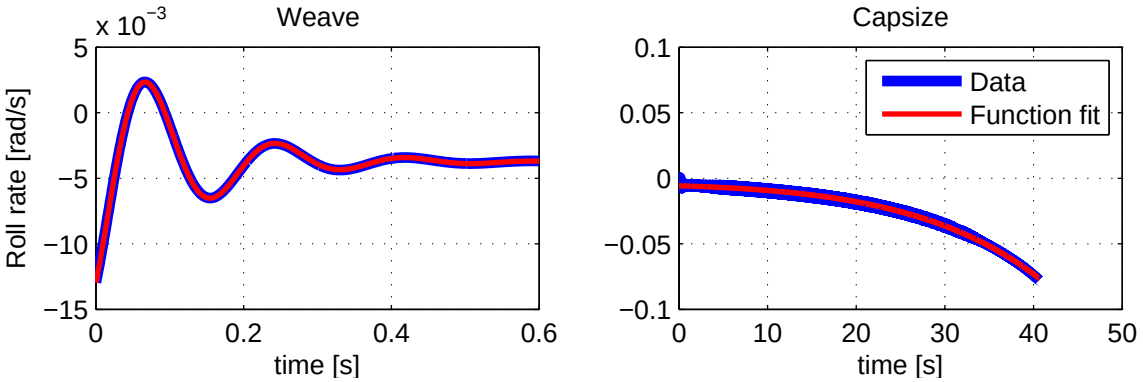

Figure 3.2: Examples of how the function fit has performed. Left: weave motion function fit (50m/s). Right: capsize motion function fit (10m/s).

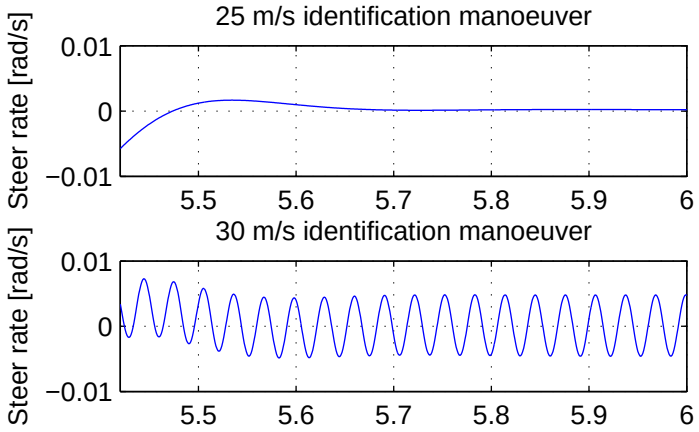

Figure 3.3: System response to the steer input on the steer rate. The response for 30 m/s shows a high frequency component, but the data for 25 m/s does not.

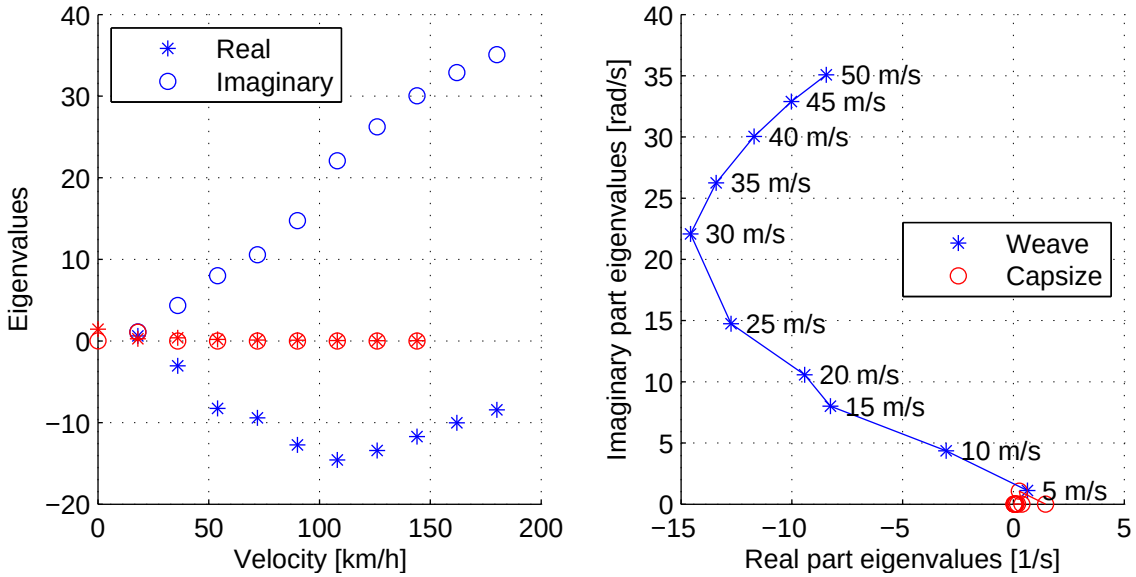

Figure 3.4: Eigenvalues of the Honda motorcycle model. The left figure shows the real and imaginary eigenvalues as function of speed. The figure on the right shows a root locus plot with increasing velocity for the weave mode.

high frequency component was so different per dataset, no conclusive data could be generated for the wobble mode.

Figure 3.4 shows the eigenvalue and root locus plot of identified eigenvalues of the Honda motorcycle dynamics model and Table 3.1 shows the specific data points. The capsize eigenmode has a small positive real part for al speeds, and an imaginary part close to 0. This behavior can also be seen in Figure 3.2 for the capsize mode, where the small positive real part results in a long time constant for the motorcycle to tip over.

The weave eigenmodes show an decrease in real part until a speed of around 30 m/s. At higher speeds, the motorcycle dynamics show an increase in the real part eigenvalue, resulting in decreased damping for the wave mode. For all speeds, it can be observed that the imaginary part of the eigenvalues increases for the weave mode. This corresponds to findings in literature [20].

3.3. Discussion

The most important observation from the motorcycle dynamics identification results is that the weave mode shows a similar curvature but with other values as described by Sharp and Alstead, from which

Table 3.1: Results from the eigenvalue identification procedure for the Honda motorcycle model.

Capsize			**Weave**		
v [m/s]	d [1/s]	ω [rad/s]	v [m/s]	d [1/s]	ω [rad/s]
0	1.45	0.01	5	0.63	1.11
5	0.38	1.14e−7	10	-5.46	0.96
10	0.38	1.15e−7	15	-8.25	8.00
15	0.18	1.19e−10	20	-9.42	10.57
20	0.20	2.18e−5	25	-12.74	14.74
25	0.10	2.49e−6	30	-14.74	22.08
30	0.20	2.18e−5	35	-13.42	26.24
35	0.04	1.04e−6	40	-11.70	30.05
40	0.03	2.23e−6	45	-10.01	32.90
			50	-8.46	35.72

the majority of parameters were taken [31]. In fact, more literature shows an increase of the imaginary part of the eigenvalues for increasing speed and in initial decrease of the real part of the eigenvalues followed by an increase in these positive eigenvalues from a certain velocity [7, 18, 20]. However, the magnitude of reported eigenvalues differ some from author to author. For the real and imaginary parts, extreme eigenvalues of -5 to -15 1/s and 20 to 30 rad/s respectively are reported [7, 20, 31]. However, it is obvious that this is mainly dependent on the parameters used in their respective motorcycle dynamics models. This is also the reason for the eigenvalues in Figure 3.4 not corresponding exactly to those reported in Sharp and Alstead: many properties are different among which tire dynamics, pitch dynamics and the rider body dynamics [31].

The capsize eigenmode in Figure 3.4 shows the same unstable behavior over the complete speed range, with decreasing negative part as the speed increases. Similar behavior has been shown by Sharp and Alstead, but in their research, the capsize eigenmode is initially stable [31]. Again, the discrepancy in this behavior could be explained by the difference in tire dynamics and other model changes.

Unfortunately, it has not been possible to identify the wobble eigenmode. It is unknown where the difference in the time-domain signals comes from with respect to the high-frequency oscillations observed in Figure 3.3. Possible sources could be numerical instability occurring only for specific velocities of the motorcycle dynamics model, instabilities of the dynamics model where the eigenfrequencies only get excited at certain velocities due to suspension elements or unknown influence(s) of specific damping characteristics. An attempt was made to log the signals at 1000 Hz to see if this enhanced the identification of a high frequent strongly damped sine wave, but no clear difference could be observed. Another possible explanation would be that the wobble eigenmode is highly damped and that the time window used was unfit for identification, but literature suggests otherwise, and it would be problematic for the function fit algorithm to fit a third oscillation on top of the weave motion and the unstable high-frequency oscillations [20, 31]. A final problem could have been that the identification maneuver was unable to excite the wobble correctly. This is however unlikely, as a steer torque input signal is closely parallel to the eigenvector of the wobble eigenmode.

For almost all identification maneuvers, the function fit algorithm was able to find the parameters to get a good fit. There was only one exception for the 5 m/s weave estimation, as the roll rate curve was more complicated than could be fit. However, by manual iteration of the starting vector yielded acceptable results in the end.

Showing that the eigenmodes of the motorcycle dynamics correspond to those reported in literature is, however, no conclusive proof that the motorcycle dynamics model behaves as a real motorcycle. To reach this goal, validation with respect to real-life data should be performed. Unfortunately, validation using a real motorcycle is an expensive and time consuming process. Development of an instrumented motorcycle, finding a test track and having a test rider perform specific maneuvers are just some of the tasks that would have needed to be fulfilled in order to obtain the experimental data. Otherwise, motorcycle manufacturing companies are reluctant to share their data. Therefore, validation using real-life telemetry was outside of the scope of this thesis.

Furthermore, where most of the motorcycle dynamics model's properties have been taken from Sharp and Alstead, the tire dynamics are mostly based on a tire properties set not specifically designed

for a motorcycle [31]. At the same time, tire dynamics play an extremely important role on vehicle dynamics [23]. Comparing the tire parameters listed in the tire properties table, Table 2.4, with figures reported by de Vries and Pacejka, it can be seen that the slip stiffnesses are moderately higher and the relaxation lengths shorter [7]. This might explain the relatively high frequencies for the weave mode, and the absence of the wobble mode. Pacejka has specifically shown that a decrease in the front and rear relaxation lengths stabilizes the wobble mode [23, p. 533]

4

Motion Platform

The motion platform consists of two dynamic systems: the Stewart platform and the steering control loader. To provide accurate cues to the user, both systems need to function within their intended design and requirements. This chapter describes the methods to evaluate the steering control loader and the Stewart platform. Results from the experiments are shown and afterwards discussed.

4.1. Method

In this section, the methods for the steering assembly frequency response analysis and Stewart platform analysis are explained.

4.1.1. Steering assembly frequency response analysis

During initial evaluation of the motorcycle simulator, the steering behavior was found not to be satisfactory. To obtain an objective measurement on the steering assembly behavior, a frequency response analysis was carried out. Input and output data is collected using the e2m software at 1000 Hz. Some of the recorded signals include steering reference angle, steering angle, steering torque and motor current. A specific input sequence for the reference angle is sent from the motorcycle model to the controller. Two approaches for input sequence were chosen. The first approach was a chirp signal, ranging from 0.5 Hz to 40 Hz. A chirp signal is a sinusoidal signal with increasing frequency. By using this signal, it is expected that all frequencies of the system are excited. The second approach uses a Gaussian uniformly distributed random number, also known as white noise, as this has a constant spectral density and should excite all system frequencies too. During initial experiments, it was found that the white noise required a too large control input. Therefore, a second order filter was implemented on the white noise signal in the form of

$$H(s) = \frac{1}{(\tau s + 1)^2}, \tag{4.1}$$

where τ is an arbitrary constant, resulting in a colored noise input signal.

Next, the input and output response could be compared in the frequency domain. Using the fast Fourier transform (FFT), the Fourier transform of the input and output data can be obtained. Let $X(j\omega)$ and $Y(j\omega)$ be the input and output Fourier transforms respectively, the complex frequency transfer function

$$H(j\omega) = \frac{Y(j\omega)}{X(j\omega)} \tag{4.2}$$

is obtained. Taking the absolute value $|H(j\omega)|$ and the angle $\angle H(j\omega)$ yield the magnitude and phase of the complex transfer function respectively and can be used to generate a Bode plot.

A more advanced method of transfer function estimation relies on the Signal Processing Toolbox from MATLAB®. The function `tfestimate(x,y,window,..,Fs)` uses among others input data `x`, output data `y`, a window function `window` and the sampling time `Fs` in Hz to calculate the relationship

between the cross power spectral density P_{yx} of `x` and `y` and the power spectral density P_{xx} of `x` [40]. This relationship is given by

$$H(j\omega) = \frac{P_{yx}(j\omega)}{P_{xx}(j\omega)}. \tag{4.3}$$

Welch's averaged periodogram method is used by MATLAB to estimate the power of the signals, making the transfer function estimation less sensitive to noise compared to using Equation (4.2). As window function, a symmetric N-point Hanning window is used and is created by the function `hanning(N)`. The magnitude and phase are constructed the same way as mentioned before. Using `mscohere(x,y,window,..,Fs)`, the magnitude squared coherence estimate can be found, which indicates how well `x` corresponds to `y`.

The control algorithm of the handlebar angle uses a spring-mass damper system, see Section 2.3.2. When it was found that the handlebar response behavior was not satisfactory, the bandwidth of the control loop had been increased by changing ω_0 from 15 rad/s to 500 rad/s. Both settings were evaluated in the scope of this research. The damping of both systems has remained unchanged at ζ = 0.7 [-].

4.1.2. Stewart platform analysis

A similar approach as for the control loader identification has been used for the Stewart platform. Besides the frequency response identification, also four maneuvers were simulated to compare time-series plots. In stead of using a chirp or white noise function as has been done with control loader identification, the platform was excited at specific frequencies from 1 to 20 Hz in steps of 1 Hz with a pure sine function with an amplitude of 1 m/s^2 for translations and 0.7 rad/s^2 for rotations. This sine function imposed a reference acceleration on all six degrees of motion individually (surge, sway, heave, roll, pitch, yaw). Also here, `tfestimate` was used to obtain the frequency domain characteristics.

For the Stewart platform, also time domain analysis was performed. With the time domain analysis, the motion cueing scaling factors could be retrieved. Also, an intuitive evaluation of the capability to simulate the eigenmodes could be done. Four different automated maneuvers were executed on the simulator. The first three maneuvers are closely related to the identification maneuvers in Section 3.1.2 and were done for 10, 30 and 50 m/s. The fourth maneuver aims at simulating slower dynamics by imposing a reference lean angle

$$\phi_{ref}(t) = \begin{cases} 0^\circ & \text{if} \quad t < 20 \\ 30^\circ & \text{if} \quad t \geq 20 \quad \text{and} \quad t < 25 \\ 0^\circ & \text{if} \quad t \geq 25 \quad \text{and} \quad t < 30 \\ -30^\circ & \text{if} \quad t \geq 30 \quad \text{and} \quad t < 35 \\ 0^\circ & \text{if} \quad t \geq 35 \end{cases}. \tag{4.4}$$

A PI-controller minimizes the error between ϕ_{ref} and ϕ by controlling the steer torque T_d.

Contrary to the steering assembly analysis, for the motion platform, no actual sensors are available to measure the signals. However, using a state observer developed by E2M, the states of the motion platform can be estimated rather accurately by measuring the motor torques and feeding the leg extensions through a kinematics model. The observer assumes a stiff top-platform. In E2M commander, a graphical user interface developed by E2M for diagnostics purposes, these signals can be found under the denominator *backward kinematics*. For this experiment, the backward kinematics signals were logged and assumed to be the signals measured on the motion platform for position, velocity and acceleration.

4.2. Results

This sections shows results obtained with respect to the motion platform for the steering assembly and Stewart platform analysis.

4.2.1. Steering assembly

Figures 4.1 and 4.2 show the obtained results for the steering assembly frequency response analysis. It can clearly be seen that the increase of bandwidth of the jam override handlebar angle control algorithm increased the system's performance. From the magnitude plot in Figure 4.1 it can be seen that the

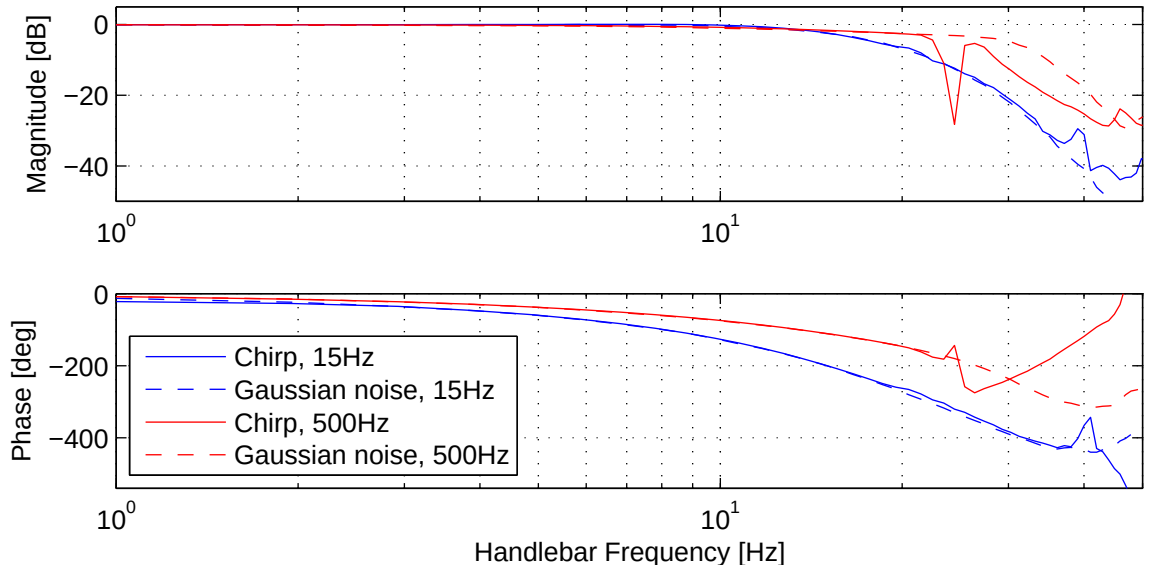

Figure 4.1: Bode plot from reference angle to achieved angle. The blue signals are achieved with a jam override frequency of 15 Hz and the red signals are obtained with a jam override frequency of 500 Hz.

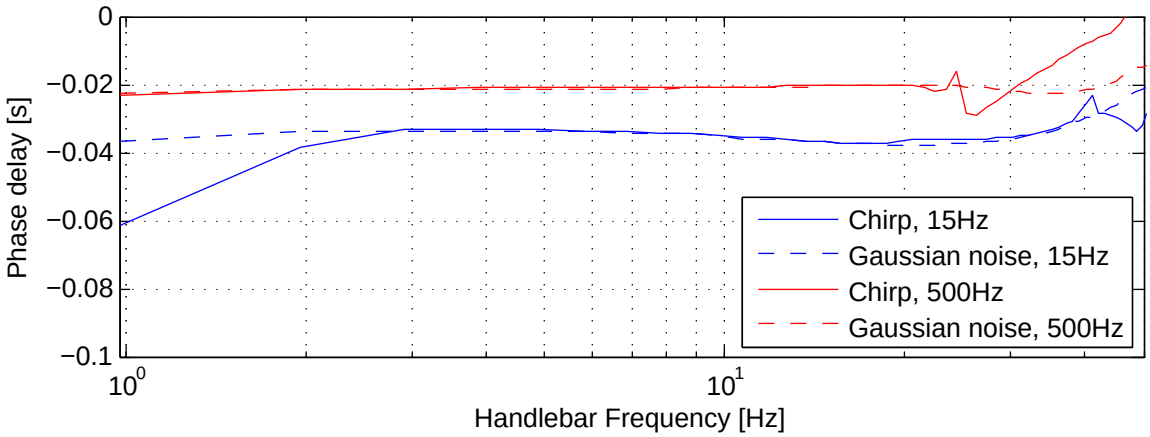

Figure 4.2: Phase delay plot from reference angle to achieved angle. The blue signals are achieved with a jam override frequency of 15 Hz and the red signals are obtained with a jam override frequency of 500 Hz. The sweep signals are obtained with the Gaussian distribution excitation.

bandwidth has increased from approximately 20 Hz to approximately 30 Hz. From Figure 4.2 it can be observed that the phase delay has been decreased with approximately 13 ms, or almost forty percent.

The coherence plot from figure 4.3 shows how well the complex transfer function has been estimated. In all cases, up to 20 Hz good coherence can be observed. However, the Gaussian noise excitation signal shows better coherence at higher frequencies. An interesting dip in the transfer function can be observed at 25 Hz for the chirp excitation for the jam override frequency of 500 Hz.

4.2.2. Stewart platform

Figure 4.4 shows the bode plot for the motion platform identification procedure. It can be seen that until 10 Hz, the magnitude remains under 2.5 dB and that the phase shift remains above approximately 10 deg. Around 11 to 12 Hz, a first natural frequency peak can be observed for the surge and sway, and to a lesser extend for pitch. At 18 Hz, the first natural frequency peak for heave can be seen.

Figure 4.5 shows the simulator's performance for the slalom maneuver as defined in Section 4.1.2. One of the first observations is that for roll angle, rate and acceleration, the scaling as described in Section 2.3 can clearly be seen and corresponds to roughly 22 percent. The acceleration signals are noisier than the position and velocity signals for roll, but still it can be seen that the motion platform is

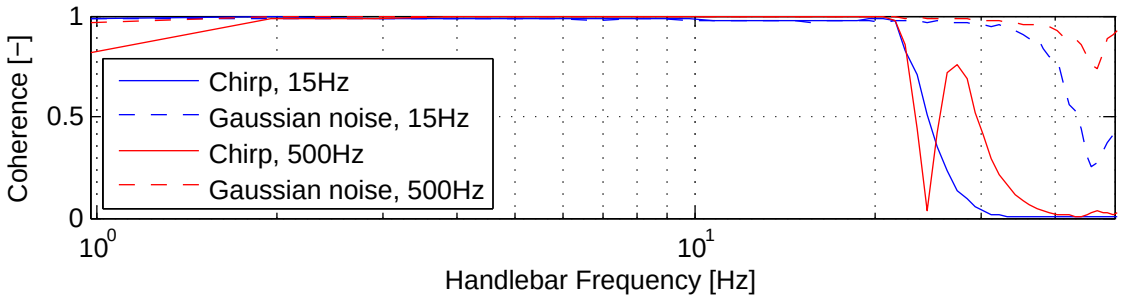

Figure 4.3: Coherence plot for the complex transfer function of reference angle to achieved angle. The blue signals are achieved with a jam override frequency of 15 Hz and the red signals are obtained with a jam override frequency of 500 Hz. The sweep signals are obtained with the Gaussian distribution excitation.

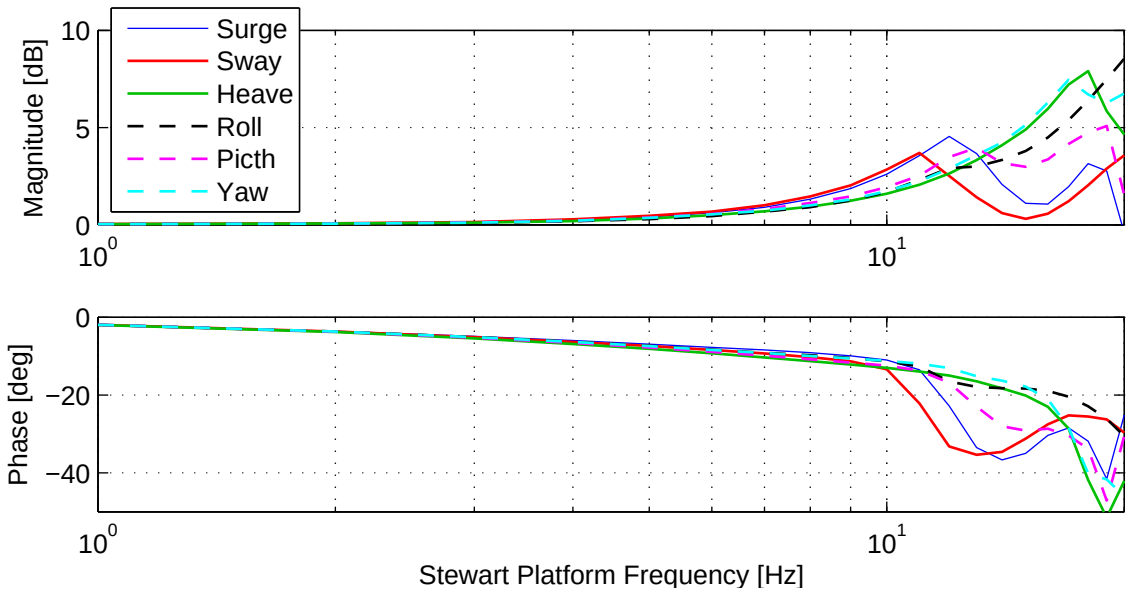

Figure 4.4: Bode plot for acceleration inputs for all 6-DoF of the motion platform. Translational and rotational motion are shown in solid and dashed lines respectively

able to simulate the model reference signal. Due to the noisy nature of the acceleration signals, it is hard to find the time delay between the peaks from the model reference to the backward kinematics signals. But when zooming in closely to the peaks it can be observed that this delay is roughly 20-40 ms for roll, pitch and yaw accelerations.

Figure 4.6 shows the identification maneuver for 30 m/s. Again, especially for the roll angle, the roll cueing scaling factor can clearly be seen. It is however not apparent that the platform's roll acceleration follows the reference signal correctly. Even more so, the pitch acceleration seems to be very noisy compared to the reference signal. Contrary to that, the yaw rate shows close correspondence, apart from a small time delay, which is around 20 ms.

4.3. Discussion

It has been shown that control system with the observer bandwidth of 500 Hz yielded the best results for the steering assembly. Not only did it decrease the phase lag, but it also increased the bandwidth of the system. The coherence plot shows that the results are reliable up to a little bit over 20 Hz. Apparently, exciting the system with a random Gaussian signal yields more robust results. Finally, testing has not showed any negative effects with respect to the stability of the handlebar actuation for the increased observer bandwidth.

In research on the effect of latency, Jay and Hubbold show that a haptic delay of more than 200 ms harms performance but that a delay on visual cues is more disastrous [15]. However, Cruden considers 200 ms delay as unsatisfactory slow. Nevertheless, with a phase delay of approximately 20 ms and a bandwidth of more than 20 Hz, the handlebar system should be able to simulate the steering feel of a motorcycle.

Although the wobble eigenmode could not be identified, literature has reported this value to be between 5-13 Hz, which is still within the limits of the handlebar's capabilities [20]. Using a smaller simulation time step, different model properties or even another modeling approach are just a few examples which can change the motorcycle dynamics enough to solve the absence of wobble.

The results from the Stewart platform identification have shown that the platform is indeed capable of simulating the motorcycle dynamic's motion. Since the maximum eigenvalues shown by the weave eigenmode at 50 m/s (Figure 3.4) have a frequency component of 35 rad/s, or 5.57 Hz, and it has been shown that the motion platform can accurately simulate motion up to at least 10 Hz, it can be assumed that the motion platform is capable of accurately simulating the weave motion of the motorcycle.

It should be noted however that there was no person sitting on the motorcycle simulator at the moment of the frequency tests. A person sitting on the simulator inevitably adds to the inertia and weight, and decreases the performance of the platform. On the other hand, the motion platforms are usually bolted to the workshop floor to form a rigid connection to te ground. Since this motorcycle simulator is a prototype and has to be moved through the workshop from time to time, the motion simulator has only been bolted to the ground with one bolt which decreases its stiffness and thus its performance.

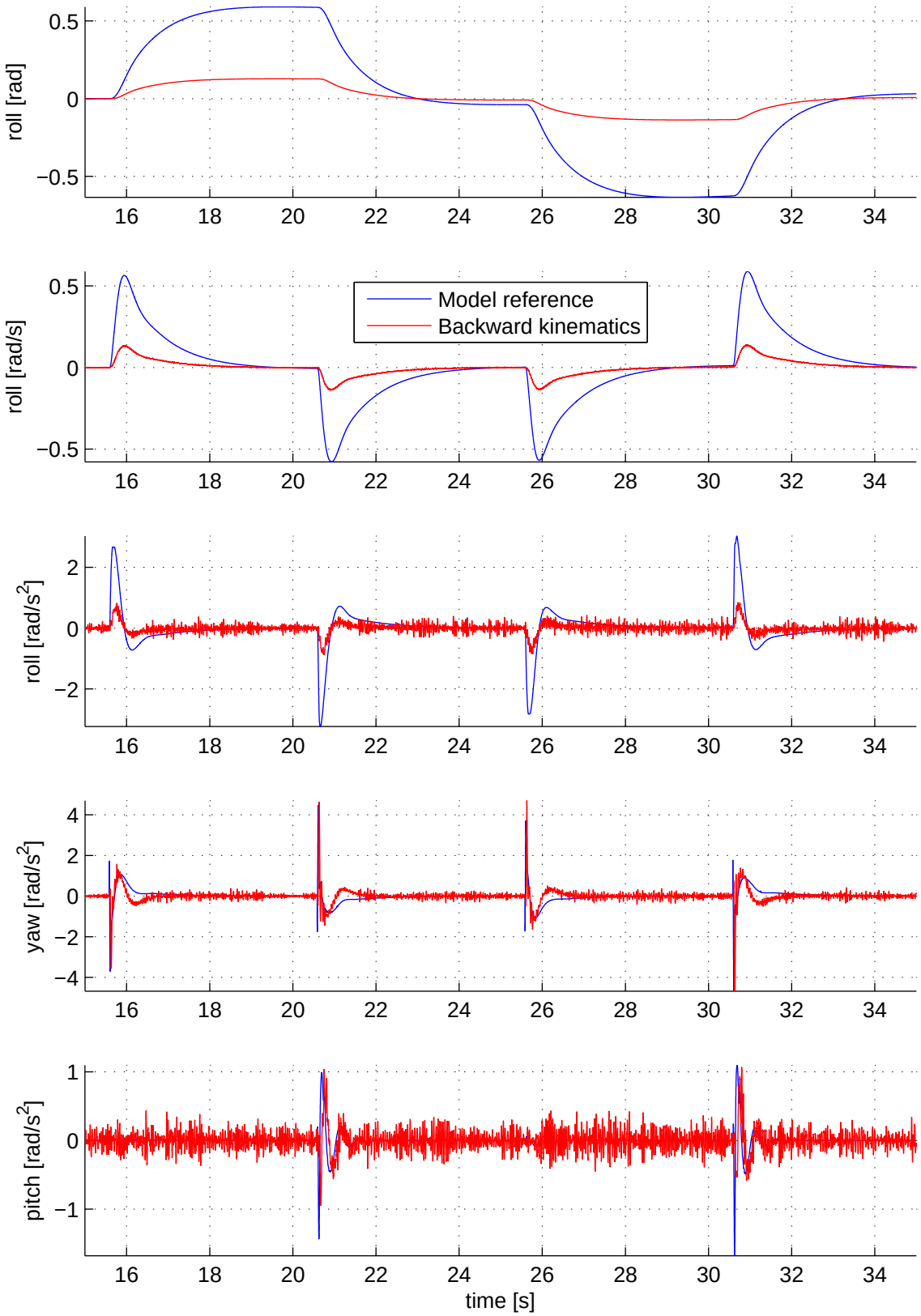

Figure 4.5: Roll, roll rate and roll, yaw and pitch accelerations for the slalom maneuver. The *model reference* signal comes from the vehicle dynamics model. The *backward kinematics* signal is an estimation of the real performance of the motion platform.

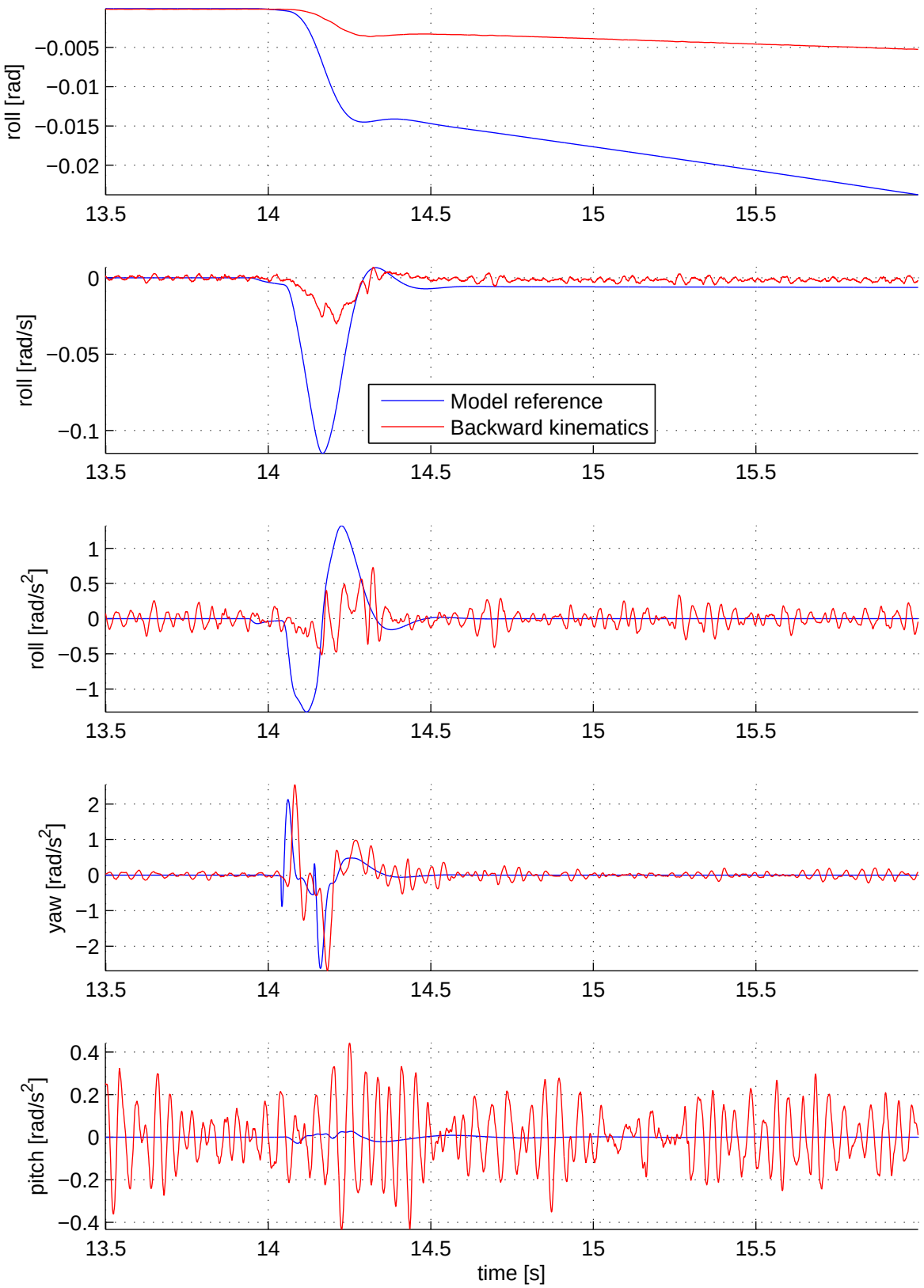

Figure 4.6: Roll, roll rate and roll, yaw and pitch accelerations for the 30 m/s identification maneuver. The *model reference* signal comes from the vehicle dynamics model. The *backward kinematics* signal is an estimation of the real performance of the motion platform.

5

Human Research

A human research approach was used to answer the research questions as stated in Section 1.3 with respect to speed perception, motion and upper body tracking. This chapter describes in detail how the human research has been conducted in Section 5.1, what the results were from the experiments in Section 5.2 and how these can be interpreted in Section 5.3.

5.1. Method

This section describes the methods used during the human research experiments.

5.1.1. Participant recruitment

Participants were recruited via the social network of the author (friends, colleagues). 16 participants were recruited all having a valid motorcycle license. The average age of the participants was 29, with a standard deviation of 11 years. Most of the participants were students at the Delft University of Technology. Table 5.1 shows the distribution of years of ownership of a motorcycle license and the amount of kilometers ridden each year. Appendix A gives a complete overview of the participant demographics.

Table 5.1: Distribution of license ownership and kilometers ridder per year of the participants.

License ownership				
0-1 years	1-2 years	2-5 years	5-10 years	more than 10 years
1	2	2	7	4
km's ridden per year				
0-1000	1000-2000	2000-6000	6000-15000	more than 15000
5	5	3	3	0

5.1.2. Test track development

Before the experiment, a test track was developed with the specific maneuvers for the participants to complete. At the basis, Cruden's Dynamic Area was used for the body tracking and motion experiments, see Figure 5.1 for an impression. This track has no elevation and features buildings, trees, guardrails and other objects which are non-collidable, so a participant can just drive through them with the virtual motorcycle.

For the trajectory following maneuver, the participants were asked to ride in a 2 m wide lane between cones on each side, consisting of straights and curves. Figure 5.2 shows the parametrization of the trajectory and Figure 5.3 shows how the trajectory is represented in the Cruden Dynamic Platform. The radii of the corners decrease the further the participant gets along the trajectory. As can be seen from Figure 5.2, the trajectory is approximately 1.3 km long and consists of 4 180 ° corners. The straights between the corners are all 60 m long so that if a participant fails to keep in the lane in a corner, the straight is long enough to return to the track. The participants were asked to ride 50 km/h along all of

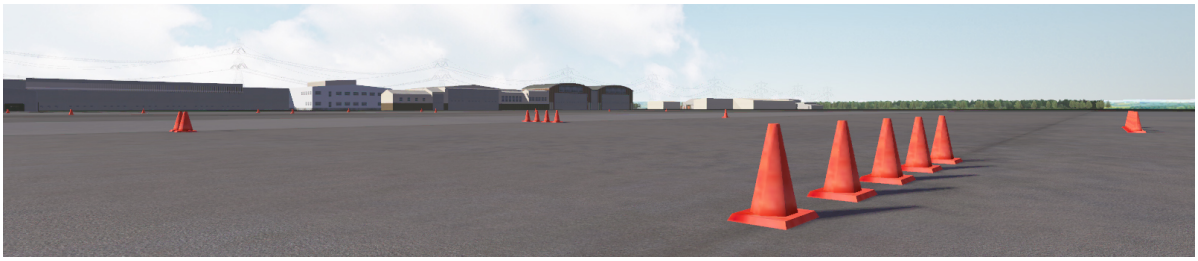

Figure 5.1: The Dynamic Area with some cones.

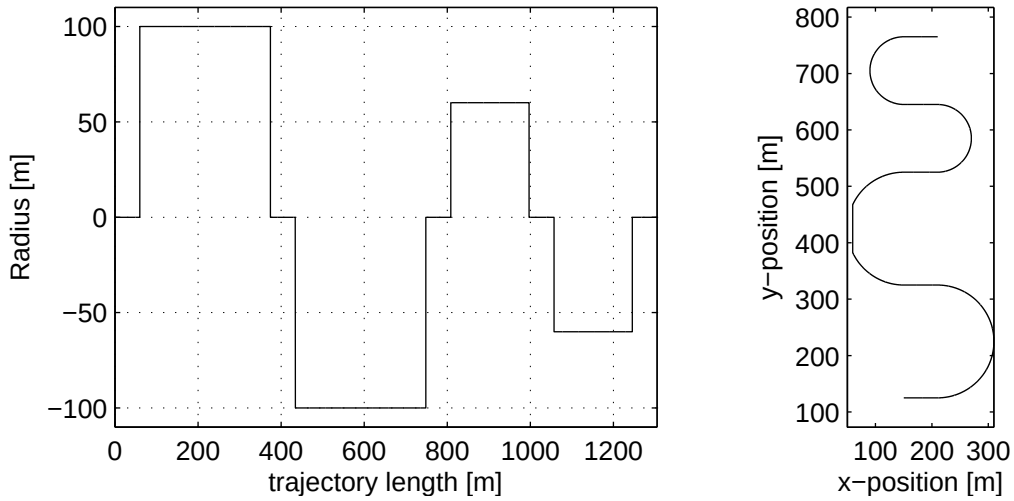

Figure 5.2: Parametrization of the trajectory following maneuver. On the left, the curvature of the maneuver can be seen. On the right, the maneuver is represented in the x, y-plane showing the top view of the track.

the track. For 50 km/h, the corners are mild, as the lateral accelerations are 1.9 m/s^2 and 3.2 m/s^2 for the radii of 100 m and 60 m respectively.

The Dynamic Area also features a 9 kilometer long 10 lane highway, see Figure 5.4. On this highway, the speed perception experiments were conducted. The width of each lane is 3.5 m, the lines are 3 m long with 4.5 m between them.

5.1.3. Experimental design

The effects of two motorcycle simulator levels have been evaluated: platform motion and upper body tracking. Both levels had two settings which were on and off. This resulted in a 2x2 experimental design.

The experiments carried out within this research are so-called within-subject experiments. With a within-subjects experiment, every participant undergoes each experimental condition. To avoid carry-

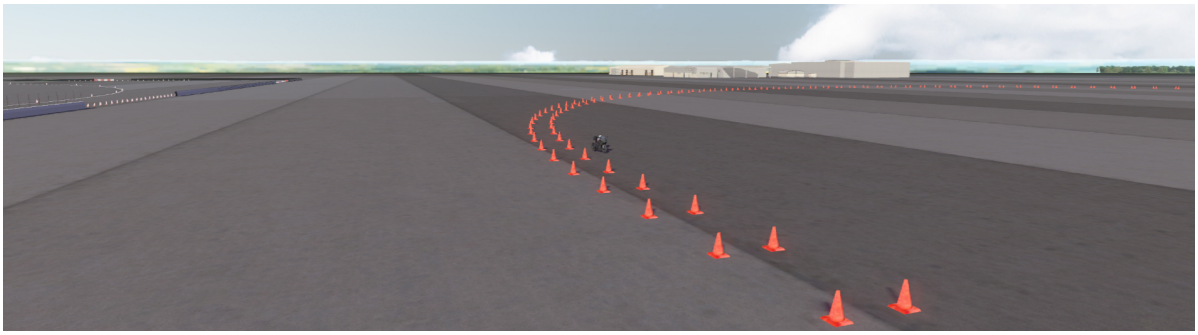

Figure 5.3: A part of the trajectory following maneuver in the Dynamic Area.

Figure 5.4: The 10 lane highway in the Dynamic Area.

over effects which include fatigue, interaction between conditions and the learning effect, several measures have been taken. First of all, the experiments in each category were counterbalanced. The order in which the participants had to complete the experiment was randomized using MATLAB. Secondly, an extensive practice session was performed before the experiment, in which the participants were able to get accustomed to the motorcycle controls, the Oculus Rift, the safety procedures and the scenario of crashing the virtual motorcycle. Thirdly, breaks were held in between the experiments to let the participant get some rest and have the participant fill in questionnaires about their experience.

The tasks themselves have not been counterbalanced on purpose. The experiments in the speed perception category were conducted first followed by the trajectory tracking experiments. This has been done for several reasons. The main reason was that it was expected that the participants would show a strong learning effect. As it was the goal test the hypothesis separately in each category, it would have been negative for the validity of the results if certain participants had more experience riding the motorcycle simulator in specific scenarios than others. A second reason was that there is a difference in how demanding the experiments in each category are. For example, the trajectory tracking experiments are more demanding than the speed perception experiments. Finally, if all experiments would need to be counterbalanced, the number of experiments would need to be much higher.

Since it was expected that the speed perception category would be the least demanding, this was conducted first. Reasons for it being less demanding than the trajectory tracking experiment is that a minimum of lateral control is required and that the speed perception experiments take less time than those in the other category. Also, the tracking experiments has a higher chance to elicit motion sickness, which could lead to drop outs or reduced performance in the speed perception tasks if performed as second task. Furthermore, for the participants to have some experience in controlling the speed of the motorcycle would be beneficial for the tests in the trajectory tracking experiments.

The participants were told to which category the experiments belonged and what their task was, but the specific condition was not disclosed. This had been done to avoid preconceptions about the experimental condition. However, certain conditions, like the no motion condition, were probably easy to identify by the participants.

Tables 5.2 and 5.3 show how the experiments are subdivided and what identifiers will be used throughout this report for reference.

Before the experiments

First, the participants had to complete the intake questionnaire (see Appendix B). The intake questionnaire consisted of items such as demographics, travel and riding behavior and previous experience with simulators. Next, the participants were instructed on the operation of the motorcycle simulator, the safety procedures and the experiments, after which the informed consent form was signed. Finally, a simulator practice simulator session was performed.

During the simulator practice session, which took around 10 minutes per participant, the participants were encouraged to ride both fast and slow and experience the dynamics of the motorcycle simulator. The participants were also asked to crash the motorcycle on purpose to experience such event.

The speed perception experiment

The speed perception test was conducted on the Cruden Dynamic Area highway. The order of SP1-SP9 had been randomized before the start of the experiment. After a set of 3 experiments, a break

Table 5.2: Experimental condition identifiers for the speed perception experiments. All were performed with platform motion and upper-body tracking.

Experiment	Instructed Velocity	Identifier
Speed Perception	50 km/h	SP50-1
		SP50-2
		SP50-3
	80 km/h	SP80-1
		SP80-2
		SP80-3
	120 km/h	SP120-1
		SP120-2
		SP120-3

Table 5.3: Experimental condition identifiers for the trajectory tracking experiments.

Experiment	Motion	Body Tracking	Identifier
Trajectory Tracking	Motion	Tracking	M1T1
		No Tracking	M1T0
	No Motion	Tracking	M0T1
		No Tracking	M0T0

was held to complete a questionnaire.

The trajectory tracking experiment
In the trajectory tracking category, the participants were asked to perform the trajectory tracking in a predetermined randomized order. After each experiment, a questionnaire had to be completed. The participants were not told to actively move their upper body and were just asked to ride normally.

To have no body tracking during the simulation, the signals from the body lean sensors were simply ignored. This resulted in the simulation of a stiff rider on the motorcycle.

After the experiments
After all experiments had been completed, the participants were asked to fill in one final form with general questions about the experiment and the motorcycle simulator. If there was some time left, the participants were invited to ride a few laps on one of the racing circuits available at the simulator, like Jerez or Zandvoort GP. The total duration of the experiments can be seen in table 5.4.

5.1.4. Data acquisition and performance metrics

With the motorcycle simulator, real-time data could be logged in two ways. The first way was via the data logger in the Simulink model and the second way was using the E2M Commander software. With the E2M commander software, signals from the motion platform and the control loader could be logged at 1000 Hz. However, since all signals that were interesting for this experiment could be logged with the data logger, and a sample rate of 100 Hz was deemed sufficient, this was the only method used to gather data for the human research experiments.

Another way data was collected was by using questionnaires that had to be completed after the experiments. A digital questionnaire has been developed to gather all the data. Since some of the questionnaire would risk losing validity by changing their appearance, the questionnaires were made

Table 5.4: Time planning for the experiments.

Activity	Duration
Intake	10 min.
Training	20 min.
Speed Perception	30 min.
Trajectory Tracking	60 min.
Total	**120 min.**

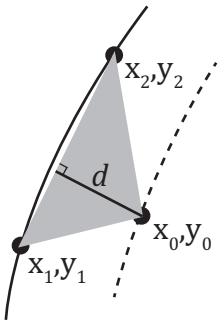

Figure 5.5: By calculating the surface of the triangle, the distance d can be determined.

in HTML and CSS with PHP form handling, sending the form data to a My-SQL database on a local server. This way, complete freedom of appearance had been ensured.

In the speed perception experiment, the main metric of interest was the participant's estimated velocity. When the participant thought he or she was riding the correct speed, he had to disengage the clutch and give a verbal stop sign. The experimenter stopped the simulation after the stop sign, while the clutch was still disengaged. This way, the point for which the participant perceived to be riding the required speed could easily be extracted by hand by looking at the clutch signal. This was done by plotting the clutch signal and using the `getpts` command in MATLAB for each speed perception experiment. `getpts` returns the x and y position from the cursor in the plot window if clicked. Next, `find` was used to find the closest point to the right of the clicked value where the clutch signal > 0.1. With this approach, all data points could quickly be extracted from the gathered data in an automated script.

For each instructed velocity, the achieved velocities were averaged per participant before final analysis, e.g. SP1 to SP3 were averaged, SP4 to SP6 were averaged etc. This results in one velocity per participant per asked velocity, and has been done to reduce the sensitivity to outliers.

Steering torque

For the trajectory tracking experiment, the steering torque was used as a control effort metric. Both the mean and standard deviation of absolute values of steering torque were used.

Lane deviation

As performance metric for the trajectory tracking maneuver, the deviation from the center of the lane could be calculated by using the reference trajectory and the ridden trajectory. For each logged position, the deviation was determined by sorting the distance from that specific position to all points of the trajectory. With the two closest points on the trajectory, a triangle was formed. By calculating the height of this triangle (with the two points of the triangle as base), the closed distance to the reference trajectory was determined. Figure 5.5 shows a graphical representation of how the calculation can be performed. The algebraic equation for calculation of d is

$$d = \frac{(y_2 - y_1)x_0 - (x_2 - x_1)y_0 + x_2y_1 - y_2x_1}{\sqrt{(y_2 - y_1)^2 + (x_2 - x_1)^2}}. \tag{5.1}$$

With this method however, a small error is made in curves since a straight line is calculated through x_1, y_1 and x_2, y_2. However, since these coordinates are spaced apart 10 cm by definition and the smallest radius curve is 60 m, the error is maximally $30 - \sqrt{30^2 - 0.1^2} = 0.083$ mm. Since the metrics are averaged over the total number of samples, this error is negligible.

Interesting performance metrics are the mean absolute deviation and the standard deviation of the lane deviation from the lane center, as they describe how well the rider was able to follow the trajectory. Also, the total count of times the rider left the 2 m wide trajectory is used as a performance metric and is called *lane departures*. The start point and end point of the data were selected automatically by finding the closest distance to both points respectively.

NASA Task Load Index

The NASA Task Load Index (NASA-TLX) is a widely used questionnaire used to evaluate the perceived workload of a task [12]. Initially, it was designed for the aviation industry, but it was soon used as a tool in research fields beyond its initial application [11]. In this research, the NASA-TLX was used to asses the workload of the participant as another metric for control effort. The questionnaires that the participant had to fill in after each experiment included the questions from the NASA-TLX. Finally, the overall task load index was used in statistical analysis.

After each trajectory tracking experiment, the first part of the TLX had to be completed (Appendix B). After all trajectory tracking experiments were completed, also the second part with the weighting sub scales had to be completed (Appindex B). The tallies of each weight scale element is counted as its respective weight. The total task load index is calculated by summing the workload scores multiplied with the weighting scores and then dividing by 15 to get a score of 0-100.

Motion Sickness Susceptibility Questionnaire

As part of the questionnaires that the participants had to fill in before the experiment, the Motion Sickness Susceptibility Questionnaire (MSSQ) evaluated the particpants' susceptibility to motion sickness [10]. The questionnaire consists of questions regarding past motion sickness experiences both as a child and over the past 10 years. With this metric, the participant composition could be compared to the general population with respect to motion sickness tolerance. For the questionnaire itself, see Appendix B. First, the susceptibility during childhood is calculated by

$$\text{MSSQA} = \frac{2.64 \times (\text{total sickness score child}) \times 9}{(\text{number of types experienced as a child})}. \tag{5.2}$$

Next, the susceptibility over the past ten years is calculated by

$$\text{MSSQB} = \frac{2.64 \times (\text{total sickness score adult}) \times 9}{(\text{number of types experienced as an adult})}. \tag{5.3}$$

Finally, the motion sickness susceptibility of the individual is calculated by

$$\text{MSSQ raw score} = \text{MSSQA} + \text{MSSQB}. \tag{5.4}$$

Simulator Sickness Questionnaire

The Simulator Sickness Questionnaire (SSQ) was developed to provide a scale to indicate motion sickness under less severe conditions of simulation [17]. The questionnaire consists of 16 symptoms which can each be scored from 0 – 3. Using specific weighting, results in three categories Occulomotor (O), Disorientation (D) and Nausea (N) can be distinguished. On top of that, an overall score called the Total Severity (TS) score can be established. The participants were asked to fill in this questionnaire after each experimental condition.

Presence Questionnaire & Immersive Tendencies Questionnaire

The degree to which a user experiences being in another place than he or she actually is, for example in a motorcycle simulator, is defined as presence [27, 44, 45]. Witmer & Singer developed a questionnaire which can be used to measure presence, the Presence Questionnaire (PQ) [45]. It is suggested that presence relates to the perceived quality of a simulator by assessing the involvement and immersion of the user in the simulator. Control, sensory, distraction and realism factors all contribute towards a final presence value. In this research, a slightly modified PQ was used, omitting questions that were not applicable to the motorcycle simulator. The PQ can be found in Appendix B.

Besides measuring the presence of the users in the simulator, before the tests the Immersive Tendencies Questionnaire (ITQ) had to be completed. The ITQ is also developed by Witmer & Singer and measures the user's capability or tendency to be involved or immersed [45]. Using values from the ITQ, it could be assessed how likely users were to experience presence and put the presence values in a broader perspective. The ITQ can be found in Appendix B.

5.1.5. Statistical analysis

The independent variables in the trajectory tracking experiment were Motion level and Body Tracking level. In each case, several dependent variables were measured like effort (subjective) and steer torque (objective). Every participant completed all combinations of Motion level and Body Tracking level, which is known as repeated measures.

Data for lane keeping performance is usually not normally distributed as the lane deviation metrics are sensitive to single lane departures. For that reason, the Wilcoxon signed rank test `signrank` was used to obtain the p and Z-values for the different metrics, testing the hypotheses that results for the motion category come from the same ranked distribution as results from the no-motion category, and the same for the body tracking level [39]. Effect sizes were calculated by

$$r = \frac{Z}{\sqrt{N}}, \tag{5.5}$$

where $N = 14$ is the sample size.

For the motion levels, results were lumped, as it was observed that the participants were hardly using their upper bodies to control the motorcycle simulator. Lumping was done by averaging the performance of each participant for each metric combining the with tracking and without tracking results. The results of the upper body tracking experiments were compared without lumping and for each motion level separately.

As this research is exploratory, a small sample size is used and the simulator's performance is evaluated per metric in stead of all metrics at the same time, a significance level $\alpha = 0.05$ has been used. So, if $p < \alpha$, the results are deemed significantly different.

5.2. Results

In this section, the results for the velocity estimation experiments and the trajectory tracking experiments are shown.

5.2.1. Velocity estimation

To start with how the data has been acquired, Figure 5.6 shows an example of a clutch and speed profile. It can be seen that, when the rider disengages the clutch for the final time, as signal that the required velocity is reached, the speed is extracted from the velocity signal accordingly. The extraction algorithm ensures that only the last clutch action is used. There have been no situations where this method failed and this approach was clear to the riders. One participant was unable to continue the experiments after the practice session, so the number of participants used in this experiment is N =15.

Figure 5.7 shows three box plots for the required velocities of 50,80 and 120 km/h. More descriptive statistics can be found in Table 5.5, where the mean and median values for achieved velocities are shown, how much these differ from the asked velocities and what extreme values were ridden. Interestingly, a large difference can be observed for the estimated velocities. Nevertheless, the median and mean values of estimated velocity for the three different velocities are rather close to the required velocity. Another important observation is that the maximum achieved velocity for a reference velocity of 120 km/h was 199.9 km/h, since the motorcycle is limited on 200.0 km/h. Bearing in mind that these values are already averaged per per participant (SP120-1 – SP120-3), this means that one of the participants was constantly riding the maximum velocity of the motorcycle for the reference velocity of 120 km/h.

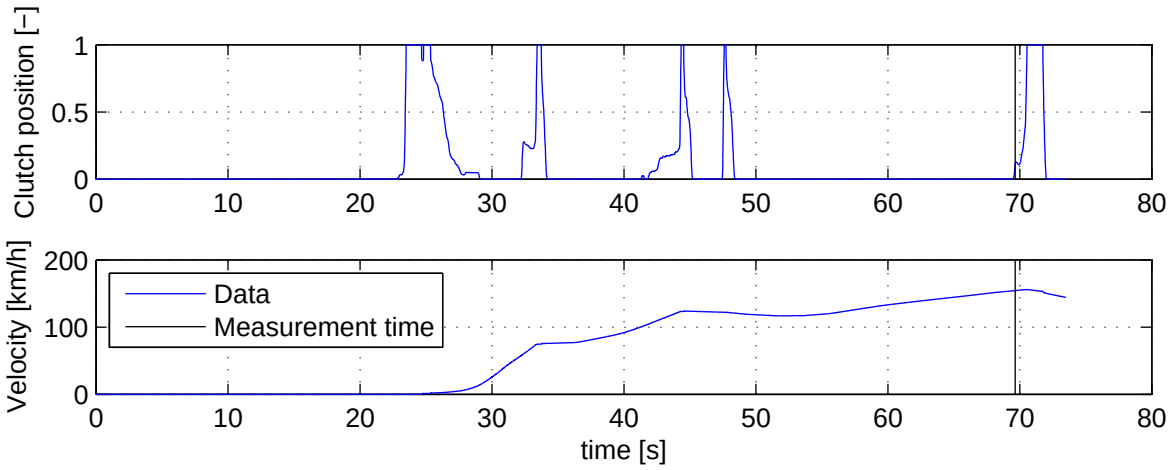

Figure 5.6: Clutch position and velocity profile for the SP9 experiment from participant P007. The black line shows where MATLAB has calculated that the clutch position > 0.1, and which speed has been taken as data snapshot.

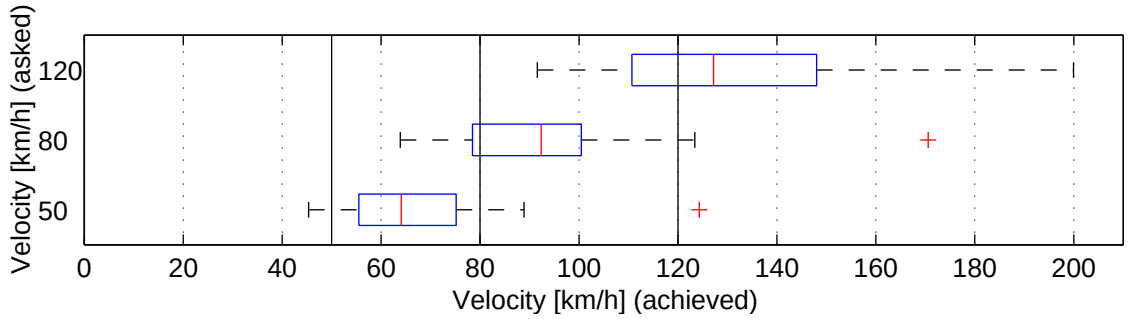

Figure 5.7: Boxplot showing the estimated speed distribution for all participants for all instructed speeds. The vertical solid black lines emphasize the velocities of 50, 80 and 120 km/h. The red line in each box is the dataset median, the edges of the blue box are the 25th and 75th percentiles. The whiskers are the lowest and highest values considered in the data set. The red pluses are outliers.

Table 5.5: Median, mean and standard deviation (SD) with percentual differences for the velocities ridden by all participants.

Instructed	**Median**	diff.	**Mean**	diff.	min	max	**SD**
50 km/h	64.06 km/h	+28%	67.96 km/h	+36%	45.35 km/h	124.3 km/h	19.23 km/h
80 km/h	92.36 km/h	+15%	95.07 km/h	+19%	63.88 km/h	170.6 km/h	25.66 km/h
120 km/h	127.2 km/h	+6.0%	134.1 km/h	+12%	91.58 km/h	199.9 km/h	29.28 km/h

5.2.2. Trajectory tracking

During the trajectory tracking experiments, one participant was unable to complete the experiments without motion as these made him feel too uncomfortable. Including the withdrawal from the participant after the practice session, the number of participants for the trajectory tracking experiments was $N = 14$.

To show an example of the data, figure 5.8 shows the trajectory ridden by participant P007 on the required path, for the no-motion and no upper body tracking condition. Figure 5.9 shows the deviation for the same experimental condition and participant. The peak observed in Figure 5.9 around 70-75 s corresponds to the deviation which can also be observed in Figure 5.8 at the end of the first corner.

Figure 5.10 shows the lane deviations and steer torques of all participants for each motion and body tracking level. Interestingly, it can be observed that the worst lane keeping performance is achieved in the first corner. It cannot easily be seen if a difference exists in lane keeping performance with respect to the straights or the corners. An important property of the lane keeping metric can be observed here: if one participant has a large lane deviation, the mean and standard deviation values of the complete group are heavily influenced. Looking closely, it seems that the mean values for the no-motion (green + magenta) lane deviation are slightly higher on average.

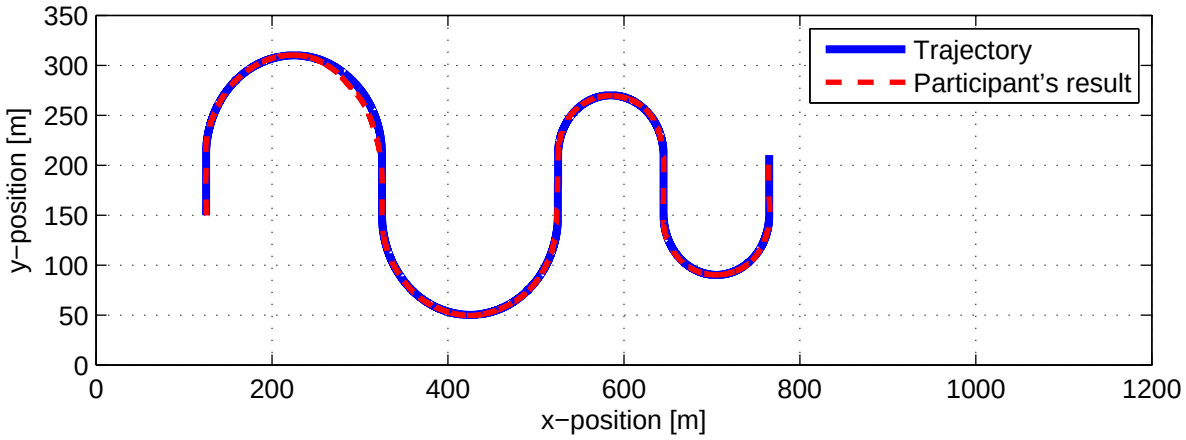

Figure 5.8: Followed trajectory of participant P007 on the required path for experimental condition M0T0 (no motion, no upper body tracking). Note that the participant entered the trajectory at the bottom left.

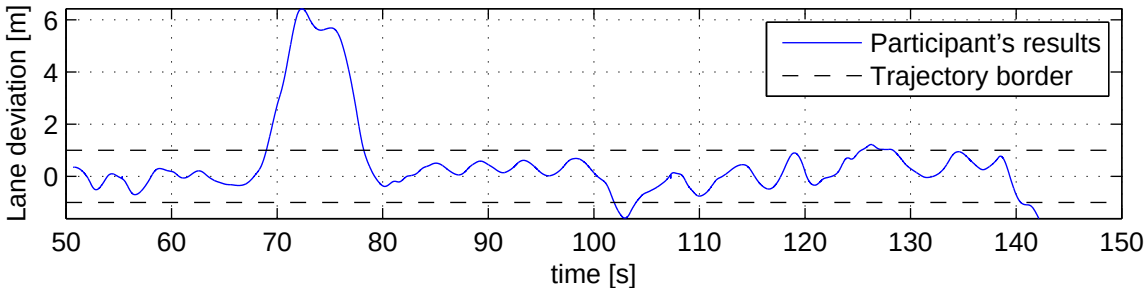

Figure 5.9: Lane deviation of participant P007 for experimental condition M0T0 (no motion, no upper body tracking)

Looking at the steering torque in Figure 5.10, peaks in steer torque can be observed at the entries and exits of the corners, since it is here where the rider wants to change the motorcycle's lean angle to go from cornering to riding in a straight line. Differences in steer torque at these points cannot be observed however. Neither can clear differences between steer torque be observed at the other points along the trajectory.

Figure 5.11 shows the boxplots for the NASA-TLX. For the weighted workload, there seems to be a clear difference between motion versus no-motion distributions. Table 5.6 shows the p-values for the Wilcoxon signed rank tests and it can be observed that the overall workload is statistically significant in favor of platform motion. As a matter of fact, all sub metrics show lower median values in favor of platform motion. However, for Mental Demand, Performance and especially Temporal demand, no statistical significant differences were found.

Figure 5.12 shows boxplots for the Presence Questionnaire. Contrary to the TLX scores, higher values are regarded as better. The top boxplots shows the total Presence scores. It can be observed that Presence is higher with motion than without motion. For the control factors, the same results can be observed, but the other factors are harder to interpret, and it might even seem that no motion scores higher for the Sensory Factors. When looking at the p-values in Table 5.6, only a statistical significant difference can be observed for the motion level for the overall Presence.

Results from the Simulator Sickness Questionnaire can be seen in Figure 5.13 and Figure 5.14. Especially for this metric, non-normally distributed results are observed. Hence, it is difficult to tell from the boxplots whether motion or upper body tracking levels are significantly different for the simulator sickness metrics. The cumulative distribution in Figure 5.14 shows that most participants reported low scores for Total Severity. Looking at the Wilcoxon signed rank test results in Table 5.6, no significant differences can be found for the motion levels. Figure A.4 in Appendix A shows that the participants were less susceptible to motion sickness than a baseline group.

Completely different results are observed for the lane deviation metrics. In figure 5.15 it can clearly be seen that the medians for motion results are lower than the medians of the no motion results. This

Table 5.6: Wilcoxon signed rank test results for the main metrics and sub metrics. The motion and no-motion columns show the data medians for each lumped category respectively. Statistically significant p-values are boldfaced ($p < 0.05$).

	Motion	**No-motion**			
Metric	*Med.*	*Med.*	p	Z	r
NASA-TLX					
Overall workload	43.75	56.75	**0.0131**	2.48	0.66
Mental Demand -	11.00	12.75	0.0684	1.82	0.49
Physical Demand -	8.00	11.75	**0.0302**	2.17	0.58
Temporal Demand -	7.50	7.75	0.5911	0.54	0.14
Performance -	8.50	10.0	0.1871	1.32	0.35
Effort -	10.75	14.00	**0.0169**	2.39	0.64
Frustration -	7.50	9.00	**0.0125**	2.50	0.67
Presence Questionnaire					
Overall presence	95.75	85.75	**0.0097**	2.59	0.69
Control factors -	48.25	44.00	0.2345	1.19	0.32
Sensory factors -	32.25	24.00	0.4797	0.72	0.19
Realism factors -	17.75	18.50	0.2345	1.19	0.32
Distraction factors -	9.75	9.00	0.2846	1.07	0.29
Simulator Sickness Questionnaire					
Total severity	3.37	13.97	0.2210	1.22	0.33
Nausea -	14.31	23.85	0.0685	1.82	0.49
Oculomotor discomfort -	7.58	13.27	0.1962	1.29	0.35
Disorientation -	24.36	13.92	1.0000	0.00	0.00
Lane keeping					
Lane departures	1.50	4.50	**0.0037**	2.91	0.78
Mean absolute lane center deviation	0.30 m	0.59 m	**0.0132**	2.48	0.66
Standard deviation lane center deviation	0.26 m	0.52 m	**0.0110**	2.54	0.68
Steer torque [Nm]					
Mean absolute steer torque	4.66	4.48	0.5098	0.66	0.18
Standard deviation steer torque	3.89	3.94	0.5098	0.66	0.18
Velocity [km/h]					
Average velocity	50.89	51.28	0.8261	0.22	0.06

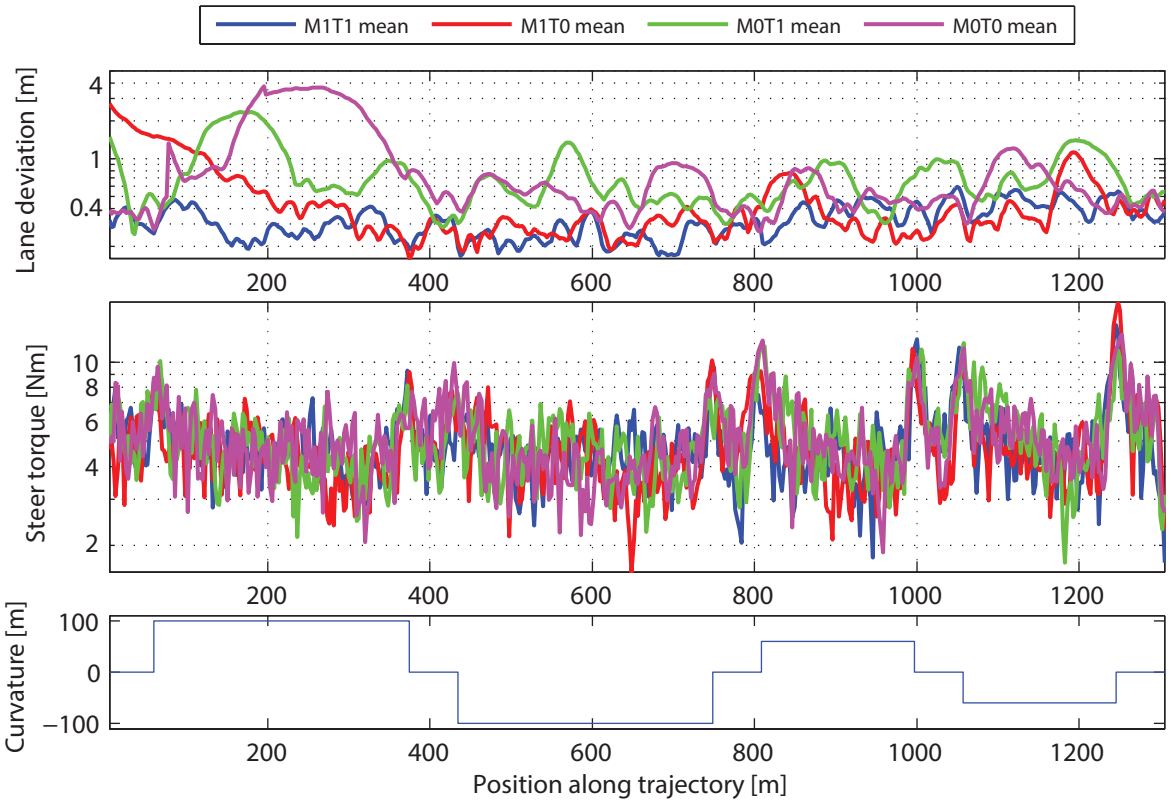

Figure 5.10: Mean absolute and standard deviation for the lane deviation and steer torque over all participants for each point along the trajectory. The bottom plot shows the curvature along the trajectory.

observation is strengthened by the Wilcoxon signed rank tests as it can be observed in Table 5.6 that the two motion levels are significantly different for all three lane keeping metrics.

Figure 5.16 shows boxplots for the steer torque metrics. From these figures, no clear observation can be established, as it seems that the medians of all experimental conditions are very close together for both the Mean absolute steer torque and standard deviation of steer torque. The difficulty in interpreting the boxplots is backed up by the results from the Wilcoxon signed rank tests in Table 5.6, where no p-values shows any significant differences between levels.

Finally, the last row in Table 5.6 shows that the average velocity ridden by the participants do not statistically differ per experimental condition.

Tables 5.7 and 5.8 show results regarding the upper body tracking results for platform motion and without platform motion respectively. As could be expected from the results observed in the boxplots in Figures 5.11, 5.12, 5.13, 5.15 and 5.16, no clear observations can be made with respect to the upper body tracking. Interestingly, the p-value for the Total Severity of Simulator Sickness for the body tracking levels without platform motion is smaller that 0.05 (Table 5.8). However, the large difference in the medians for both tracking levels, and the lack of this difference for the body tracking levels with platform motion most likely would make it a type II error if this result would be assumed significant.

Finally, Tables 5.6, 5.8 and 5.7 show that the average velocity between experimental conditions do not significantly differ from each other, so the results are not influenced by large differences in speed for completing the trajectory.

5.3. Discussion

Like the Method and Results sections, the speed perception experiments are discussed first, followed by the trajectory tracking experiments.

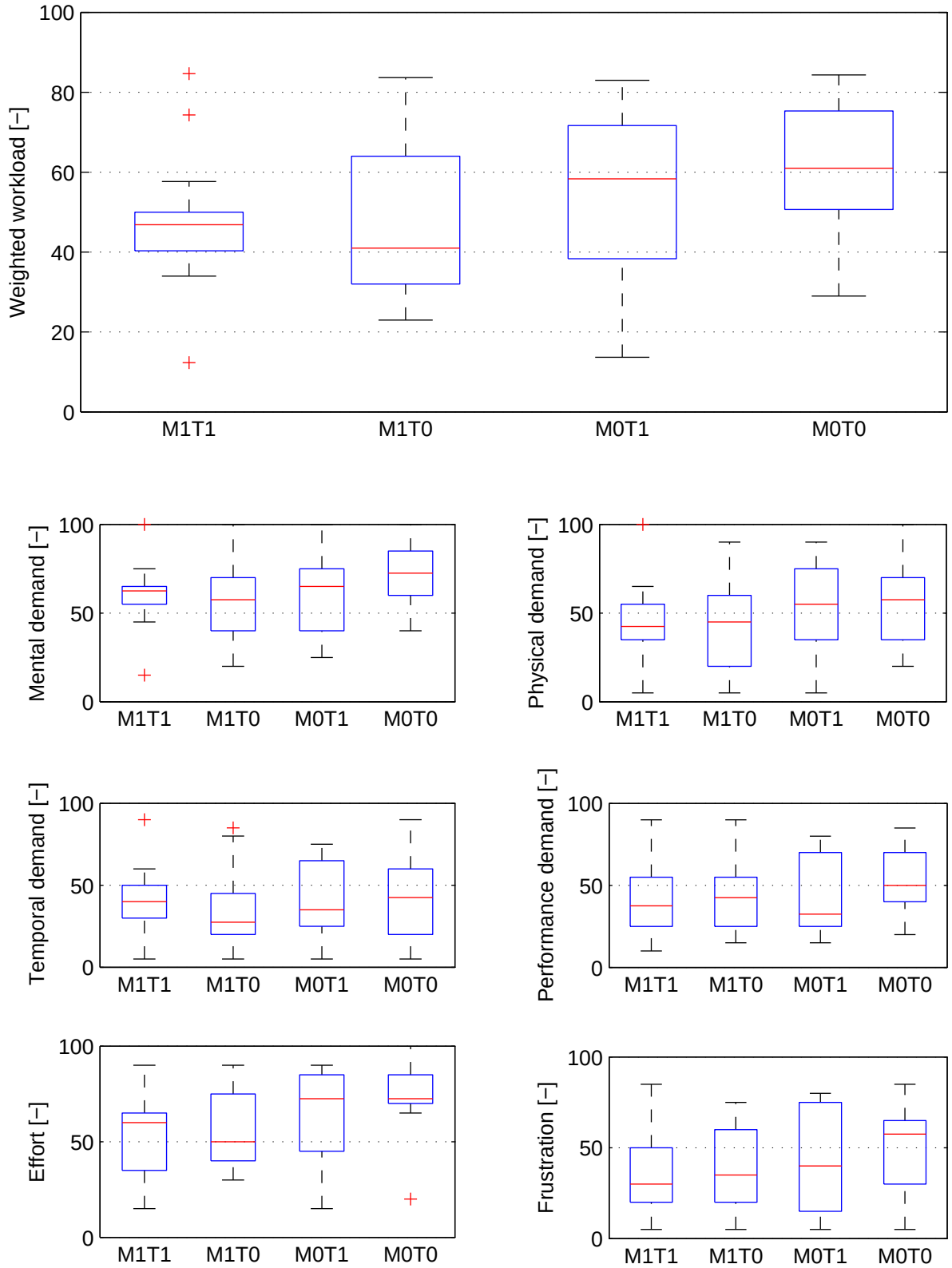

Figure 5.11: Boxplots for each participant score for the Task Load Index (TLX) questionnaires. The top boxplots show the weighted scores for each participant. The bottom six plots show the scores for each category of the questionnaire separately.

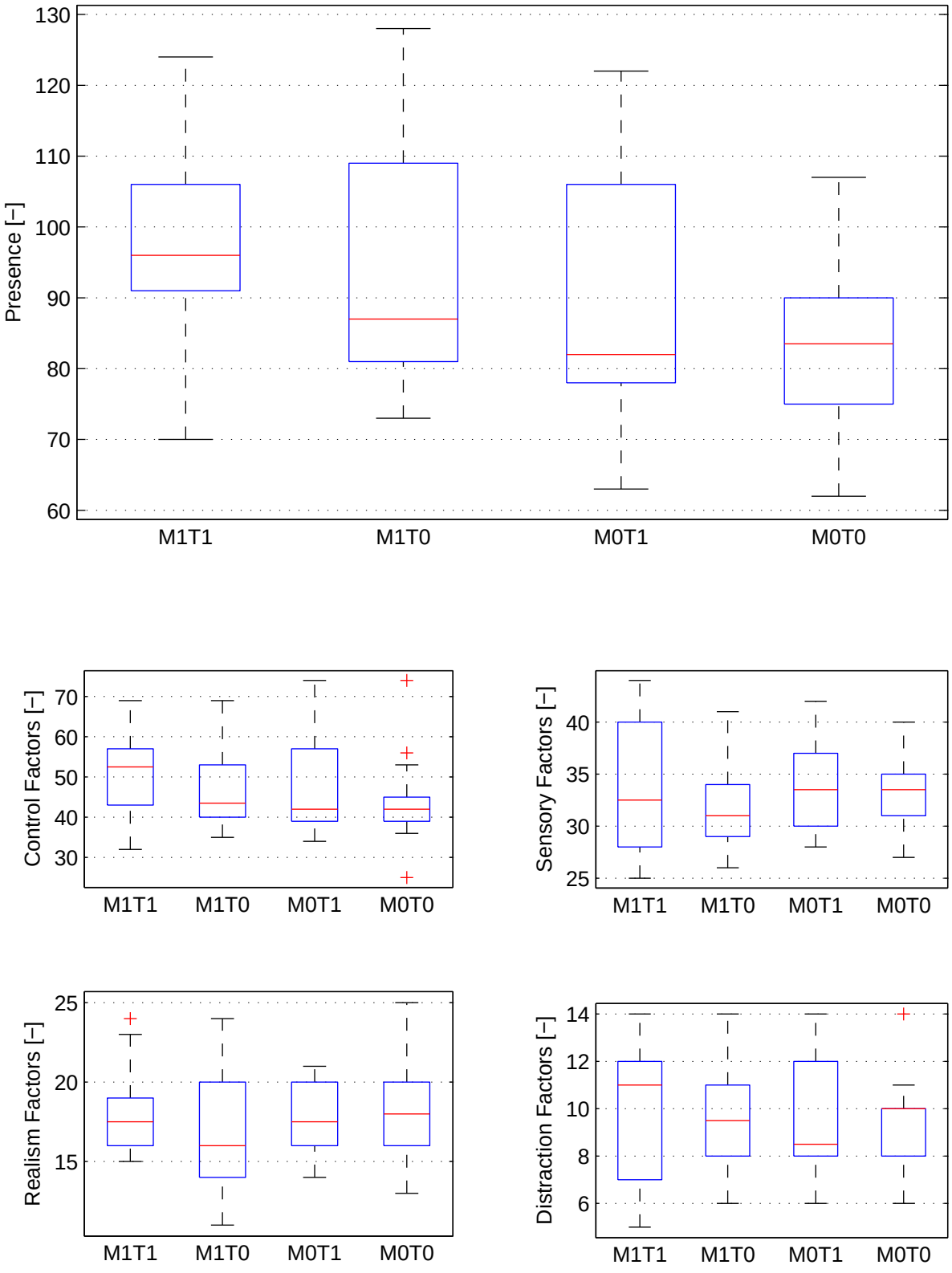

Figure 5.12: Boxplots showing the results from the presence questionnaires. The top figure shows the complete presence scores, and the bottom figures show the subcategories of presence: Control Factors, Sensory Factors, Realism Factors and Distraction Factors.

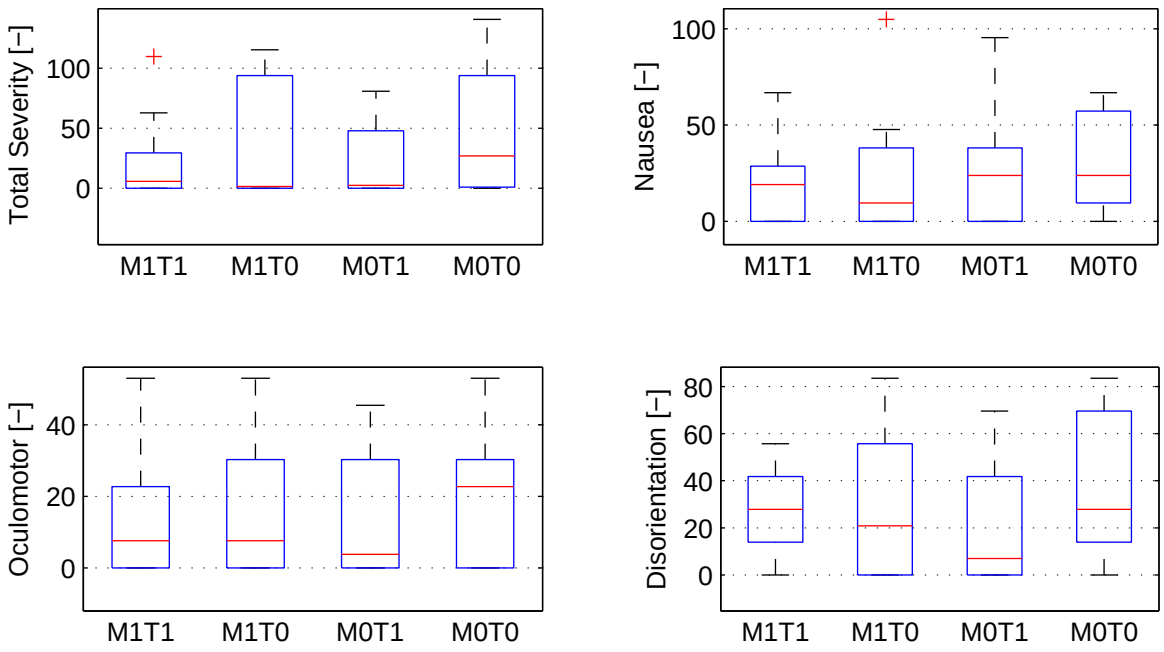

Figure 5.13: Boxplots showing the results for the Simulator Sickness Questionnaires (SSQ's). The top left shows the total severity score, the other three show the subcategories of simulator sickness.

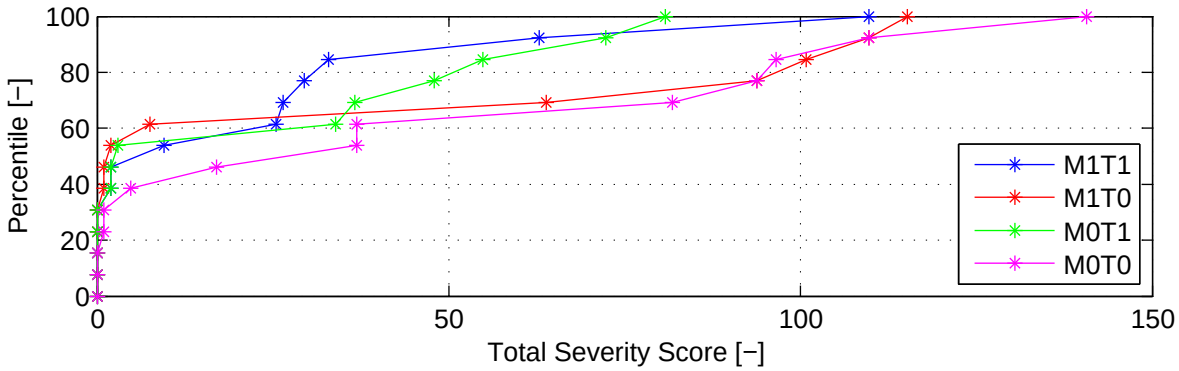

Figure 5.14: Cumulative distribution for the Total Severity scores of the SSQ for the four simulator settings.

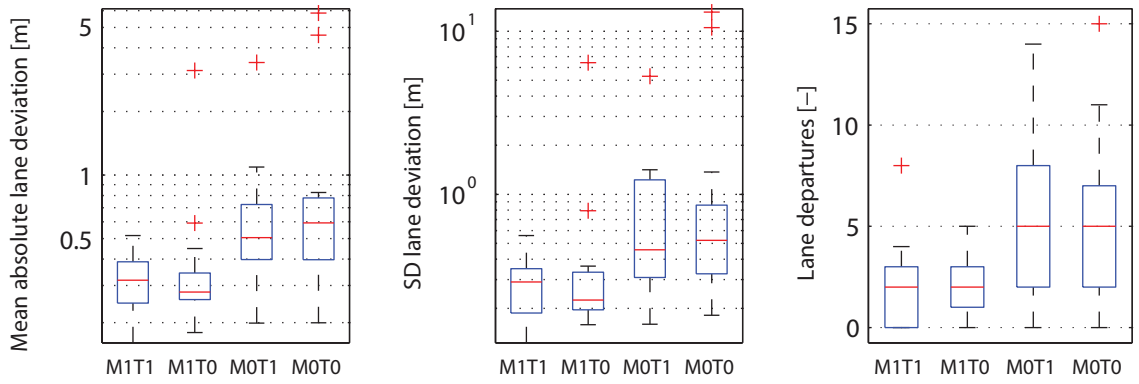

Figure 5.15: Boxplots for the mean absolute lane deviation, Standard Deviation (SD) of lane deviation and number of lane departures. Note that the y-axis is logarithmic to better show the distribution of data points for the mean absolute lane deviation and the standard deviation of lane deviation.

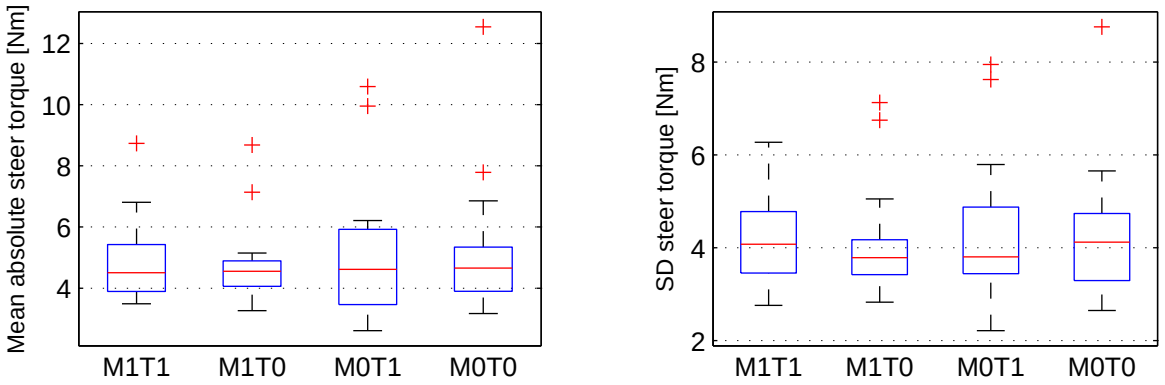

Figure 5.16: Boxplots showing the mean absolute steer torque and Standard Deviation (SD) of steer torque.

Table 5.7: Wilcoxon signed rank tests results for the main metrics for the upper body tracking **with** platform motion (M1T1 - M1T0).

	Body tracking	**No body tracking**			
Metric	*Med.*	*Med.*	p	Z	r
NASA-TLX					
Overall workload	46.83	41.00	0.8261	0.22	0.06
Presence Questionnaire					
Overall presence	96.00	87.00	0.9249	0.09	0.03
Simulator Sickness Questionnaire					
Total severity	5.74	1.50	0.2357	1.19	0.32
Lane keeping					
Lane departures	2.00	2.00	0.6175	0.50	0.13
Mean absolute lane center deviation	0.32 m	0.28 m	0.8753	0.16	0.04
Standard deviation lane center deviation	0.29 m	0.22 m	0.8261	0.22	0.06
Steer torque [Nm]					
Mean absolute steer torque	4.51	4.55	0.9250	0.09	0.03
Standard deviation steer torque	4.07	3.79	0.6378	0.47	0.13
Velocity [km/h]					
Average velocity	51.22	50.82	0.9250	0.09	0.02

Table 5.8: Wilcoxon signed rank tests results for the main metrics for the upper body tracking **without** platform motion (M0T1 - M0T0).

	Body tracking	**No body tracking**			
Metric	*Med.*	*Med.*	p	Z	r
NASA-TLX					
Overall workload	58.33	61.00	0.4324	0.79	0.21
Presence Questionnaire					
Overall presence	82.00	83.50	0.3301	0.97	0.26
Simulator Sickness Questionnaire					
Total severity	2.50	26.94	0.0410	2.04	0.55
Lane keeping					
Lane departures	5.00	5.00	0.9721	0.04	0.01
Mean absolute lane center deviation	0.50 m	0.59 m	0.6378	0.47	0.13
Standard deviation lane center deviation	0.46 m	0.52 m	0.5509	0.60	0.16
Steer torque [Nm]					
Mean absolute steer torque	4.62	4.66	0.5936	0.53	0.14
Standard deviation steer torque	3.80	4.12	0.6832	0.41	0.11
Velocity [km/h]					
Average velocity	51.06	51.01	0.5936	0.53	0.14

5.3.1. Speed perception experiments

The results from the speed perception experiments have shown that the participants overestimated their velocity, what was to be expected from literature [24, 44]. When looking at the hypotheses, which have been based mostly on the research by Recarte and Nunes on car driving, the results posted in Table 5.5 show very close resemblance, albeit that somewhat larger standard deviation is observed and that more extreme outliers are present. Nevertheless, it can be concluded that the participants were just as bad at estimating their velocity in the motorcycle without speedometer compared to people driving in a car without a speedometer. Following this line of thought, it can be concluded that the sum of all cues is reasonable for experiencing speed like in a real vehicle or on a real motorcycle.

One important side note however is that the contribution of wind noise was very limited compared to riding on a real motorcycle, and multiple participants had remarks about this. Better simulation of wind noise would probably result in a decrease of estimated speeds, especially for the higher speeds. This could also reduce outliers observed in large overestimations of velocity.

Interestingly, all participants were very curious on how 'well' they performed and were mostly unable to tell whether or not they were close to the asked speed. This illustrates how difficult it is to estimate one's speed without a speedometer and how interesting it is that most participants underestimate their actual speed in general.

5.3.2. Trajectory tracking experiments

For the two motion levels, it has become clear that a difference could be observed in favor of simulation with motion. For the overall values of workload and presence, and for all metrics of lane deviation, significant results have been reported to back this statement. Interestingly though, about one-third of the participants were unable to tell whether they were riding with or without motion after the experiments were completed. At the same time, one of the participants was unable to complete the experiments without motion. Therefore, there seems to be a large personal preference with respect to motion level, as also observed by [25]. Since the velocities ridden by the participants for the with and without motion conditions do not differ significantly, it can be assumed that the results are not influenced by large differences in velocity.

Since the participants in this experiments reported lower motion sickness susceptibility than a baseline group, it is not surprising that a large number of participants reported low levels of simulator sickness, or no simulator sickness at all (see Figure A.4). This makes the SSQ less reliable. Concurrently, no results were found where simulator sickness provided a clear distinction between simulator settings. Nevertheless, the results with respect to motion sickness favor the motorcycle simulator, as 14 participants were all able to complete the experiments without getting too sick to continue, and as some participants did not even report motion sickness at all.

Regarding the steer torque results, no significant differences were found. A possible explanation for this is that the participants did not change their control behavior depending on the experimental condition, and the amount of torque they put on the handlebar is largely influenced by what they use during normal riding behavior.

When looking at the upper body tracking results, it cannot be concluded that body tracking has a significant influence on the performance or quality of the motorcycle simulator. It was observed during the experiments that some of the riders were not using their upper body as much as expected, and this could be explained by the layout of the experiment's trajectory. While riding 50 km/h, completing the corners did not require the participants to seek out the limits of the motorcycle's handling capabilities, and thus did not require the riders to use their upper body to steer the motorcycle. Hence, the use of the upper body was rather limited, and this could explain the absence of clear results with respect to the upper body tracking.

Furthermore, the upper body tracking system to account for rider movement on the motorcycle as used in this thesis might be too limited to accurately steer the motorcycle. It could be that the upper body tracking system lacks sensitivity to the small upper body displacements used to negotiate mild turns as was required in this research. If the upper body tracking system was not sensitive enough to do this, then it is no surprise that the results were also insignificant.

For the lane deviation metrics, less is assumed to be better. However, this relies on the assumption that, with a real motorcycle, little lane deviation is observed. Showing that lane deviation performance with motion is significantly better than without motion therefore only demonstrates the participant's capability to keep to the center of the lane with motion is easier than without motion. Again, real-

life experiments with a motorcycle and the same trajectory are needed to give indisputable evidence that a motion based simulator shows indeed higher validity than without, because only then a good comparison between lane deviation metrics can be made.

On a final note, subjective assessments of the participants indicated that the motorcycle simulator is impressive and riding it is close to riding a real motorcycle. However, most participants also said there is still room for improvement and mentioned that the steer torque required is rather high and that they felt that they could usually steer their own motorcycle more by using body motion.

6

Conclusion

To evaluate the motorcycle simulator, three aspects of the simulator have been assessed and have showed that the simulator can be used for research and development of motorcycles and motorcycle systems. In the first part, the motorcycle dynamics model has shown to behave similar to a real motorcycle. Next, the motion platform has been tested to show that the simulator can simulate the motorcycle dynamics. And finally, with a human research approach, speed perception and rider performance have shown to be satisfactory.

The motorcycle dynamics model developed in this thesis based on a Honda CB750 shows the same non-minimum phase behavior as a real motorcycle: if one wants to steer to the right, a counterclockwise torque needs to be exerted on the handlebar to make the motorcycle lean in to the right and make a right hand turn. More detailed analysis of the motorcycle dynamics model has shown that the eigenvalues of capsize and weave motion are qualitatively similar to those of a real motorcycle. With these results, it can be concluded that the motorcycle dynamics model can be used for simulation of a real motorcycle within the application range for which the motorcycle simulator has been designed.

Using data from the identification of the motorcycle dynamics, it has been shown that the motion platform can cue the dynamics of a motorcycle. Furthermore, the bandwidth of the Stewart platform and handlebar control loader are sufficient to simulate motorcycle models with even higher frequency dynamics, and the delays in these systems are small enough not to be noticeable by the rider. Therefore, the hypothesis that the motion platform can capture the dynamics of a motorcycle is confirmed.

The first question from the human research experiments was whether riders of the motorcycle simulator were able to estimate their speed like they would do in real life. Results showed that speed perception corresponded closely to what had previously been discovered in a real vehicle. Although in both cases the human was rather unable to estimate its speed correctly, the errors were very similar, and therefore speed perception in the motorcycle simulator is similar to that in real life.

The second question was whether riders actually need motion and upper body tracking to have the highest fidelity on the motorcycle simulator. While no clear conclusions can be drawn with respect to the upper body tracking system, motion showed significantly better results than no-motion. Therefore, if one wants to build a motorcycle simulator for research purposes, and high fidelity is required, a motion platform is necessary to provide the rider with all the cues needed to ride a motorcycle properly.

Ultimately, results from this research can help in the development of a new generation of motorcycle simulators, but it has been demonstrated that the Cruden motorcycle simulator can already be used in other motorcycle related research. The use of motorcycle simulators will open a way to a new area of research which could eventually make riding motorcycles safer and development of motorcycles faster and better.

7

Future Work

Even though the Cruden motorcycle simulator can be used for research and entertainment purposes, it is still not as easy to ride as a real motorcycle. What needs to be done to reach this goal is not clear at this point, but advances in hardware technology and even further reducing the delays present in the system are some of the first steps that can be undertaken. Using a large x-y platform in combination with a Stewart platform could open the possibility to cue the cornering dynamics better, but the gain of doing this might not weigh up to both the exorbitant effort and cost of such solution.

The results from the speed perception experiments have now been compared with results reported in literature where speed perception was measured in a car without a speedometer. A more valid method would have been to do the same experiment on a real motorcycle on a comparable track. It could be that motorcyclists are better able to estimate their speed on a motorcycle without speedometer than car drivers in a car without a speedometer.

To get a better understanding of steering the motorcycle with upper body steering by the rider, a new experiment needs to be designed focusing more on the limit handling of a motorcycle where the rider needs to use his upper body to steer the motorcycle. Since different riders use different control methods for steering the motorcycle, the risk remains that some riders use their upper body while others do not. Riding on the limits of the motorcycle, or even racing the motorcycle ensures that riding with upper body movement is used. This problem could also be addressed by having participants ride on a real motorcycle and on a motorcycle simulator. Further research on the implementation of rider movement could improve the interaction with the simulator too, making this part of research even more interesting.

Although the handlebar dynamics already show high performance, advances in this area could still improve the motorcycle simulator even more, given that the handlebar feel is rather important. In stead of using only a reference angle from the virtual vehicle dynamics, also a reference velocity and reference acceleration could be used to obtain a Multiple Input Single Output (MISO) system, where the output is the motor current, and improve the handlebar's behavior by using a better performing control scheme.

To be sure that the motorcycle dynamics model is correct, input and output responses need to be compared with a real motorcycle with the same properties for a number of test maneuvers. Even though the motorcycle dynamics model used in this work does show the most important properties of a real motorcycle, the exact behavior might still be different from a real motorcycle. To do this validation, the inertial properties of a real motorcycle need to be measured, and this same motorcycle needs to be used in real-life experiments. Data from these experiments are consequently used in the validation process.

But maybe even more important dynamics behavior can be accounted to the tire dynamics. Using a validated tire dynamics model for a motorcycle could even further improve the motorcycle model dynamics validity and also improve the steering behavior of the motorcycle. For example, the remarks from the participants that a large steering torque is needed to steer the motorcycle could possibly be solved by other tire models or just its parametrization.

Bibliography

[1] Shingo Chiyoda, Kenichi Yoshimoto, Daisuke Kawasaki, Yoshifumi Murakami, and Takayuki Sugimoto. Development of a motorcycle simulator using parallel manipulator and head mounted display. In *The Proceedings of the International Conference on Motion and Vibration Control 6.1*, pages 599–602. The Japan Society of Mechanical Engineers, 2002.

[2] Keith Code. *A Twist of The Wrist Volume II*. California Superbike School, Inc., 1993.

[3] Vittore Cossalter and Roberto Lot. A motorcycle multi-body model for real time simulations based on the natural coordinates approach. *Vehicle system dynamics*, 37(6):423–447, 2002.

[4] Vittore Cossalter, Roberto Lot, and Stefano Rota. Objective and subjective evaluation of an advanced motorcycle riding simulator. *European transport research review*, 2(4):223–233, 2010.

[5] Vittore Cossalter, Roberto Lot, Matteo Massaro, and Roberto Sartori. Development and validation of an advanced motorcycle riding simulator. *Proceedings of the Institution of Mechanical Engineers, Part D: Journal of Automobile Engineering*, 225(6):705–720, 2011.

[6] Mehmet Dagdelen, Gilles Reymond, Andras Kemeny, Marc Bordier, and Nadia Maïzi. Model-based predictive motion cueing strategy for vehicle driving simulators. *Control Engineering Practice*, 17(9):995–1003, 2009.

[7] Edwin JH de De Vries and Hans B Pacejka. Motorcycle tyre measurements and models. *Vehicle System Dynamics*, 29(S1):280–298, 1998.

[8] Johannes Drosdol and Ferdinand Panik. The daimler-benz driving simulator a tool for vehicle development. Technical report, SAE Technical Paper, 1985.

[9] D Ferrazzin, FBACA Salsedo, F Barbagli, CA Avizzano, G Di Pietro, A Brogni, M Vignoni, M Bergamasco, L Arnone, M Marcacci, et al. The moris motorcycle simulator: an overview. Technical report, SAE Technical Paper, 2001.

[10] John F Golding. Motion sickness susceptibility questionnaire revised and its relationship to other forms of sickness. *Brain research bulletin*, 47(5):507–516, 1998.

[11] Sandra G Hart. Nasa-task load index (nasa-tlx); 20 years later. In *Proceedings of the human factors and ergonomics society annual meeting*, volume 50, pages 904–908. Sage Publications Sage CA: Los Angeles, CA, 2006.

[12] Sandra G Hart and Lowell E Staveland. Development of nasa-tlx (task load index): Results of empirical and theoretical research. In *Advances in psychology*, volume 52, pages 139–183. Elsevier, 1988.

[13] Jacob A Houck, Robert J Telban, and Frank M Cardullo. Motion cueing algorithm development: Human-centered linear and nonlinear approaches. 2005.

[14] Hirohide Imaizumi, Takehiko Fujioka, and Manabu Omae. Rider model by use of multibody dynamics analysis. *JSAE review*, 17(1):75–77, 1996.

[15] Caroline Jay and Roger Hubbold. Delayed visual and haptic feedback in a reciprocal tapping task. In *Eurohaptics Conference, 2005 and Symposium on Haptic Interfaces for Virtual Environment and Teleoperator Systems, 2005. World Haptics 2005. First Joint*, pages 655–656. IEEE, 2005.

[16] Andras Kemeny and Francesco Panerai. Evaluating perception in driving simulation experiments. *Trends in cognitive sciences*, 7(1):31–37, 2003.

[17] Robert S Kennedy, Norman E Lane, Kevin S Berbaum, and Michael G Lilienthal. Simulator sickness questionnaire: An enhanced method for quantifying simulator sickness. *The international journal of aviation psychology*, 3(3):203–220, 1993.

[18] Cornelis Koenen. *The dynamic behaviour of a motorcycle when running straight ahead and when cornering*. PhD thesis, Delft University of Technology, 1983.

[19] JDG Kooijman, AL Schwab, and Jacob Philippus Meijaard. Experimental validation of a model of an uncontrolled bicycle. *Multibody System Dynamics*, 19(1-2):115–132, 2008.

[20] David JN Limebeer and Robin S Sharp. Bicycles, motorcycles, and models. *IEEE control systems*, 26(5):34–61, 2006.

[21] Lamri Nehaoua, Salim Hima, Hichem Arioui, Nicolas Seguy, and Stéphane Espié. Design and modeling of a new motorcycle riding simulator. In *American Control Conference, 2007. ACC'07*, pages 176–181. IEEE, 2007.

[22] NHTSA. Motorcycles traffic safety fact sheet (dot-hs810-990). `https://crashstats.nhtsa.dot.gov/Api/Public/ViewPublication/810990`, 2007. accessed: 14-11-2017.

[23] Hans B. Pacejka. Chapter 11 - motorcycle dynamics. In Hans B. Pacejka, editor, *Tire and Vehicle Dynamics (Third Edition)*, pages 59 – 85. Butterworth-Heinemann, Oxford, third edition edition, 2012. ISBN 978-0-08-097016-5. doi: https://doi.org/10.1016/B978-0-08-097016-5.00002-4. URL `https://www.sciencedirect.com/science/article/pii/B9780080970165000024`.

[24] Miguel A Recarte and Luis M Nunes. Perception of speed in an automobile: Estimation and production. *Journal of experimental psychology: applied*, 2(4):291, 1996.

[25] Lloyd D Reid and Meyer A Nahon. Response of airline pilots to variations in flight simulator motion algorithms. *Journal of Aircraft*, 25(7):639–646, 1988.

[26] Gilles Reymond, Andras Kemeny, Jacques Droulez, and Alain Berthoz. Role of lateral acceleration in curve driving: Driver model and experiments on a real vehicle and a driving simulator. *Human factors*, 43(3):483–495, 2001.

[27] Rainer Scheuchenpflug, Cecilia Ruspa, and Silvia Quattrocolo. Presence in virtual driving simulators. *Human Factors in the Age of Virtual Reality. Shaker Publishing, Maastricht, NL*, pages 143–148, 2003.

[28] Chris Schwarz, Tad Gates, and Yiannis Papelis. Motion characteristics of the national advanced driving simulator. In *Proceedings of the Driving Simulation Conference*, 2003.

[29] Amit Shahar, Virginie Dagonneau, Séphane Caro, Isabelle Israël, and Régis Lobjois. Towards identifying the roll motion parameters of a motorcycle simulator. *Applied ergonomics*, 45(3):734–740, 2014.

[30] Robin S Sharp. The stability and control of motorcycles. *Journal of mechanical engineering science*, 13(5):316–329, 1971.

[31] RS Sharp and CJ Alstead. The influence of structural flexibilities on the straight-running stability of motorcycles. *Vehicle system dynamics*, 9(6):327–357, 1980.

[32] RS Sharp, Simos Evangelou, and David JN Limebeer. Advances in the modelling of motorcycle dynamics. *Multibody system dynamics*, 12(3):251–283, 2004.

[33] JJ Slob. State-of-the-art driving simulators, a literature survey. *DCT report*, 107, 2008.

[34] Alex W Stedmon, Benjamin Hasseldine, David Rice, Mark Young, Steve Markham, Michael Hancox, Edward Brickell, and Joanna Noble. 'motorcyclesim': an evaluation of rider interaction with an innovative motorcycle simulator. *The Computer Journal*, 54(7):1010–1025, 2009.

[35] Doug Stewart. A platform with six degrees of freedom. *Proceedings of the institution of mechanical engineers*, 180(1):371–386, 1965.

[36] E2M Technologies. ef-dd-20/50/130. https://www.e2mtechnologies.eu/productpage-ef-dd-2050130/, 2018. Accessed June 12, 2018.

[37] E2M Technologies. em6-300-1500. https://www.e2mtechnologies.eu/productpage-em6-300-1500/, 2018. Accessed June 12, 2018.

[38] Intel RealSense Technology. Intel realsense camera sr300. https://software.intel.com/en-us/realsense/sr300, 2018. Accessed June 12, 2018.

[39] Inc. The MathWorks. Wilcoxon signed rank test. https://www.mathworks.com/help/stats/signrank.html, 2018. Accessed June 26, 2018.

[40] Inc. The MathWorks. Transfer function estimate. https://nl.mathworks.com/help/signal/ref/tfestimate.html, 2018. Accessed June 20, 2018.

[41] David H Weir and Allen J Clark. A survey of mid-level driving simulators. Technical report, SAE Technical Paper, 1995.

[42] Francis JohnWelsh Whipple. The stability of the motion of a bicycle. *Quarterly Journal of Pure and Applied Mathematics*, 30(120):312–321, 1899.

[43] Walter W Wierwille, John G Casali, and Brian S Repa. Driver steering reaction time to abrupt-onset crosswinds, as measured in a moving-base driving simulator. *Human Factors*, 25(1):103–116, 1983.

[44] Sebastian Will. *Development of a presence model for driving simulators based on speed perception in a motorcycle riding simulator*. Inaugural-dissertation, Fakultät für Humanwissenschaften der Julius-Maximilians-Universität Würzburg, 2017.

[45] Bob G Witmer and Michael J Singer. Measuring presence in virtual environments: A presence questionnaire. *Presence*, 7(3):225–240, 1998.

[46] Goro Yamasaki, Katsuhito Aoki, Yukio Miyamaru, and Koichiro Ohnuma. Development of motorcycle training simulator. *JSAE Review*, 19(1):81 – 85, 1998. ISSN 0389-4304. doi: https://doi.org/10.1016/S0389-4304(97)00057-X. URL http://www.sciencedirect.com/science/article/pii/S038943049700057X.

A

Participant Demographics

This chapter of the Appendix shows participant demographics in Figures A.1 to A.3. This data has been gathered using the Intake Questionnaire shown in Appendix B. Figure A.4 shows the cumulative distribution of the motion sickness susceptibility of the participants in this research. It can be observed that they report to have experienced less motion sickness than the baseline group in the studies of Golding [10].

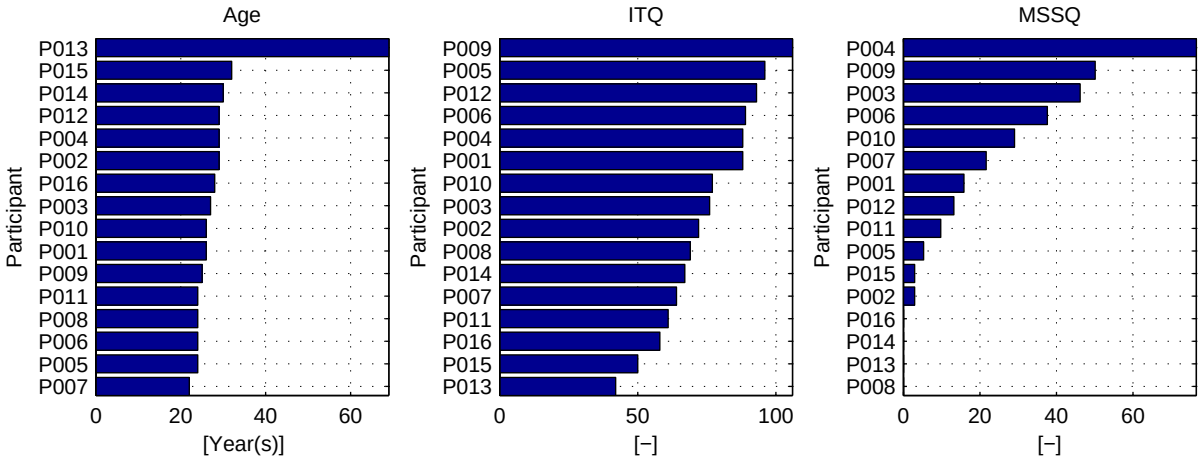

Figure A.1: Participant demographics showing age (left), Immersive Tendencies Questionnaire (ITQ) results (middle) and Motion Sickness Susceptibility Questionnaire results (right).

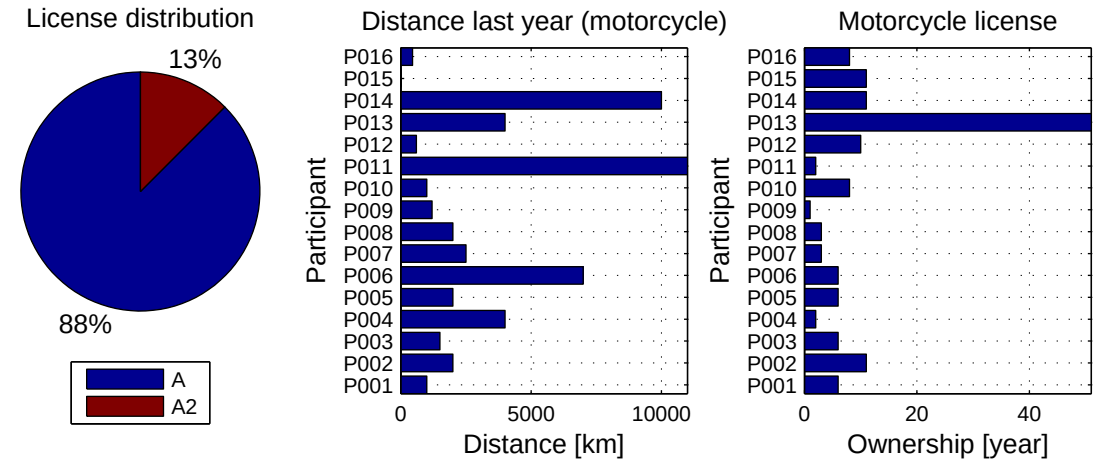

Figure A.2: Participant demogrpahics showing license distribution (left), distance ridden on a motorcycle during last year (middle) and the number of years the participant has had a motorcycle license (right).

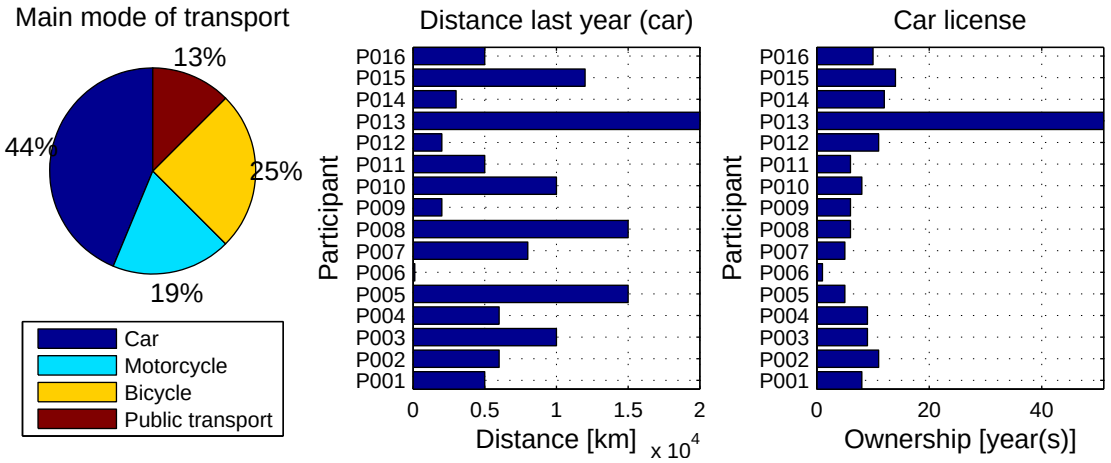

Figure A.3: Participant demographics showing the main mode of transport for the participants (left), distance driven in a car during last year (middle) and the number of years the participant has had a valid car license.

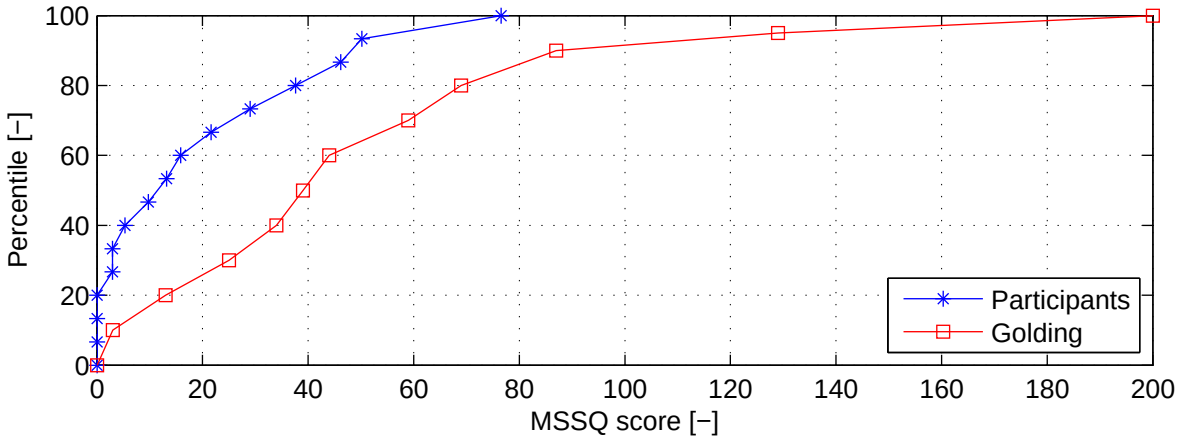

Figure A.4: Cumulative distribution of Motion Sickness Susceptibility Questionnaire results for the participants of the experiments in this research and the baseline from Golding [10].

B

Questionnaires

The questionnaires used in this report are displayed on the following pages. The intake questionnaire starts at 59. The questionnaire used after the practice session and after the speed perception experiments starts at page 64. The two other questionnaires start at 65 and 67, where the last questionnaire is mostly equal to the second-last questionnaire apart from the weighting scale for the NASA-TLX. The second-last questionnaire is administered after the first three trajectory tracking experiments, and the last questionnaire is administered after the last trajectory tracking experiment.

The questionnaires displayed below have been optimized for a computer display. Hence, on the following pages, scaled down versions of the questionnaires are shown to make them fit on A4-paper.

Intake Questionnaire

Participant Demographics

Participant ID.		
Age		years
Gender	Male ○	Female ○
Do you have normal vision or corrected to normal vision?	Yes ○	No ○
Have you suffered from motion sickness, vertigo or migraine in the past?	Yes ○	No ○
Have you been diagnosed with epilepsy?	Yes ○	No ○
What is your primary mode of transport?	Car ○	Motorcycle ○ Moped ○ Bicycle ○ Walking ○ Public Transport ○
Which motorcycle license do you have?	A1 ○	A2 ○ A2(80) ○ A ○
For how many years have you had a motorcycle license (approximately)		years
How many kilometers did you ride on a motorcycle in the last 12 months (approximately)		km
For how many years have you had a B car driver license (approximately)		years
How many kilometers did you drive in a car in the last 12 months (approximately)		km

Motion Sickness Susceptibility Questionnaire

Section A: **Your CHILDHOOD Experience Only** (before 12 years of age)

For each of the following types of transport or entertainment please indicate:

As a **Child (before age 12),** how often you **Travelled or Experienced** (tick boxes):

	Never	1 to 4 trips	5 to 10 trips	11 or more trips
Cars	○	○	○	○
Busses or Coaches	○	○	○	○
Trains	○	○	○	○
Aircraft	○	○	○	○
Small Boats	○	○	○	○
Ships, e.g. Channel Ferries	○	○	○	○

Swings	○	○	○	○
Roundabouts: playgrounds	○	○	○	○
Big Dippers, Funfair Rides	○	○	○	○

As a **Child (before age 12),** how often you **Felt Sick or Nauseated** (tick boxes):

	Never	**Rarely**	**Sometimes**	**Frequently**	**Always**
Cars	○	○	○	○	○
Busses or Coaches	○	○	○	○	○
Trains	○	○	○	○	○
Aircraft	○	○	○	○	○
Small Boats	○	○	○	○	○
Ships, e.g. Channel Ferries	○	○	○	○	○
Swings	○	○	○	○	○
Roundabouts: playgrounds	○	○	○	○	○
Big Dippers, Funfair Rides	○	○	○	○	○

As a **Child (before age 12),** how often you **Vomited** (tick boxes):

	Never	**Rarely**	**Sometimes**	**Frequently**	**Always**
Cars	○	○	○	○	○
Busses or Coaches	○	○	○	○	○
Trains	○	○	○	○	○
Aircraft	○	○	○	○	○
Small Boats	○	○	○	○	○
Ships, e.g. Channel Ferries	○	○	○	○	○
Swings	○	○	○	○	○
Roundabouts: playgrounds	○	○	○	○	○
Big Dippers, Funfair Rides	○	○	○	○	○

Section B: **Your Experience over the Last 10 Years (approximately)**

For each of the following types of transport or entertainment please indicate:

Over the **Last 10 years,** how often you **Travelled or Experienced** (tick boxes):

	Never	**1 to 4 trips**	**5 to 10 trips**	**11 or more trips**
Cars	○	○	○	○
Busses or Coaches	○	○	○	○
Trains	○	○	○	○
Aircraft	○	○	○	○
Small Boats	○	○	○	○
Ships, e.g. Channel Ferries	○	○	○	○
Swings	○	○	○	○

Roundabouts: playgrounds	○	○	○	○
Big Dippers, Funfair Rides	○	○	○	○

Over the **last 10 years,** how often you **Felt Sick or Nauseated** (tick boxes):

	Never	Rarely	Sometimes	Frequently	Always
Cars	○	○	○	○	○
Busses or Coaches	○	○	○	○	○
Trains	○	○	○	○	○
Aircraft	○	○	○	○	○
Small Boats	○	○	○	○	○
Ships, e.g. Channel Ferries	○	○	○	○	○
Swings	○	○	○	○	○
Roundabouts: playgrounds	○	○	○	○	○
Big Dippers, Funfair Rides	○	○	○	○	○

Over the **last 10 years,** how often you **Vomited** (tick boxes):

	Never	Rarely	Sometimes	Frequently	Always
Cars	○	○	○	○	○
Busses or Coaches	○	○	○	○	○
Trains	○	○	○	○	○
Aircraft	○	○	○	○	○
Small Boats	○	○	○	○	○
Ships, e.g. Channel Ferries	○	○	○	○	○
Swings	○	○	○	○	○
Roundabouts: playgrounds	○	○	○	○	○
Big Dippers, Funfair Rides	○	○	○	○	○

Immersive Tendencies Questionnaire

Do you easily become deeply involved in movies or TV dramas?	Not	○ ○ ○ ○ ○ ○ ○	Very
Do you ever become so involved in a television program or book that people have proplems getting your attention?	Not	○ ○ ○ ○ ○ ○ ○	Very
How mentally alert do you feel at the present time?	Not	○ ○ ○ ○ ○ ○ ○	Very
Do you ever become so involved in a movie that you are not aware of things happening around you?	Not	○ ○ ○ ○ ○ ○ ○	Very
How frequently do you find yourself closely identifying with the characters in a story line?	Not	○ ○ ○ ○ ○ ○ ○	Very
Do you ever become so involved in a video game that it is as if you are inside the game rather than moving a joystick and watching the screen?	Not	○ ○ ○ ○ ○ ○ ○	Very
How physically fit do you feel today?	Not	○ ○ ○ ○ ○ ○ ○	Very
How good are you at blocking out external distractions when you are involved in	Not	○ ○ ○ ○ ○ ○ ○	Very

something?			
When watching sports, do you ever become so involved in the game that you react is if you were one of the players?	Not	○ ○ ○ ○ ○ ○ ○	Very
Do you ever become so involved in a daydream that you are not aware of things happening around you?	Not	○ ○ ○ ○ ○ ○ ○	Very
Do you ever have dreams that are so real that you feel disoriented when you awake?	Not	○ ○ ○ ○ ○ ○ ○	Very
When playing sports, do you become so involved in the game that you lose track of time?	Not	○ ○ ○ ○ ○ ○ ○	Very
How well do you concentrate on enjoyable activities?	Not	○ ○ ○ ○ ○ ○ ○	Very
How often do you play arcade of video games? (OFTEN should be taken to mean every day or every two days, on average.)	Not	○ ○ ○ ○ ○ ○ ○	Very
Have you ever gotten excited during a chase or fight scene on TV or in the movies?	Not	○ ○ ○ ○ ○ ○ ○	Very
Have you ever gotten scared by something happening on a TV show or in a movie?	Not	○ ○ ○ ○ ○ ○ ○	Very
Have you ever remained apprehensive or fearful long after watching a scary movie?	Not	○ ○ ○ ○ ○ ○ ○	Very
Do you ever become so involved in doing something that you lose all track of time?	Not	○ ○ ○ ○ ○ ○ ○	Very

Simulator Sickness Questionnaire

Please indicate from 0 - 3 for each of the 16 symptoms.

General discomfort	○ ○ ○ ○
Fatigue:	○ ○ ○ ○
Headache:	○ ○ ○ ○
Eyestrain:	○ ○ ○ ○
Difficulty focusing:	○ ○ ○ ○
Increased salivation:	○ ○ ○ ○
Sweating:	○ ○ ○ ○
Nausea:	○ ○ ○ ○
Difficulty concentrating:	○ ○ ○ ○
Fullness of head:	○ ○ ○ ○
Blurred vision:	○ ○ ○ ○
Dizzy (eyes open):	○ ○ ○ ○
Dizzy (eyes closed):	○ ○ ○ ○
Vertigo:	○ ○ ○ ○
Stomach awareness:	○ ○ ○ ○
Burping:	○ ○ ○ ○

Send Questionnaire

Participant Info

Participant ID.:

Experiment No.:

Simulator Sickness Questionnaire

Please indicate from 0 - 3 for each of the 16 symptoms.

General discomfort	○	○	○	○
Fatigue:	○	○	○	○
Headache:	○	○	○	○
Eyestrain:	○	○	○	○
Difficulty focusing:	○	○	○	○
Increased salivation:	○	○	○	○
Sweating:	○	○	○	○
Nausea:	○	○	○	○
Difficulty concentrating:	○	○	○	○
Fullness of head:	○	○	○	○
Blurred vision:	○	○	○	○
Dizzy (eyes open):	○	○	○	○
Dizzy (eyes closed):	○	○	○	○
Vertigo:	○	○	○	○
Stomach awareness:	○	○	○	○
Burping:	○	○	○	○

Send Questionnaire

Participant Info

Participant ID.:
Experiment No.:

NASA Task Load Index

Mental Demand - How mentally demanding was the task?

Very Low | | | | | | | | | | | | | | | | | | | | Very High

Physical Demand- How physically demanding was the task?

Very Low | | | | | | | | | | | | | | | | | | | | Very High

Temporal Demand - How hurried or rushed was the pace of the task?

Very Low | | | | | | | | | | | | | | | | | | | | Very High

Performance - How successful were you in accomplishing what you were asked to do?

Perfect | | | | | | | | | | | | | | | | | | | | Failure

Effort - How hard did you have to work to accomplish your level of performance?

Very Low | | | | | | | | | | | | | | | | | | | | Very High

Frustration - How insecure, discouraged, irritated, stressed and annoyed were you?

Very Low | | | | | | | | | | | | | | | | | | | | Very High

Simulator Sickness Questionnaire

Please indicate from 0 - 3 for each of the 16 symptoms.

General discomfort ○ ○ ○ ○
Fatigue: ○ ○ ○ ○
Headache: ○ ○ ○ ○
Eyestrain: ○ ○ ○ ○

Difficulty focusing: ○ ○ ○ ○
Increased salivation: ○ ○ ○ ○
Sweating: ○ ○ ○ ○
Nausea: ○ ○ ○ ○

Difficulty concentrating: ○ ○ ○ ○
Fullness of head: ○ ○ ○ ○
Blurred vision: ○ ○ ○ ○
Dizzy (eyes open): ○ ○ ○ ○

Dizzy (eyes closed): ○ ○ ○ ○
Vertigo: ○ ○ ○ ○
Stomach awareness: ○ ○ ○ ○
Burping: ○ ○ ○ ○

Presence Questionnaire

How much were you able to control events? Not ○ ○ ○ ○ ○ ○ ○ Very
How responsive was the environment to actions that you imitated (or performed) Not ○ ○ ○ ○ ○ ○ ○ Very
How natural did your interaction with the enviroment seem? Not ○ ○ ○ ○ ○ ○ ○ Very
How much did the visual aspects of the environment involve you? Not ○ ○ ○ ○ ○ ○ ○ Very

How much did the auditory aspects of the environment involve you? Not ○ ○ ○ ○ ○ ○ ○ Very

How natural was the mechanism which controlled movement through the environment?	Not	○	○	○	○	○	○	○	Very
How compelling was your sense of objects moving through space?	Not	○	○	○	○	○	○	○	Very
How much did your experiences in the virtual environment seem consistent with your real world experiences?	Not	○	○	○	○	○	○	○	Very
Were you able to anticipate what would happen next in response to the actions that you performed?	Not	○	○	○	○	○	○	○	Very
How completely were you able to actively survey or search the environment using vision?	Not	○	○	○	○	○	○	○	Very
How well could you identify sounds?	Not	○	○	○	○	○	○	○	Very
How wel could you localize sounds?	Not	○	○	○	○	○	○	○	Very
How compelling was your sense of moving around inside the virtual environment?	Not	○	○	○	○	○	○	○	Very
How involved were you in the virtual environment experience?	Not	○	○	○	○	○	○	○	Very
How much delay did you experience between your actions and expected outcomes?	Very	○	○	○	○	○	○	○	Not
How quickly did you adjust to the virtual environment?	Not	○	○	○	○	○	○	○	Very
How proficient in moving and interacting with the virtual environment did you feel at the end of the experience?	Not	○	○	○	○	○	○	○	Very
How much did the visual display quality interfere or distract you from performing assigned tasks or required activities?	Very	○	○	○	○	○	○	○	Not
How much did the control devices interfere with the performance of assigned tasks or with other activities?	Very	○	○	○	○	○	○	○	Not
How well could you concentrate on the assigned tasks or required activities rather than on the mechanisms used to perform those tasks or activities?	Not	○	○	○	○	○	○	○	Very

Send Questionnaire

Participant Info

Participant ID.:
Experiment No.:

NASA Task Load Index

Mental Demand - How mentally demanding was the task?

Very Low | | | | | | | | | | | | | | | | | | | | Very High

Physical Demand- How physically demanding was the task?

Very Low | | | | | | | | | | | | | | | | | | | | Very High

Temporal Demand - How hurried or rushed was the pace of the task?

Very Low | | | | | | | | | | | | | | | | | | | | Very High

Performance - How successful were you in accomplishing what you were asked to do?

Perfect | | | | | | | | | | | | | | | | | | | | Failure

Effort - How hard did you have to work to accomplish your level of performance?

Very Low | | | | | | | | | | | | | | | | | | | | Very High

Frustration - How insecure, discouraged, irritated, stressed and annoyed were you?

Very Low | | | | | | | | | | | | | | | | | | | | Very High

Simulator Sickness Questionnaire

Please indicate from 0 - 3 for each of the 16 symptoms.

General discomfort ○ ○ ○ ○
Fatigue: ○ ○ ○ ○
Headache: ○ ○ ○ ○
Eyestrain: ○ ○ ○ ○

Difficulty focusing: ○ ○ ○ ○
Increased salivation: ○ ○ ○ ○
Sweating: ○ ○ ○ ○
Nausea: ○ ○ ○ ○

Difficulty concentrating: ○ ○ ○ ○
Fullness of head: ○ ○ ○ ○
Blurred vision: ○ ○ ○ ○
Dizzy (eyes open): ○ ○ ○ ○

Dizzy (eyes closed): ○ ○ ○ ○
Vertigo: ○ ○ ○ ○
Stomach awareness: ○ ○ ○ ○
Burping: ○ ○ ○ ○

Presence Questionnaire

How much were you able to control events? Not ○ ○ ○ ○ ○ ○ ○ Very
How responsive was the enviroment to actions that you imitated (or performed) Not ○ ○ ○ ○ ○ ○ ○ Very
How natural did your interaction with the environment seem? Not ○ ○ ○ ○ ○ ○ ○ Very
How much did the visual aspects of the environment involve you? Not ○ ○ ○ ○ ○ ○ ○ Very

How much did the auditory aspects of the environment involve you? Not ○ ○ ○ ○ ○ ○ ○ Very

How natural was the mechanism which controlled movement through the environment?	Not	Very
How compelling was your sense of objects moving through space?	Not	Very
How much did your experiences in the virtual environment seem consistent with your real world experiences?	Not	Very
Were you able to anticipate what would happen next in response to the actions that you performed?	Not	Very
How completely were you able to actively survey or search the environment using vision?	Not	Very
How well could you identify sounds?	Not	Very
How wel could you localize sounds?	Not	Very
How compelling was your sense of moving around inside the virtual environment?	Not	Very
How involved were you in the virtual environment experience?	Not	Very
How much delay did you experience between your actions and expected outcomes?	Very	Not
How quickly did you adjust to the virtual environment?	Not	Very
How proficient in moving and interacting with the virtual environment did you feel at the end of the experience?	Not	Very
How much did the visual display quality interfere or distract you from performing assigned tasks or required activities?	Very	Not
How much did the control devices interfere with the performance of assigned tasks or with other activities?	Very	Not
How well could you concentrate on the assigned tasks or required activities rather than on the mechanisms used to perform those tasks or activities?	Not	Very

NASA-TLX Sources of workload

Tick the box that represents the more important contributor to workload in the specific task(s) you performed in this experiment.

Mental Demand:	How mentally demanding was the task?
Physical Demand	How physically demanding was the task?
Temporal Demand:	How hurried or rushed was the pace of the task?
Performance:	How succesfull were you in accomplishing what you were asked to do?
Effort:	How hard did you have to work to accomplish your level of performance?
Frustration:	How insecure, discouraged, irritated, stressed and annoyed were you?

Effort	- or -	Performance
Temporal Demand	- or -	Frustration
Physical Demand	- or -	Effort
Physical Demand	- or -	Frustration
Performance	- or -	Frustration
Physical Demand	- or -	Temporal Demand
Physical Demand	- or -	Performance
Temporal Demand	- or -	Mental Demand
Frustration	- or -	Effort
Performance	- or -	Mental Demand
Performance	- or -	Temporal Demand
Mental Demand	- or -	Effort
Mental Demand	- or -	Physical Demand
Effort	- or -	Physical Demand
Frustration	- or -	Mental Demand

Send Questionnaire

C

Steps for Conducting the Experiments

C.1. List of Steps

Before the participant arrives:

1. Determine specific sequence of the experiments for the participant.
2. Create a file folder tree for the experiments on a USB stick.
3. Print the informed consent form.
4. Assign participant ID. to the participant.
5. Turn on the PC's.
6. Turn on the motion platform.
7. Turn on the sound systems.
8. Test ride the motorcycle simulator for the practice session scenario.

Before the experiments:

1. Check if the participant has read, understood and signed the informed consent form.
2. Have the participant complete the intake questionnaire.
3. Answer any question from the participant.

Practice session:

1. Explain the operation and safety procedures of the motorcycle simulator.
2. Have the participant take position on the motorcycle simulator.
3. Load the *"Cruden Dynamic Area"* track.
4. Start the practice sessions and start the timer.
5. Urge the participant to perform certain maneuvers to familiarize himself with the simulator.
6. End the practice session after 10 minutes.
7. Administer the *"During speed perception"* questionnaire (SSQ) with experimental condition *"PRC"*.

Speed perception experiments:

1. Explain the procedure of the trajectory tracking experiment.
2. Load the *"Cruden Dynamic Area"* track.
3. Ensure that the dashboard is shut off in *"views.ini"* (so there is no speedometer).
4. For each experimental condition:
   (a) Check the required experimental condition.
   (b) Copy the corresponding setup files.
   (c) Perform the speed perception experiment.
   (d) Have the participant complete the *"during speed perception"* questionnaire after every three conditions (SSQ).
   (e) Copy the `.rtd` log files to the correct file folder in the file folder tree.
5. Check that all `.rtd` log files are present.

Trajectory tracking experiments:

1. Explain the procedure of the speed perception experiment.
2. Load the *"Cruden Dynamic Area with cones"* track.
3. For each experimental condition:
   (a) Check the required experimental conditions (Motion/ Body tracking).
   (b) Copy the corresponding setup files.
   (c) Perform the trajectory tracking experiment.
   (d) Have the participant complete the *"during trajectory"* questionnaire after each condition (TLX, SSQ, PQ).
   (e) Copy the `.rtd` log files to the correct file folder in the file folder tree.
4. Have the participant complete the *"after trajectory tracking"* questionnaire (TLX, SSQ, PQ, TLX-sources).
5. Check that all `.rtd` log files are present in the file folder tree.

After the experiments:

1. Thank the participant for participating in the experiments.
2. Back-up all data collected during the experiments.
3. Turn of motion platform, PC's and audio systems.
4. (If after closing time) Notify workshop manager the experiments are completed and close the building.

C.2. Order of Administration

Table C.1: Randomized order of administration for the speed perception and trajectory tracking experiments.

P001	**P002**	**P003**	**P004**	**P005**	**P006**	**P007**	**P008**
			Speed perception				
SP120-3	SP50-2	SP50-2	SP50-3	SP120-1	SP50-1	SP80-3	SP80-2
SP80-1	SP120-1	SP120-2	SP120-3	SP80-2	SP120-1	SP50-3	SP80-1
SP50-3	SP120-2	SP50-1	SP80-2	SP50-1	SP80-3	SP80-1	SP50-1
SP50-1	SP80-3	SP80-2	SP80-3	SP50-2	SP120-2	SP50-2	SP120-1
SP50-2	SP80-1	SP80-1	SP120-1	SP80-1	SP120-3	SP120-1	SP120-2
SP120-2	SP120-3	SP120-3	SP50-2	SP50-3	SP50-3	SP120-2	SP120-3
SP120-1	SP80-2	SP120-1	SP120-2	SP120-2	SP50-2	SP120-3	SP50-3
SP80-3	SP50-3	SP50-3	SP50-1	SP120-3	SP80-1	SP80-2	SP80-3
SP80-2	SP50-1	SP80-3	SP80-1	SP80-3	SP80-2	SP50-1	SP50-2
			Trajectory tracking				
M0T1	M0T0	M0T1	M0T0	M0T1	M1T1	M1T1	M1T0
M1T1	M1T1	M1T1	M1T1	M1T0	M1T0	M0T0	M0T1
M0T0	M0T1	M0T0	M0T1	M0T0	M0T0	M1T0	M1T1
M1T0	M1T0	M1T0	M1T0	M1T1	M0T1	M0T1	M0T0

P009	**P010**	**P011**	**P012**	**P013**	**P014**	**P015**	**P016**
			Speed perception				
SP50-3	SP120-2	SP120-3	SP120-2	SP120-3	SP50-1	SP50-2	SP120-3
SP50-2	SP50-1	SP80-2	SP80-3	SP50-1	SP50-3	SP80-1	SP80-3
SP120-3	SP50-2	SP50-2	SP50-1	SP120-1	SP80-1	SP50-1	SP80-2
SP80-2	SP80-1	SP120-2	SP50-3	SP50-3	SP120-2	SP120-2	SP50-3
SP120-1	SP80-2	SP120-1	SP120-3	SP120-2	SP50-2	SP120-1	SP50-2
SP120-2	SP120-1	SP80-1	SP50-2	SP50-2	SP80-2	SP80-3	SP120-1
SP80-1	SP80-3	SP50-3	SP120-1	SP80-1	SP80-3	SP80-2	SP50-1
SP50-1	SP120-3	SP50-1	SP80-2	SP80-3	SP120-3	SP50-3	SP120-2
SP80-3	SP50-3	SP80-3	SP80-1	SP80-2	SP120-1	SP120-3	SP80-1
			Trajectory tracking				
M0T1	M1T1	M1T0	M0T0	M0T0	M1T0	M1T0	M1T0
M0T0	M0T0	M0T0	M0T1	M0T1	M0T1	M0T0	M0T0
M1T1	M0T1	M1T1	M1T1	M1T1	M0T0	M1T1	M1T1
M1T0	M1T0	M0T1	M1T0	M1T0	M1T1	M0T1	M0T1

D

Informed Consent Form

This consent form used for the experiments is shown in this chapter of the appendix in the following six pages.

1 Research Group

1.1 Researchers in charge of the project

Bernhard E. Westerhof[1]	MSc. Student	Delft University of Technology
Edwin J.H. de Vries[3]	Senior Modeling & Simulation Engineer	Cruden B.V.
Arend L. Schwab[1,2]	Assistant Professor	Delft University of Technology
Riender Happee[1,2]	Associate Professor	Delft University of Technology

1.2 Organizations

1. Vehicle Engineering, Department of Mechanical Engineering, Faculty of Mechanical, Maritime and Materials Engineering, Delft University of Technology, Delft, the Netherlands
2. Department of Biomechanical Engineering, Faculty of Mechanical, Maritime and Materials Engineering, Delft University of Technology, Delft, the Netherlands
3. Cruden B.V., Amsterdam, the Netherlands

---

2 This document

This Informed Consent Form has two parts:

- **Information Sheet,** pages 1 - 5
- **Certificate of Consent,** page 6

Before agreeing to participate in this study, you are asked to read this document carefully. The Information Sheet describes the purpose, procedures, and risks of this study. After reading the Information Sheet, we will be happy to explain any points that seem unclear, or sections that you do not understand. You should feel comfortable to speak to any of the researchers involved to answer any questions you may have at any time. After you have read this Information Sheet and we have answered all of your questions or discussed any concerns, you can decide if you would like to be involved. At the end of this document, we would like to ask you to sign a written Certificate of Consent to confirm your agreement to participate. Your signature is required for participation.

You will be given a copy of the full Informed Consent Form.

---

3 Purpose of the research

Although motorcycle simulators are much less common than flight or automotive simulators, they could play an important role in research, design optimization and simulator testing. This

research is conducted to evaluate Cruden's motorcycle simulator and to obtain design criteria for future motorcycle simulators. With the knowledge obtained in this research, a better understanding in the human-machine interaction between motorcycles and riders is obtained and the development of new motorcycle simulators can be improved. This in turn enables more detailed research into motorcycle dynamics, human factors, safety systems and rider assistance systems.

4 Participation

4.1 Location of the experiment

Participation will involve to complete one in-person session at Cruden B.V. Global Headquarters, Pedro de Medinalaan 25, 1086 XP Amsterdam, the Netherlands.

4.2 Eligibility criteria

You are invited to participate in this project if:

- You are 18 years or older.
- You are over 1.50 meter in length.
- You have a motorcycle license.
- You have normal or corrected-to-normal vision (i.e. glasses or contact lenses).
- You have not experienced (simulator) motion sickness in the past.
- You do not have heart, back or neck issues.
- You have not been diagnosed with epilepsy.
- You are not pregnant/think that you may be pregnant.
- You have not recently had surgery.
- You are not physically disabled.
- You are not under the influence of drugs, alcohol or prescription substances that my compromise the comfort when operating a motion-based motorcycle simulator using a head-mounted display.

The researchers reserve the right at any time to refuse or excuse (from an in-progress session) any participant who does not meet/no longer meets the study requirements or who are behaving in an unnecessarily unsafe manner.

4.3 Voluntary participation and right to refuse or withdraw

Your participation in this project is completely voluntary. We welcome you to contact us to ask any questions and to discuss your possible involvement in the project, but it is your choice whether to participate or not. If you do agree to participate you have the right to withdraw from the project at any moment without comment or penalty.

5 Procedure

5.1 Your tasks

You will be asked to perform several maneuvers for different simulator settings. The experiments can be divided in three categories: motion, body tracking and speed perception. The simulated motorcycle is a Honda CB-750 classic bike. You control the simulator using the same inputs as on the real motorcycle: throttle, front and rear brake, gear selector, clutch and steering torque. In some of the simulations, also body lean can be used to control the motorcycle.

5.1.1 Speed perception

During the speed perception experiment, you are asked to ride either 50, 80 or 120 km/h with the absence of a speedometer. For each speed, three repetitions will be performed. Between each set of three tries, you will get a break. The speed perception experiments are conducted on a highway environment.

5.1.2 Trajectory tracking

In the trajectory tracking task, you will be asked to ride between a trajectory of cones at 50 km/h. In this case, the speedometer is available and you are advised to make use of it. Different settings of the motorcycle simulator will be used to evaluate its performance. No matter how far you have deviated from the center of the trajectory, you should try to finish the experiment.

5.2 Prior to the simulator sessions

Prior to the simulator sessions, the informed consent form will be sent to you. When you visit the simulator sessions, the study details will be explained to you, an informed consent form will be signed, and baseline questionnaires on workload and simulator sickness will be completed.

Next, a safety instruction will be given on operating the motorcycle simulator. The operation of the emergency switches will be shown and it will be stressed that the experiment can be stopped at any time.

5.3 Practice simulator sessions

The experiment starts with some practice to familiarize yourself with the simulator, the virtual environment and the procedure of starting an experiment. The first practice session takes around 10 minutes and you are encouraged to ride both fast and slow to get a feeling of the dynamics of the motorcycle. After the practice session, you are asked to complete another questionnaire.

5.4 Testing simulator sessions

The speed perception experiments will be conducted first. After a break, the trajectory tracking experiments will begin. Between each experimental condition in the trajectory tracking experiment, a break will be held in which questionnaires are to be completed.

5.5 Duration and time commitment

The whole experiment will take approximately 2 hours and involves signing a consent form, practice simulator sessions, testing simulator sessions, breaks and completing questionnaires.

6 Expected benefits

It is not expected that the project directly benefits you. However, your participation in this study will add to our understand of riding performance and motorcycle simulator performance and in this way your participation will assist in developing new approaches to making motorcycle riding safer for riders.

7 Risks associated with participation

Participants may experience simulator motion sickness. In case a participant experiences such sickness, the experiment can be stopped at any time. An emergency switch is available on the handlebar of the motorcycle mock-up with which you can shut-down the simulation instantaneously. The head-mounted display can be easily removed so that you will no longer receive visual cues. It is advised to remove the head-mounted display as soon as the emergency switch is enabled to avoid motion sickness. Prior to the experiment you will be instructed on the safety procedures. Taking place on the simulator requires you to climb up a small staircase, which might result in an accidental fall. The participant may only enter the simulator when the simulator is shut-down, to avoid tripping due to motion of the simulator. During the experiment, an operator ensures safe conduct of operation of the motorcycle simulator. If the operator notices unsafe or unwanted behavior of the simulator or participant, the experiment may be terminated prematurely.

There are several ways for you to lose control of the virtual motorcycle. Some of these are losing stability at low speed and braking too hard in corners. The experience of a crash can be emotionally and physically demanding, as the motion base and head mounted display simulate right to the point of crashing the virtual motorcycle. Finally, in some test tracks, guard rails, buildings and other objects are non-solid objects, so a participant can ride through them. Riding through a non-solid object can be an emotionally uncomfortable experience.

8 Privacy and confidentiality

All comments and responses are anonymous and will be treated confidentially unless required by law. The names of individual persons are not required in any of the responses. Publications or presentations of the results will not include any information that could identify you.

Any data collected as part of this project will be stored securely as per TU Delft's Research Data Management policy. Only the researchers involved in the project will have access to this

information. Please note that non-identifiable data from this project may be used as comparative data in future projects or stored on an open access database for secondary analysis.

9 Sharing of results

Results of the study might be presented in scientific and traffic safety seminars and conferences, and published as PhD theses and articles in scientific journals. Data might also be used in related studies on rider behavior, training, training in simulators, design of motorcycle/scooter safety systems, and human-machine interface design for motorcycles/scooters.

10 Responsibility

The researchers, funding bodies or institutions involved do not bear any responsibility for possible inconveniences or damages during travel to or from the location of the experimental activity.

11 Questions/further information about the project

If you wish to ask questions about the project or require further information, please contact one of the researchers below:

Researcher	**E-mail**	**Phone**
Bernhard E. Westerhof	b.e.westerhof@student.tudelft.nl	+31(0)6 1600 9860
Edwin J.H. de Vries	e.devries@cruden.com	
Arend L. Schwab	a.l.schwab@tudelft.nl	
Riender Happee	r.happee@tudelft.nl	

12 Ethical approval and complains regarding the conduct of the project

This study has been approved by the Human Research Ethics Committee (HREC), Approval Number 378(2018). If needed, verification of approval can be obtained either by writing to P.O. Box 5015, 2600 GA Delft, The Netherlands or by sending an email to HREC@tudelft.nl. If you do have any concerns or complaints about the ethical conduct of the project you may contact the HREC on the above mentioned addresses. The HREC is not connected with the research project and can facilitate a resolution to your concern in an impartial manner.

Certificate of consent

Title of study: Motorcycle simulator evaluation

Participant ID: .....

To be read and signed by the participant

I declare that I clearly understand the nature, methods and purpose of this research as well as my responsibilities as a participant. I know that the data and results of this study shall be treated anonymously and confidentially. My questions and doubts, regarding the above, have been answered satisfactorily.

I declare that I meet all eligibility criteria written in the Information Sheet (pages 1 - 5).

I have been made aware of all possible risks and discomforts present in this study.

I agree entirely voluntarily to participate in this study. I reserve the right to withdraw my participation at any time during the study, without needing to provide a reason. My withdrawal shall not negatively affect me in any way.

Name of participant: .....

Date, Place: .....

Signature of participant: .....

To be read and signed by the researcher

I have provided a sufficient oral and written explanation of this study. I will answer any other questions of the participant to the best of my abilities. The participant will not suffer any adverse consequences due to premature termination of the study.

Name of researcher: .....

Date, Place: .....

Signature of researcher: .....